Study of the Cell Biological Role of Lowe Syndrome Protein OCRL1

Adam Graham Grieve

This thesis is submitted to the University College of London
for degree of Doctor of Philosophy

February 2009

Department of Cell Biology
UCL Institute of Ophthalmology
11-43 Bath Street
London
EC1V 9EL

Abstract

Oculocerebrorenal syndrome of Lowe (OCRL) is caused by mutations in a phosphatidylinositol 5-phosphatase, OCRL1, and is believed to lead to an elevation of its preferred substrate, PI(4,5)P2. To date, much of the work on OCRL1 has centred on its role at Golgi and endosomal membranes. However, there is also evidence of plasma membrane activity for OCRL1, where its PI(4,5)P2 substrate is known to be highly abundant. PI(4,5)P2 regulates a wide array of downstream cellular functions such as cytoskeletal dynamics, membrane trafficking and signalling. The tight regulation of PI(4,5)P2 levels and localisation, like other phosphoinositides, provides a framework upon which many of these cellular processes work. In this thesis, effects of OCRL1 loss have been tested through siRNA depletion of OCRL1, focussing where possible on multiple PI(4,5)P2-dependent mechanisms, and also focussing on cells forming polarised epithelia. Firstly, we have visualised the localisation of PI(4,5)P2 in living HeLa cells lacking OCRL1 through immunostaining for Annexin A2, which showed a marked translocation to the plasma membrane. This change in distribution of Annexin A2 suggested that OCRL1 depletion may have an effect on intracellular calcium dynamics as well as PI(4,5)P2 localisation. We also used a GFP-chimera of the well characterised PI(4,5)P2-binding pleckstrin homology domain of PLCδ1. This showed no difference in localisation upon OCRL1 depletion. As OCRL1 is highly enriched at the TGN, we fused the pleckstrin homology domain of PLCδ1 to a mutated pleckstrin homology domain of OSBP known to bind

ARF1 at the TGN, to act as a coincidence detector for PI(4,5)P2 at the TGN. This construct also showed no reproducible effect of OCRL1 depletion.

Secondly we tested the effect of loss of OCRL1 on cytosolic calcium levels. Using two phospholipase C (PLC) agonists, and a SERCA pump inhibitor, we found no consistent differences in calcium handling upon depletion of OCRL1. Thirdly, we have assessed the potential specialised role that OCRL1 has in polarised epithelial cells, which might relate to the clinical picture in Lowe Syndrome. We found that OCRL1 targets the tight junctions of immortalised lines and primary cells. Through co-immunoprecipitation, we found OCRL1 in complexes with the tight junction scaffold protein ZO-1. Most significantly, we found that depletion of OCRL1 in human polarised epithelial cell lines interfered with epithelial differentiation, reducing cell number and altering morphology, to produce large flat cells. We attribute this phenotype, stronger than any other so far described experimentally, to a defect in tight junction maturation.

Declaration

I, Adam Graham Grieve, confirm that the work presented in this thesis is my own. Where information has been derived from other sources, I confirm that this has been indicated in the thesis.

London, February 2009

Acknowledgements

Firstly, I'd like to thank Matt Hayes, Becca Longbottom and Ian "Dr Evil" White, my surrogate post-docs, who have always been a huge support to me. Whenever I've been needy, required help, or more often than not, needed to buck my ideas up, I could always rely upon them for advice, a slap, a hug or a kick to the rear. You always knew which way to get the best out of me. The student team past and present: Mark Evans for the bourbons and his cider fuelled gymnastics-themed tourettes, Ah-Lai Law for the theft of her foodstuffs and all the little favours she did for me, Jay Stone for being the best sit-next-to buddy ever, Maria Dawson for being a pain in the neck, and the two other members of the greatest trio in the world, Lux "I don't have issues with dark chocolate or pronouncing the word plastic" Fatimathas and PC Jenny "I speak in a Welsh accent" Williams (Go Team Western!).

I would like to thank everyone else in the Cell Biology department for putting up with me and making the Institute such a lovely place to work. This thesis would be impossible without the help of so many people such as Anna Tsapara who was always there for help when I needed it, Veronkia Mikitova for making the Levine Group a trio, Karl Matter who (sometimes unknowingly) allowed me to pilfer his lab materials on an increasingly frequent basis, and others that bring everything together such as Claire Cox and Aida Jokubaityte. Outside the Institute, Sandip Patel and Sam Ranasinghe from the Physiology Department in UCL have helped me a great deal with calcium imaging. Also, I would like to thank Geraint Thomas and Shamshad Cockcroft for putting me on my way to a PhD- their enthusiasm for science was, and still is, infectious.

In particular I would like to thank the univocal and verbose Tim Levine for taking me on as his student. Tim has supported me every time I have needed it, understood my awful definition of deadlines and taught me so much. I have been told many times that a PhD student often becomes someone much like his or her supervisor. If I even go a small way to fulfilling that prophesy, then I

would be extremely proud of myself. You are a truly inspiring scientist and the best supervisor I could have possibly asked for.

I would like to thank the Lowe Syndrome Trust for funding my project. I sincerely hope that all the valued effort they put into funding research projects like my own yields the cure they seek.

I would like to thank other friends and colleagues for a number of reasons, for keeping me as sane as possible, food, support, housing, beer and love: Ben, Bowden, Charlie, Clare, many Emilys, Emma, Gianfranco, Jim, John Kelly, Kate, Luke, Mace, Mark, Mattea, Mike, Minoo, Natalie, Rushee, Shalini, Shweta, Stagg, and many Steves. Especially, I would like to thank my beautiful non-girlfriend, Francesca. Not being in a relationship with you for the last two years has made me the happy man I am today, submitting this thesis. Thank you for being someone I can always turn to, to support me and always make things better.

I would like to thank family, especially my Mum and Dad for everything they do and did for me, to get me to this point. My parents taught me at a young age (what has now become a bit of a cliché, but I'm sure they were the first to say it) that if I found a job that I enjoyed, it is less like a job and more like a hobby. Thank you, I do not often say this, but you were right. Furthermore, I would also like to thank Grannie and Grandpa for their unerring support and love. I would also like to thank Miss Penny Grieve, the best friend a boy could ever have, despite all her digging. Bad girl. Good girl. Come here then.

Finally, I would like to thank the very strange man at O2 Customer Services. The 100 free WAP minutes and 300 free texts on my GSM mobile have been extremely useful. Your many phone calls to me while I have been writing this thesaurus have been very motivational. I look forward to hearing from you soon.

Dedication

I would like to dedicate this thesis to my mother, Nadia.

List of Contents

List of Figures

List of abbreviations

ADP	Adenosine diphosphate
AKT	AK transforming
AP	Apurinic/apyrimidinic
AP-1	Adaptor protein 1
AP-2	Adaptor protein 2
aPKC	Atypical protein kinase C
APPL1	Adaptor protein, phosphotyrosine interaction, PH domain and leucine zipper containing 1
ARF	ADP-ribosylation factor
ASH	ASPM, SPD2, Hydin
ATP	Adenosine triphosphate
BAPTA	1,2-bis(o-aminophenoxy)ethane-N,N,N',N'-tetraacetic acid
Caco-2	Colorectal adenocarcinoma
Cdc42	Cell division cycle 42
CHC	Clathrin heavy chain
CHO	Chinese hamster ovary
CI-MPR	Cation-independent mannose-6-phosphate receptor
CLCN5	Chloride channel 5 (nephrolithiasis 2, X-linked, Dent disease)
CMV	Cytomegalovirus
COS-7	CV-1 (simian) in Origin, carrying SV40 genetic material
C-terminal	Carboxyl terminal
DAG	Diacylglycerol

DAPI	4',6-diamidino-2-phenylindole
DCC	Deleted in colorectal cancer
DMEM	Dulbecco's Modified Eagle Medium
DNA	Deoxyribonucleic acid
dNTP	Deoxynucleotide Triphosphate
DSP	Dithiobis (succinimidyl propionate)
E-cadherin	Epithelial cadherin
ECL	Enhanced chemiluminescence
ECM	Extracellular medium
EDTA	Ethylenediaminetetraacetic acid
EEA1	Early endosome antigen 1
EGF	Epidermal growth factor
EGFR	Epidermal growth factor receptor
EGTA	Ethylene glycol tetraacetic acid
EMT	Epithelial-mesenchymal transition
ENTH	Epsin N-terminal homology domain
ER	Endoplasmic reticulum
F-actin	Filamentous actin
FAPP-2	Four-phosphate adaptor protein 2
FRAP	Fluorescence Recovery After Photobleaching
FSH	Follicle-stimulating hormone
FSHR	Follicle-stimulating hormone receptor
Gα12	G protein alpha subunit 12
GAP43	Growth-associated protein 43
GFP	Green fluorescent protein

Grp1	General Receptor for Phosphoinositides 1
GTPase	Guanosine triphosphatase
HCE	Human Corneal Epithelial
HeLa	Henrietta Lacks, cervical immortalised cancer cell line
HGF	Hepatocyte growth factor
HLE-B3	Human Lens Epithelial B3
Hrs	Hepatocyte growth factor regulated tyrosine kinase substrate
IgG	Immunoglobulin G
INPP5B	Inositol polyphosphate-5-phosphatase B
IP2	Inositol (1,4)-bisphosphate
IP3	Inositol (1,4,5)-trisphosphate
JRAB/MICAL-L2	Junctional Rab 13-binding protein/molecule interacting with CasL-like 2
LLC-PK1	Pig kidney epithelial cell line
MARCKS	Myristoylated alanine-rich C-kinase substrate
MDCK	Madin-Darby Canine Kidney
N-terminal	Amino-terminal
OCRL	Oculocerebrorenal Syndrome of Lowe
OSBP	Oxysterol binding protein
PAK	p21-activated kinase
Par 3	Partitioning protein 3
Par 6	Partitioning protein 6
PBS	Phosphate buffered saline
PCR	Polymerase Chain Reaction

PDGF	Platelet derived growth factor
PDZ	Post synaptic density protein (PSD95), Drosophila disc large tumor suppressor (DlgA), and zonula occludens-1
PFA	Paraformaldehyde
PH	Pleckstrin Homology
PI(3)P	Phosphatidylinositol 3-phosphate
PI(3,4,5)P3	Phosphatidylinositol 3,4,5-trisphosphate
PI(3,5)P2	Phosphatidylinositol 3,4-bisphosphate
PI(4)P	Phosphatidylinositol 4-phosphate
PI(4)P5K	Phosphatidylinositol 4-phosphate 5-kinase
PI(4,5)P2	Phosphatidylinositol 4,5-bisphosphate
PI3K	Phosphatidylinositol 4,5-bisphosphate 3-kinase
PIP	Phosphoinositide
PIPP	Inositol polyphosphate 5-phosphatase
PKA	Protein Kinase A
PKC	Protein Kinase C
PLC	Phospholipase C
PMCA	Plasma membrane calcium ATPase
POP	PLC∂-OSBP[EE]-PH
PTB	Phosphotyrosine binding
PTEN	Phosphatase and Tensin Homolog
PVDF	Polyvinylidene Fluoride
PX	Phox-homology
Rab	Ras-like protein in brain
Rac1	Ras-related C3 botulinum toxin substrate 1

RhoGAP	Rho GTPase activating protein
SCAR	Suppressor of cAR
SDS	Sodium Dodecyl Sulphate
SH2	Src Homology 2
SH3	Src Homology 3
SHIP	SH2 containing inositol 5-phoshatase
siRNA	Small interfering ribonucleic acid
SKICH	SKIP carboxyl homology
SKIP	Skeletal muscle and kidney enriched inositol phosphatase
SOC	Store-operated calcium
Star PAP	Nuclear speckle targeted PIPKIalpha regulated-poly(A) polymerase
STxB	Shiga toxin B-subunit
TCA	Trichloroacetic acid
TER	Transepithelial Resistance
TGN	Trans-Golgi Network
TGN46	Trans-Golgi Network protein 46
TrkA	Tropomyosin-Related Kinase A
VAP	VAMP-associated protein
VASP	Vasodilator-stimulated Phosphoprotein
VPA	Valproate
WASP	Wiscott-Aldrich Syndrome Protein
ZO-1	Zona occludens-1
ZO-2	Zona occludens-2

Chapter 1: Introduction

1: Introduction

Oculocerebrorenal disease of Lowe (OCRL), otherwise known as Lowe Syndrome, is an X-linked recessive disease that manifests in patients with in-born bilateral cataract, mental retardation and a selective proximal tubulopathy. The renal disorder in Lowe Syndrome is characterised by low molecular weight proteinuria and hypercalciuria, which eventually progresses to renal failure, commonly in the second decade. The disease gene, OCRL1, was discovered in 1992; its transcript encodes an inositol polyphosphate 5-phosphatase[1]. Thus, OCRL likely arises from an inborn error in inositol lipid metabolism, and this is one of very few hereditary diseases that directly link phosphoinositides to disease.

Phosphatidylinositol is an important cellular lipid, both as a key membrane constituent and as a participant in metabolic processes, a number of its metabolites being significant signalling molecules. Phosphatidylinositol is synthesised at the endoplasmic reticulum and is delivered to other membranes either by vesicular transport or via cytosolic phosphatidylinositol transfer proteins, where it can then be modified in a number of ways [2]. The inositol ring of phosphatidylinositol can be reversibly phosphorylated at positions D3, D4 and D5. The different combinations of which give rise to seven phosphoinositide isomers [3]. Interconversion of phosphoinositides through lipid kinase and lipid phosphatase activity occurs in a manner strictly regulated spatially and temporally.

The resulting abundancies of different phosphoinositide at distinct sites within the cell (Figure 1.1) can result in the recruitment, and thereby activation, of a wide array of different proteins important in regulating a variety of cellular processes [4-6]. Phosphoinositide binding domains respond to phosphorylation events occurring at the membrane, and respond to the temporal and spatial regulation of phosphoinositide levels [7]. Many proteins demonstrated to play important roles in a wide range of cellular processes such as membrane trafficking, cell signalling and cytoskeletal organisation have phosphoinositide binding domains that drive their recruitment to sites of activity or enzyme substrates [8, 9]. The best examples of modular domains that bind phosphoinositides are the well-studied Pleckstrin homology (PH), Phox homology (PX) and epsin N-terminal homology (ENTH) domain families [10]. In order to visualise where these lipids accumulate within the cell, many of these domains have been isolated, characterised for their phosphoinositide preference and expressed in cells as green fluorescent protein (GFP) chimeras [11]. This method of detecting where certain phosphoinositides are localised within the cell has revealed a very highly ordered cellular map, with different classes of phosphoinositide accumulating at specific membranes (Figure 1.1). For example, the PH domain of oxysterol binding protein (OSBP) has been used as a coincidence detector of Golgi PI(4)P. PI(4)P generation at the Golgi coordinates many events, such as vesicular trafficking from the TGN to the plasma membrane and modification of key lipids such as glycosphingolipids . Wang *et al.* demonstrated the importance of Golgi PI(4)P generation through their studies on PI4KIIalpha [12]. By specifically generating PI(4)P at the Golgi, the cell creates a signal to recruit clathrin adaptor AP-1.

Figure 1.1: Phosphoinositides and membrane identity

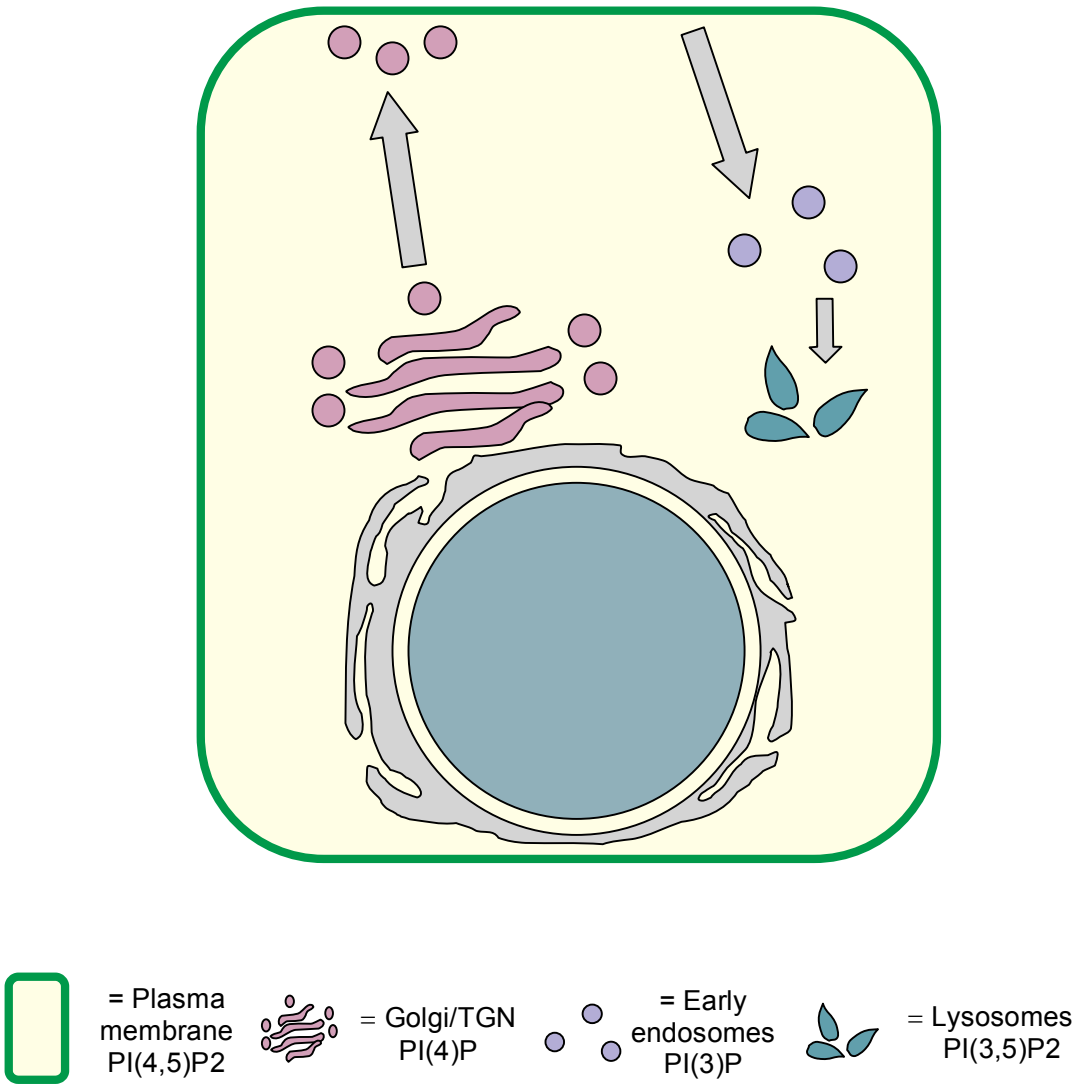

Legend

This diagram depicts a model whereby specific phosphoinositides preferentially accumulate at distinct organelles within the cell. For instance, the major pool of PI(4,5)P2 has been shown to be at the plasma membrane. However, there is also evidence of small pools of PI(4,5)P2 existing at different organelles, such as the Golgi and nucleus [13, 14]. PI(3)P has been shown to be enriched at early endosomes, and there is some evidence of

PI(3,5)P2 at the late endosome/lysosome [15-18]. Least convincingly fitting this model is PI(4)P. It has been shown that PI(4)P is highly enriched at the Golgi apparatus and plays multiple roles at this site [19-21]. However, there is some data showing that there is a pool of PI(4)P at the plasma membrane, presumably as a precursor to PI(4,5)P2 [22]. It is thought that the enrichment of these lipids at different organelles aids the recruitment of proteins to their desired site. These lipids have been shown to have a wide variety of roles, varying from PLC signalling (PI(4,5)P2) to the release of vesicles from the TGN (PI(4)P), discussed below.

This enzyme was shown to generate the majority of Golgi PI(4)P and without it, AP-1 fails to target the Golgi and AP-1 dependent post-Golgi events are inhibited. Another example of the importance of Golgi PI(4)P can be drawn from work carried out on the four phosphate adaptor protein-2 (FAPP-2). The PH domain of FAPP-2 has been used as a co-incidence detector for PI(4)P; when the ability of FAPP-2 PH to interact with phosphoinositides is disturbed, TGN to plasma membrane transport is inhibited [23]. The work with PI(4)P indicating it is more widely distributed than is commonly thought from simplistic assessment of results with a selected group of reporters, which are actually are more like co-incidence detectors, is a notion that is highly useful and applicable to PI(4,5)P2 as well. PI(4,5)P2 has classically been shown to be abundant at the plasma membrane through studies using the PH domain of phospholipase C delta (PLCδ-PH) [22, 24], but it may be that it has a wider distribution when methods do not involve coincidence detection [13]. The importance of PI(4,5)P2 abundance at the plasma membrane is described in detail later in the introduction. However, this section provides two examples of the significance of plasma membrane PI(4,5)P2. Firstly, it has been found that PI(4,5)P2 is required for the early and late events in formation of endocytic coated vesicles [25]. Furthermore, many signal transduction events work via receptor mediated PLC hydrolysis of PI(4,5)P2. In a recent study, it was shown that IP3-mediated signalling cannot occur when PI(4,5)P2 is depleted from the plasma membrane [26]. This was achieved utilising an artificial system whereby a recombinant inositol 5-phosphatase is recruited to the plasma membrane.

By contrast to 4-phosphorylated PIPs, phosphatidylinositol 3-phosphate (PI(3)P) has been demonstrated to be highly enriched at early endosomes and its levels and downstream signalling regulates proteins important in sorting endocytosed receptors from endosomes to lysosomes [27]. For example, PI(3)P-binding protein Hrs (hepatocyte growth factor regulated tyrosine kinase substrate) mediates endosomal sorting of growth factor receptors [28]. PI(3)P has also been shown to recruit a kinase that converts PI(3)P into PI(3,5)P2, named PIKfyve, an enzyme now shown to partake in multiple membrane trafficking pathways such as EGFR trafficking to the nucleus and exocytosis in neurosecretory cells [29, 30]. PI(3,4,5)P3 is present at very low levels in cells at rest. Upon many different stimuli, PI(3,4,5)P3 is generated at the plasma membrane through the actions of PI3K. PI(3,4,5)P3 engages in a variety of processes at the plasma membrane such as phagocytosis, regulated exocytosis, and cytoskeletal organisation [6, 31].

Responsibility of maintaining the identity and function of cellular membranes through the segregation of phosphoinositides falls on the shoulders of proteins able to modulate them; this can be through interconversion by phosphoinositide kinases and phosphatases, or by their hydrolysis through phospholipases [4, 32-34]. OCRL1 is a type-II inositol polyphosphate 5-phosphatase [35]. The acronym OCRL stands for Oculocerebrorenal syndrome of Lowe, an X-linked disorder. Pathological mutations in the OCRL1 gene invariably cause almost complete absence of OCRL1 protein and an elevation of its preferred substrate, PI(4,5)P2 [36].

OCRL1 has a central inositol 5-polyphosphate phosphatase domain that has been shown to be responsible for dephosphorylation of phosphoinositides and inositol phosphates at the D5 position of the myo-inositol ring [37, 38]. OCRL1 belongs to a family of ten mammalian 5-phosphatases (Figure 1.2) (four members expressed in yeast) that have been shown to have a wide range of functions, such as synaptic vesicle re-cycling, hematopoietic cell function and insulin signalling [33]. In order to appreciate where OCRL1 fits within this enzyme family, knowledge of the cellular roles played by other 5-phosphatases is required. A great amount of work has been carried out on other mammalian 5-phosphatases such as synaptojanin 1, synaptojanin 2, SHIP1 and SHIP2. 5-phosphatases identified more recently include SKIP and PIPP [39, 40]. However, there are many differences in function and activity, as well as differences in the expression pattern of this enzyme family. The full map of where these proteins act is not yet known, which causes difficulty in interpreting the level of redundancy between them. The clearest and most obvious level of redundancy can be found with studies comparing INPP5B and OCRL1. Knock-out INPP5B and OCRL1 mice are viable and have few abnormalities [41]. However, upon crossing mice deficient in OCRL1 to mice deficient in INPP5B, no live born mice were found. This demonstrates the high level of redundancy between these two proteins. The similarity between these proteins is discussed later. By definition, each member of this enzyme family contains a central conserved 5-phosphatase catalytic domain. The crystal structure of an archetypal 5-phosphatase has revealed the 5-phosphatases belong to the AP endonuclease family with a His/Asp active site pair [33].

Figure 1.2: The inositol polyphosphate 5-phosphatase family

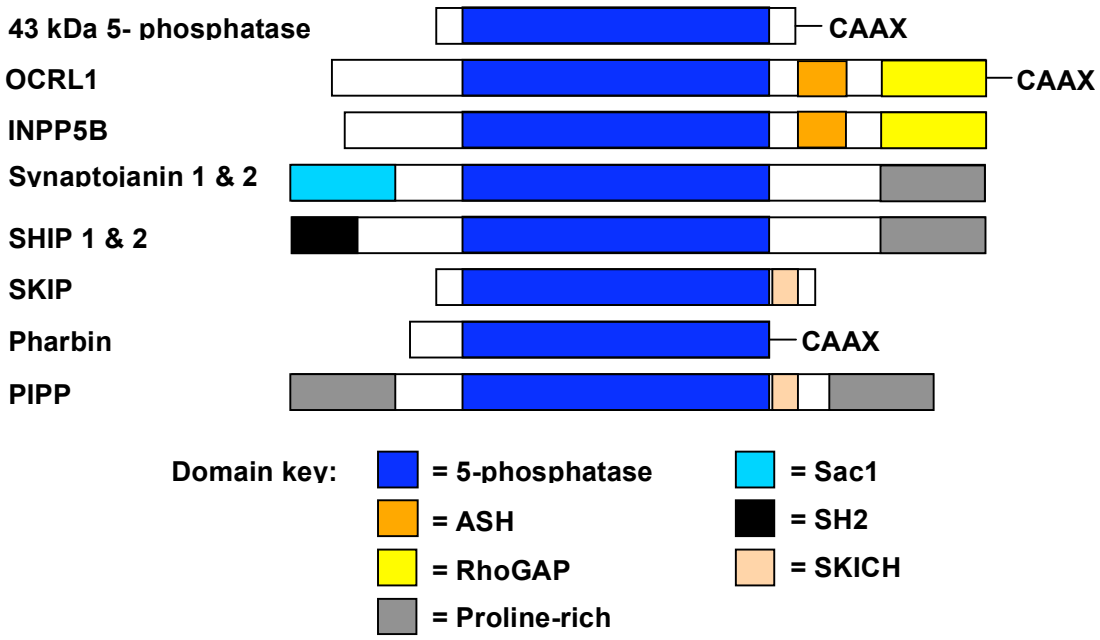

Legend

This diagram depicts the similarities and differences in domain structure between the inositol polyphosphate 5-phosphatase proteins, with the shared 5-phosphatase domain aligned to the centre. OCRL1 and INPP5B form a subfamily of 5-phosphatases with ASH and RhoGAP domains.

OCRL1 and another 5-phosphatase, INPP5B, differ from other family members by having a carboxy-terminal domain homologous to Rho-GTPase activating proteins (Figure 1.2). This domain has been shown to have no GTPase activity, but does regulate the ability of OCRL1 to bind various small GTPases, notably Cdc42 and Rac1 GTPases and ADP-ribosylation factor (ARF) family members ARF1 and ARF6 [42, 43]. A great number of the Rab family of small GTPases have also been shown to bind the OCRL1 linker region between the phosphatase domain and Rho-GAP homology domain [44, 45], now known to co-incide with the ASH (ASPM, SPD-2 and Hydin) domain. It is believed that binding to these small GTPases is the major driving factor in OCRL1 localisation to the trans-Golgi network (TGN) and the endosomal system [44, 46]. It has also been shown that OCRL1 translocates to the plasma membrane upon growth-factor stimulation in a Rac1-dependent manner [47]. Recently it has also been revealed that binding to GTP-locked Rab GTPases in vitro is sufficient to increase OCRL1 enzyme activity [44]. This suggests that OCRL1 recruitment to membranes containing these GTPases is synonymous with inositol polyphosphatase 5-phosphatase activation and is physiologically relevant to its function. These data suggest that the RhoGAP domain within OCRL1 is important in its recruitment to inositol polyphosphate 5-phosphatase substrates. These binding events may alter the conformation and activation of the full-length OCRL1 protein. The idea that overall protein structure is regulated by the ASH domain is supported by the observation that Lowe Syndrome patients express a wide spectrum of single amino-acid mutations within the ASH and Rho-GAP domains [48-50]. On either side of the central

inositol polyphosphate 5-phosphatase domain of OCRL1 are two motifs that co-ordinate binding to proteins important in clathrin-mediated endocytosis and membrane trafficking. These two short motifs within OCRL1, by single letter amino acid code: LIDLE and FEDNF, have been shown to mediate binding of OCRL1 to clathrin heavy-chain and the clathrin adaptor protein-2 (AP-2), respectively (Figure 1.3). Not only does OCRL1 bind these molecules but it has also been demonstrated *in vitro* to facilitate the formation of clathrin cages [51, 52]. Alternative splicing in an exon adjacent to the LIDLE motif of OCRL1 gives rise to two (one short and one long) isoforms of OCRL1. These isoforms arise due to tissue-specific splicing and differ by the presence or absence of a stretch of eight amino acids (EDSFLEKE), immediately downstream of the LIDLE motif. Both isoforms are expressed in all tissues, with the short isoform of OCRL1 the more abundant of the two [53]. The only exception to this arises in the brain, where only the long isoform is expressed. The significance of alternative splicing of OCRL1 and potential differences in the clathrin binding activity of each isoform has not yet been elucidated. INPP5B does not have clathrin binding motifs, but contains the same carboxy-terminal domains as OCRL1, such as the ASH and RhoGAP homology domain. INPP5B, unlike OCRL1, does however contain a carboxy-terminal CAAX box allowing it to be prenylated, thus increasing its affinity for membranes (Figure 1.3). However, the differences between OCRL1 and INPP5B proteins may not be functionally significant, as there is some evidence that the reason why Lowe syndrome affects only a few tissues is that INPP5B can compensate for it. This

Figure 1.3: Schematic of OCRL1 and INPP5B domain organisation

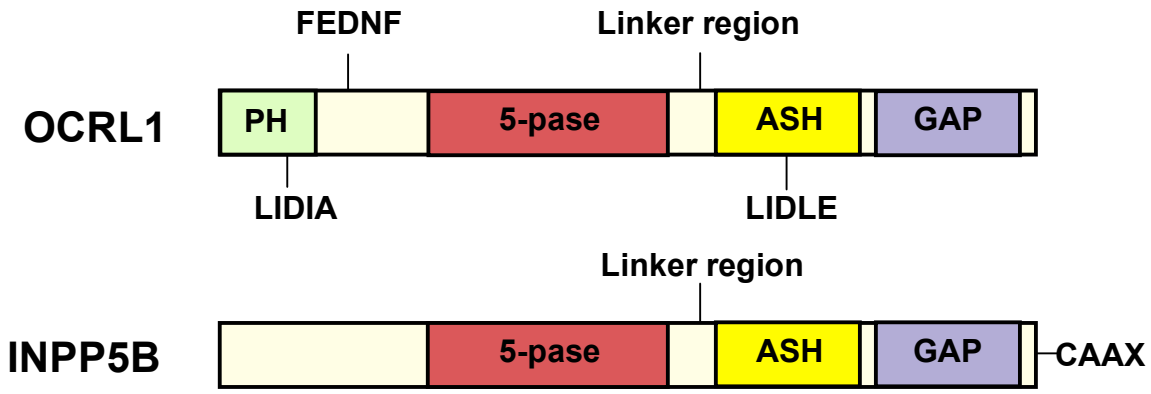

Legend

OCRL1 and INPP5B differ from the other eight 5-phosphatases by their carboxy-terminal domains with homology to Rho-GAPs. These domains do not have any GAP activity for GTPases. Nevertheless, this domain in OCRL1 facilitates binding to Rac1, Arf1, Arf6, and Cdc42 to a lesser extent, not being specific for the active forms [42, 43, 54]. The homologous domain in Inpp5b has not been studied in detail. The ASH domain in both proteins has been shown to facilitate binding to multiple Rab GTPases [44]. The overlap in specificity directs both phosphatases to early endosomes and the Golgi [52, 55]. The ASH and RhoGAP domains together of both OCRL1 and INPP5B bind to the endocytic adaptor APPL1 [54]. OCRL1 also has two motifs that interact with clathrin heavy chain (LIDLE and LIDIA), and one that binds to AP-2 (FEDNF), all these being absent from INPP5B [52]. An NMR structure has been reported for the extreme amino-terminal of OCRL1 by Prof. P de Camilli (Personal communication). This region apparently folds into a PH-like fold, but there is no electro-positive pocket, so binding to PIPs is highly unlikely.

mechanism is suggested by the work of Prof. R Nussbaum constructing a mouse model of Lowe Syndrome. While single knock-out of INPP5B or OCRL1 is viable, double INPP5B and OCRL1 knock-out in mice is lethal. This suggests that INPP5B complements the loss of OCRL1 in the mouse. To explain why INPP5B does not complement OCRL1 loss in humans, analysis of murine and human INPP5B reveals that the two genes differ in structure. There is alternative splicing at exon 7 of the murine INPP5B gene, leading to increased transcripts (though truncated at the 5' end). For this reason, work is currently being undertaken to "humanise" the 5-phosphatase pathway in mice by placing human INPP5B onto an INPP5B knock-out background and crossing this mutant with the OCRL1 knock-out mouse (personal communication, Prof. R Nussbaum).

Recently, data has shown that OCRL1 is recruited to late-stage, endocytic clathrin-coated pits and binds the Rab5 effector APPL1, on peripheral early endosomes [54]. Bioinformatics studies predicted that OCRL1 contained an ASH domain in-between its RhoGAP and 5-phosphatase domains [56]. This prediction has now been validated through structural studies of the interaction of OCRL1 with APPL1, involving the first determination of an ASH domain structure. The ASH domain was shown to have a super-immunoglobulin-like fold, similar to VAP. This interaction is mediated by the ASH and RhoGAP domains of OCRL1 and is abolished by described disease mutations [50, 54]. This study suggested that the interaction between OCRL1 and APPL1 provided links with protein networks that may be dysfunctional in Lowe Syndrome. The PTB domain of APPL1 binds directly cell surface receptors,

including DCC (deleted in colon cancer), adiponectin, FSH receptor, and TrkA [57-60]. It is possible that OCRL1 loss of function could affect one or many signalling pathways downstream of these receptors. For instance, activation of TrkA results in the generation of PI(3,4,5)P3 and the activation of AKT[61]. Interestingly, AKT has been found to be a binding partner of megalin, a protein shown to be less abundant in Lowe Syndrome patient urine [62]. It has been suggested before that abnormal recycling of megalin to the plasma membrane may be responsible for the abnormal protein reabsorption and proximal tubulopathy observed in Lowe Syndrome patients [63]. Furthermore, it has been suggested that abnormal TrkA (and other aforementioned receptors expressed in the brain) trafficking underlies the CNS defects exhibited by Lowe Syndrome patients. However attractive these models may be, it must be added that although OCRL1 translocates to clathrin-coated pits at the plasma membrane, this group observed no defect in endocytosis upon OCRL1 depletion in this studies. (Personal communication, Prof. P. de Camilli)

The confirmed localisations and binding partners of OCRL1 implicate a role in the regulation of membrane traffic, something of which was demonstrated by Choudhury *et al*. in 2005. In this study, defective trafficking of shiga toxin (STxB) from early endosomes to the TGN in cells over-expressing OCRL1 or a 5-phosphatase domain deletion mutant form of OCRL1 was demonstrated. OCRL1 depletion by RNAi results in redistribution of CI-MPR and TGN46, TGN-resident proteins, to early endosomes supporting the theory that OCRL1 regulates vesicular membrane traffic [52]. Whether this partial redistribution of

markers is PI(4,5)P2 dependent or independent is unclear. It is possible that the function of some membrane trafficking proteins may be regulated by changes in phosphoinositide levels due to OCRL1 loss. For instance, if Golgi PI(4)P is less abundant upon OCRL1 loss, it is possible that the previously described effects of loss of PI4KIIα function could be reproduced [12]. This general theory may prove to be true if OCRL1 activity is targeted to Golgi pools of phosphoinositides.

However, loss of OCRL1 may affect the normal function of proteins through PI(4,5)P2-independent mechanisms, such as scaffolding of other proteins, including small GTPases. The activity of proteins integral in regulation of TGN-to-endosome vesicular trafficking may potentially be altered by OCRL1 depletion. Trafficking of STxB is regulated by Rab6 [64]. It is possible that OCRL1 plays pivotal roles in the availability of Rab6, suggested by the finding that STxB trafficking is perturbed by over-expression of OCRL1 [52]. This may be a general mechanism for all small GTPases that bind OCRL1. Overall, effects may be a result of both PI(4,5)P2-dependent and PI(4,5)P2-independent mechanisms.

PI(4,5)P2- dependent mechanisms have been suggested to be responsible for an altered actin phenotype in Lowe Syndrome patient fibroblasts. As previously suggested, upon loss of OCRL1 function, PI(4,5)P2 may become elevated at sites OCRL1 is normally resident. PI(4,5)P2 has been shown to have dramatic effects upon the regulation of proteins instrumental in the organisation of the actin cytoskeleton such as gelsolin and proflin [65]. This

raises the possibility that dysregulation of PI(4,5)P2 levels at internal sites within the cell may be responsible for the actin phenotype in Lowe Syndrome patient cells. Fibroblasts from Lowe Syndrome patients have increased punctate actin staining that colocalises with actin-modulating proteins previously shown to bind or be activated by PI(4,5)P2. This punctate pattern of actin is concomitant with a loss of actin stress-fibres [66].

Whether PI(4,5)P2 accumulates at internal membranes after OCRL1 depletion is uncertain. The potential to generate PI(4,5)P2 at internal membranes is suggested by studies that show PI(4)P5K activity is present in isolated Golgi membrane fractions [67]. Furthermore, PI(4)P5Ks can be stimulated through ARF activity, linking levels of PI(4,5)P2 with vesicular trafficking [68]. However, the presence of PI(4,5)P2 at these internal membranes has not been shown directly, apart from one study by Watt *et al.* in 2002 (discussed later) [13]. There is an important question in analysing the cellular role of OCRL1: is it possible to accurately visualise the phosphoinositides with which it interacts and creates? The nature of the lipid molecule creates a problem; there is no perfect tool available to enable direct visualisation of endogenous lipids within the cell. This means that visualisation of subcellular sites of lipids is limited to the affinity and accuracy of fluorescent probes that can bind them. For example, GFP chimeras of the PH domain of PLCδ are used to visualise PI(4,5)P2, a phosphoinositide known to be highly abundant at the plasma membrane [11, 69]. However, the localisation of PLCδ-PH-GFP to the plasma membrane is due to PI(4,5)P2 head-group specific interactions in combination with an affinity for anionic environments at the

plasma membrane[70, 71]. This leads to confusion in interpreting the PLCδ-PH-GFP signal; localisation at the plasma membrane is not wholly driven by PI(4,5)P2 levels. The general affinity of PLCδ-PH-GFP for the plasma membrane means that visualising potential sites of PI(4,5)P2 elevation at the Golgi apparatus or endosomes upon loss of OCRL1 may not be possible, although previous work in yeast by Stefan *et al.* in 2002 demonstrated increases in PI(4,5)P2 upon inactivation of the cell's complement of synaptojanins, leaving no 5-phosphatase activity [72]. PI(4,5)P2 accumulated in intracellular compartments, reported through use of 2xPLCδ-PH fused to GFP. Interestingly, this study also revealed cellular phenotypes similar to those demonstrated in Lowe Syndrome patient fibroblasts and OCRL1 depleted cells. Synaptojanin-like protein inactivation led to a loss of organisation of the actin cytoskeleton and impaired clathrin mediated membrane traffic [72]. Loss of OCRL1 function and inactivation of the inositol polyphosphate 5-phosphatase domain of the synaptojanin-like proteins lead to similar cellular phenotypes. This suggests that a common PI(4,5)P2 mechanism is in place and warrants further investigation. As referred to earlier in this section, evidence of low levels PI(4,5)P2 at internal membranes has been demonstrated through immuno-electron microscopical analysis of on-section labelling with PLCδ-PH [13]. In this study, PLCδ-PH labelling of ultra thin cell sections verified the high abundance of PI(4,5)P2 at the plasma membrane. In addition to this, but to a lesser extent, PLCδ-PH was also detected on the Golgi stack, endosomes and in the nucleus. Potentially, this low level of PI(4,5)P2 on internal membranes is increased upon loss of

OCRL1 function. This shows that under some circumstances PLCδ-PH can detect PI(4,5)P2 on internal membranes.

OCRL1 and calcium handling

An alternative way of analysing the downstream effects of OCRL1 loss is by looking at the localisation of proteins that are known to either bind to or be activated by PI(4,5)P2. OCRL1 loss or depletion increases the substrate of members of the phospholipase C (PLC) family. This suggests there may be an effect upon second messengers downstream of it, namely inositol(1,4,5)-trisphosphate (IP3), 1,2-diacylglycerol (DAG) and calcium. Annexin A2 is a phospholipid binding protein known to share OCRL1 binding partners such as Rac1 and clathrin adaptor AP-2 [73, 74]. Annexin A2 also binds PI(4,5)P2 and membranes in a calcium-dependent manner [75-77]. These reports and the endosomal localisation of Annexin A2 suggest that it may have an important relationship with OCRL1. For these reasons, we have investigated Annexin A2 localisation upon OCRL1 depletion, with the hypothesis that Annexin A2 would translocate to sites of PI(4,5)P2 elevation in the presence of a hypothesised elevation in cytosolic calcium. A similar translocation of Annexin A2 occurs upon inactivation of the proton-chloride antiporter CLCN5, which makes it a candidate for an active participant in Lowe's syndrome [78].

The link between OCRL1 and CLCN5 was first established because mutations in CLCN5 lead to a condition known as Dent's Disease, which shares a very similar selective renal tubulopathy with Lowe Syndrome [79]. The similarity in the pathology of these patients is supported further by the finding

that 20% of patients with the Dent's phenotype have mutations in OCRL1, not in CLCN5. These data are suggestive of a single, shared pathophysiological mechanism in both CLCN5 -/- and OCRL1 -/- patients, and it is therefore plausible that Annexin A2 has a role in Lowe Syndrome [80].

From the above, it might be hypothesised that OCRL1 depletion has an effect on the PLC pathway. The hydrolysis of PI(4,5)P2 to second-messengers IP3 and DAG by members of the PLC family triggers the release of intracellular calcium stores and the recruitment of protein kinase C (PKC) to the plasma membrane, respectively [81, 82]. There are many possible effects that OCRL1 depletion may have on this process. Firstly, raised PI(4,5)P2 levels may cause an increase in the speed and amount of calcium release, by providing increased substrate availability for members of the PLC family. The Golgi apparatus has been shown to be a bona fide calcium store and can liberate calcium upon IP3 stimulation through endogenous IP3 receptors [83, 84]. If OCRL1 depletion leads to an elevation of PI(4,5)P2 at the Golgi, local PLC mediated PI(4,5)P2 hydrolysis may occur at this site [83]. This may affect the responsiveness of Golgi calcium stores. Other evidence for a potential increase in IP3 responses upon OCRL1 can be drawn from work carried out with synaptojanin-1. Over-expression of the synaptojanin-1 inositol polyphosphate 5-phosphatase domain has an inhibitory effect on calcium store release in response to ATP. This inhibition of calcium signalling coincided with GFP-PLCδ-PH being less associated with the plasma membrane [85]. In a similar study, rapid translocation of an inositol polyphosphate 5-phosphatase, closely related to OCRL1, to the plasma

membrane caused significant differences in calcium handling in COS-7 cells with rapid termination of calcium signals in the cytoplasm [26]. This was shown to be due to interference with the sustained generation of IP3, rather than a block of capacitative calcium entry. These data led to the hypothesis that when the opposite situation arises, as in Lowe Syndrome, with depletion of proteins with inositol polyphosphate 5-phosphatase activity, there may be an increase in IP3 responses.

Alternatively, there are well-described mechanisms by which depletion of OCRL1 may have a negative impact on calcium signalling. Studies have shown that PI(4,5)P2 inhibits the IP3 receptor. This raises the possibility that increased PI(4,5)P2 at sites apposing the IP3 receptor may inhibit the PLC signalling pathway [86]. In addition, PI(4,5)P2 has been shown to have positive and negative roles in many different channels and pumps integral to calcium signalling [87]. The overall sum effect of these interactions is hard to predict, but worth investigating further.

OCRL1 and intercellular junctions

As described earlier in the introduction, phosphoinositides build up in a specific spatial and temporal manner. This particular arrangement controls many cellular processes, such as aforementioned membrane trafficking and signal transduction. Phosphoinositides also regulate the formation and function of many different intercellular junctions. There is also a clear cross-talk between these processes, for instance, regulation of membrane trafficking can affect the formation of the tight junction, and recruitment of effector

proteins to the tight junction can affect certain signalling cascades. The complex regulation of these different processes is in some part controlled through generation and destruction of different phosphoinositides.

To date, cell biological studies of OCRL1 have tended to use non-polarised cells, most frequently fibroblasts [44, 52, 54]. However, Lowe Syndrome is a disease that manifests itself in polarised cell types such as epithelia and cells of the CNS. The key difference between polarised and non-polarised cell types is the presence of intercellular junctions. Because regulation of phosphoinositides is closely related to many aspects of intercellular junction activity, we believed that the inability to find a phenotype for OCRL1 loss might be a consequence of studying non-polarised cell types. For these reasons we felt a study of OCRL1 in polarised cell types was warranted to determine if there is a role for OCRL1 at intercellular junctions.

Junction biogenesis and maintenance

Eukaryotic cells have evolved to interact with one another through many different specialised junctions, the most studied and understood being adherens, tight and gap junctions. These junctions control a wide range of cellular processes such as cellular differentiation, signal transduction, apoptosis and proliferation [88, 89]. Gap junctions are specialised channels that connect the cytoplasm of two cells and allow various molecules and ions, such as IP3 and calcium, to pass in a regulated manner between cells [90, 91]. Gap junctions are composed of and defined by their structure: 6 homo- or heterotypic connexins are incorporated into connexons (or hemichannels), one provided by each neighbouring cell, which connect across the intercellular

space. These channels are important in cellular events such as electrical and metabolic coupling between cells, adhesion and tumor suppression [91]. Gap junctions can be linked to the pathological effects of OCRL1 loss in humans, as gap junction dysregulation can lead to cataract formation [92]. Adherens junctions are a specialised apical bridge between two epithelial cells, normally basally located in relation to the tight junction. They are defined by the presence of proteins such as cadherins and catenins and are thought to function as a bridge between the actin cytoskeleton and intercellular junctions [93]. Again, these junctions are integral to adhesion between cells and also provide the platform for signalling pathways and formation of other types of junction [88]. The other main type of junction between epithelial cells is the tight junction. These junctions form a physical barrier to diffusion of fluid and macromolecules and also function to couple cells together, and so can be used to define epithelia as leaky or tight, a definition based on the number of tight junction strands and ability to restrict fluid movement. These independent strands form a complex network that seals the apical membrane and blocks passage of solutes between cells. Proteins such as occludins and claudins characterise the tight junction. These proteins, like adherens junction proteins, also link the actin cytoskeleton between cells [93]. An important function of both tight and adherens junctions is to act as physical barriers within the membrane. These junctions serve to restrict the lateral movement of proteins within the membrane. This process of compartmentalisation along the apical-basolateral plane of the membrane is integral to cellular functions such as endocytosis, exocytosis and cell signalling.

Intercellular junction formation in mammalian epithelia occurs in a strict spatio-temporal manner. As cells make contact with one another, a “primordial adherens junction” is formed. Beneath the membrane, this structure is supported by filamentous F-actin, which later develops into a peripheral F-actin ring that plays a supportive and restrictive role, discussed in the later section entitled “Epithelial polarisation and the actin cytoskeleton”. After the formation of the primordial adherens junction, F-actin polymerisation occurs alongside the development of the tight junction, apical to the adherens junction [94-96]. These two types of junction then go on to mature fully and separately; this junctional maturation is supported by the underlying actin cytoskeleton and is aided by delivery of junctional components through vesicular trafficking (discussed later in the section entitled “Membrane trafficking”).

Upon maturation of these junctions however, the proteins are not stable and inert but continuously remodelled and active in many processes such as cell signalling and cell division, discussed in later sections. A few recent papers have highlighted the continuous and dynamic nature of junctional proteins harnessed the ability of fluorescence-recovery after photobleaching (FRAP) to investigate the movement of proteins in and out of the membrane. One of these studies, looking at the movement of three tight junction proteins, ZO-1, occludin and claudin-1, revealed that each had very different stabilities at the membrane [97]. Striking results show that approximately 70% of occludin is motile within the plane of the plasma membrane, and nearly 70% of ZO-1 moves dynamically between plasma membrane pools and intracellular pools.

However, 76% of claudin-1 is stable within the plasma membrane. These data revealed that the tight junction complex is rapidly and continuously remodelled in an energy-dependent manner, even when epithelia and intercellular junctions are “fully matured”. These data challenged the previously thought model of static, scaffold like-junctions. Furthermore, each protein analysed had a different mechanism of exchange at the tight junction, highlighting the dynamic and specific nature of junctional remodelling, even at time-points previously thought to be quite stable.

Epithelial polarisation and the actin cytoskeleton.

The cell cytoskeleton plays key roles in junction formation and the resultant polarisation of cells. The characteristic tall cuboidal shaping of polarised cells, displaying distinct apical and basolateral membranes, occurs partly as a result of cytoskeletal rearrangements. There are distinct differences and changes in cytoskeletal elements that occur during intercellular junction formation. The cell contains three main kinds of cytoskeletal filaments, which are microfilaments (e.g. actin), intermediate filaments (e.g. vimentin/keratin), and microtubules (e.g. α-tubulin). These cytoskeletal filaments provide the cell with structure and shape. Of these, actin microfilaments have been linked to OCRL1 cell biology, but to-date only in non-polarised skin fibroblasts from Lowe Syndrome patients. In one of these studies, it was shown that Lowe Syndrome fibroblasts show a much-reduced number of actin stress fibers or bundles and some small punctate vesicular actin at perinuclear regions of the cell [66]. Also, in a recent study by our group and that of Prof, SE Moss, we have shown that this “vesicular” actin takes the form of an actin “rocket” or

“comet”, an elongated, arborescent form of actin that propels a vesicle through the cytoplasm. Actin rockets form in Lowe Syndrome patient fibroblasts at rest [98, 99], which is a sign of increased actin polymerisation. The presence of actin rockets in Lowe Syndrome fibroblasts might be caused by increased PI(4,5)P2, and so, possibly ties in with OCRL1 loss [100].

Actin has key roles in junction formation and also in the maturation of epithelia from large flat cells to tall cuboidal cells [101]. The polarisation of epithelia is thought to occur in a specific sequence of events. At early stages of polarisation, it is thought that actin is recruited to junctions in order to restrict movement of proteins out of and within the plane of the membrane. By doing so, the specific spatial (namely apical to basolateral) ordering of junctional components is established. In the later stages of polarisation, peripheral circular actin bundles play a supportive, protective and active role in cell shape and are co-incident with cell-cell junctions.

There are two very good examples of the importance of actin at cell-cell contacts in polarised cell types. The first is demonstrated by a mammalian study showing two distinct pools of filamentous actin that are dynamically altered upon cell-cell adhesion: a continuous line of junctional actin and peripheral thin bundles [102]. These two types of actin filaments differ in their actin dynamics, mode of formation and have distinct roles in the polarisation process. This “two-pool” theory has recently been corroborated in a different model, looking at epithelial development in Drosophila embryogenesis. In this recent study, the relationship between E-cadherin and actin was assessed

[103]. At intercellular contacts, cells concentrate E-cadherin and in perijunctional regions F-actin is accumulated. However, there is a different level of complexity in that E-cadherin is not distributed uniformly in cell–cell contacts. E-cadherin is shown to concentrate in discrete spots or clusters thought to be “spot-adherens” junctions. Using FRAP and photoactivation techniques, clustered E-cadherin was shown to be much more stable than the E-cadherin found at perijunctional regions of the cell. Like the earlier study described, there seemed to be a similar “two-pool” mechanism in place, where different forms of actin may differentially regulate different pools of junctional components such as E-cadherin. It was found that the clustered E-cadherin was stable despite perijunctional actin disruption with injected latrunculin A, which inhibits actin filament assembly, or in mutant flies that have a fragmented junctional actin network. Interestingly, latrunculin A treatment caused this clustered E-cadherin to become much more mobile within the membrane. In contrast, lateral mobility of E-cadherin was decreased through expression of proteins that promote actin assembly, such as Wiscott-Aldrich Syndrome protein (WASP), a protein that is regulated by PI(4,5)P2. These findings suggest a model whereby a dynamic pool of junctional actin restricts the movement of stable cadherin clusters. It seems that there is a relatively stable pool of actin filaments in close proximity to the E-cadherin clusters as well as a dynamic pool at intercellular contacts. This evidence adds weight to the view that different pools of actin differentially control specific maturational events junctions.

In sum, OCRL1 loss has a dramatic effect on the actin cytoskeleton in non-polarised fibroblast cells. There is added complexity within the actin cytoskeleton of polarised cells. This means that a previously unseen effect of OCRL1 loss may be revealed in a polarised cell type. Furthermore, OCRL1 contains a Rho-GAP homology domain at its carboxy-terminus, known to bind Cdc42 and Rac1. The role of the Rho GTPase family and the actin cytoskeleton is well characterised. OCRL1 binding to Cdc42 and/or Rac1 may lead to unanticipated changes in the way they regulate actin at intercellular contacts. For example, studies in MDCK cells using constitutively active and dominant negative mutants of Rho, Cdc42 and Rac1 revealed that these proteins have a high potential to interfere with specific functions localised to the tight junction [104, 105]. Clathrin-dependent endocytosis (which involves OCRL1) is highly dependent upon dynamic changes in actin polymerisation at the plasma membrane. If OCRL1 had a specific role at junctions, it is possible that OCRL1 partakes in clathrin-mediated endocytosis of junctional proteins, which would not be observed in non-polarised cells. In support of this, adherens and tight junction proteins such as E-cadherin and occludin are internalised in a clathrin-dependent manner [106]. These findings suggest that an investigation of OCRL1 and the actin cytoskeleton in polarised cells is warranted.

Membrane trafficking in polarised cells

To maintain the functionally and structurally different plasma membranes in a polarised cell, junctional and polarity proteins must be trafficked selectively to

their correct and desired sites. The maintenance of apico-basolateral polarity requires the activity of membrane trafficking proteins to sort proteins from endocytic and biosynthetic origin [88].

Of the many classes and types of proteins important in membrane trafficking, one of the largest and most important is the Rab family of small GTPases [107, 108]. A recent study has shown that OCRL1 has extremely broad binding specificity for the Rab GTPases [45]. Of the many Rab proteins that bind OCRL1, there is some evidence that two specific Rab GTPases are vital to trafficking of junctional proteins to the plasma membrane. Rab 8 has been shown to play an *in vivo* role in the localisation of apical membrane and junction proteins [109, 110]. Another member of the Rab GTPase family, Rab 13 has been shown to localise to the tight junction [111]. Interestingly endogenous Rab 13 localises to intracellular vesicles in non-polarised CHO cells. However, when in polarised cell types such as Caco-2 and LLC-PK1, the protein is very specifically localised to the apical plasma membrane, at the level of the tight junction as shown by strong colocalisation with ZO-1. In this same study, the junctional localisation of Rab 13 was also confirmed in frozen intestinal sections from mouse [112].

While Rab 13 has a role outside polarisation, regulating membrane trafficking of proteins between the TGN and endosomes in MDCK cells, it was shown that Rab 13 mutants inhibit specific surface delivery of cargo proteins to apical and basolateral membranes [113]. Moreover, upon over-expression of dominant-active Rab 13, not only is the structure of the tight junction affected, but

functional read-outs of tight junctional integrity such as trans-epithelial resistance and measurement of fence function are greatly disturbed [111]. This causes a delay in tight junction formation, which the authors propose to be due to impaired endocytic recycling of tight junction proteins such as claudin-1 and occludin. These data are verified by work showing that Rab 13 mediates the continuous trafficking of occludin in and out of the membrane [114]. This was shown by partial colocalisation of vesicular, endocytosed occludin with endogenous Rab 13. Furthermore, this study showed that over-expression of constitutively active Rab 13 caused the specific and striking movement of occludin to intracellular vesicles.

Another example of the importance of membrane trafficking proteins in junction formation can be drawn from a study assessing the roles of JRAB/MICAL-L2 in adherens and tight junction formation. JRAB/MICAL-L2 is a cytoplasmic protein that binds to both Rab 8 and Rab 13 and regulates the endocytic recycling of tight junction proteins occludin and claudin-1 [115]. Interestingly, depletion of JRAB/MICAL-L2 and expression of its Rab 13 binding domain inhibited traffic of occludin and claudin-1, but also traffic of adherens junction protein E-cadherin [109]. Knockdown of Rab 8 also caused impaired trafficking of E-cadherin in this study. Given the theory that the polarised tissues affected by OCRL1 loss (lens, kidney, neurons/glia) are uncompensated for by its homologue INPP5B, one extremely interesting observation is that OCRL1, but not INPP5B, binds Rab 1 4, which regulates specific apical targetting in polarised cell types [44, 55, 116]. The difference in Rab binding may be important, despite the hypothesis that OCRL1 and INPP5B

are redundant (discussed above), as this latter hypothesis has yet to be tested fully. Altogether, these findings provide possible molecular pathways by which OCRL1 might regulate junctional activities.

The trafficking of proteins to their desired locations serves to place them at their sites of activity. Previous studies, discussed above, describe how altered activity of Rab 13 causes a plethora of defects in tight junction assembly and function. Interestingly, this happens due to a cross talk between membrane trafficking and signal transduction. Constitutively active Rab 13 causes the inhibition of VASP phosphorylation by protein kinase A (PKA) in polarised cell types [117]. This is thought to be due to Rab-GTP binding to VASP, and perhaps leading to it being sequestered away from the tight junction. Interestingly, restoration of tight junction structure was achieved upon stimulation of PKA signalling by forskolin, emphasising the importance of trafficking and activity of signalling proteins in tight junction function. The importance of cell signalling at the junction is the topic of the next section.

Cell signalling derived from cell-cell junctions

The cytoplasmic face of intercellular junction complexes provides a scaffold by which cell-cell interaction and related activities at junctions feed back to many different signalling pathways that regulate cellular processes such as cell differentiation and proliferation [88, 118]. Due to the multitude of different pathways downstream of intercellular junctions, this section will concern itself with signalling to and from tight junctions, and will suggest the most likely pathways within which OCRL1 may function.

OCRL1 is a phosphatidylinositol polyphosphate 5-phosphatase, with a preference for dephosphorylating PI(4,5)P2 [119]. Apart from its roles in recruiting proteins to its sites of existence, PI(4,5)P2 is also a signalling lipid. PI(4,5)P2 can be converted into two second messengers, inositol (1,4,5)-triphosphate and phosphatidylinositol (3,4,5) triphosphate, through the actions of phospholipase C (PLC) and phosphatidylinositol 3-kinase (PI3K), respectively. These second messengers have been shown to be important to the function, maintenance and structure of tight junctions. Given the localisation of these lipids to junctions, and that enzymes that act upon them, such as PLCβ3, bind to junctional proteins, there are many avenues to investigate [120]. For instance, the tight junction protein ZO-1 is a scaffolding protein for Gα12 [121]. Through binding to the SH3 domain of ZO-1, Gα12 may co-ordinate signalling events downstream of the tight junction such as PLCε hydrolysis of PI(4,5)P2 [122]. If levels of PI(4,5)P2 at tight junctions are regulated by OCRL1, downstream effects such as the barrier function and viability of tight junctions may be affected. This is discussed further in the section, “Intercellular junctions and phosphoinositides”

As mentioned earlier, there are a wide number of signalling proteins that are linked to OCRL1 function by virtue of their ability to bind APPL1 [58-61]. It has been shown that changes in phosphoinositide levels or localisation affect the formation of junctions and the cell polarisation process [123]. If OCRL1 contributes to the strictly controlled apico-basolateral segregation of phosphoinositides, either PI(4,5)P2 or PI(3,4,5)P3, then it may play a role in

cell polarisation. It is also possible that in a polarised context, the ability of OCRL1 to dephosphorylate PI(3,4,5)P3 may become significant [119]. Finally, loss of OCRL1 may also affect, directly or indirectly, the shuttling of APPL1 in and out of the nucleus. If this were to occur, a pathway that regulates proliferation via APPL1 and Rab 5 may become dysregulated [124] .

Intercellular junctions and phosphoinositides

Several aspects of junction formation and regulation may feasibly require OCRL1. The potential ability of OCRL1 to dephosphorylate PI(4,5)P2 at intercellular junctions has many possible outcomes. One study has shown PI(4,5)P2 is important in gap junction communication [120]. PI(4,5)P2 is highly enriched at the plasma membrane. Through use of a novel regulated system, in which a 5-phosphatase domain highly homologous to the OCRL1 5-phosphatase domain is forcibly driven to the plasma membrane, the functions of PI(4,5)P2 at gap junctions was investigated. Using this system, it was found that depletion of PI(4,5)P2 was sufficient to close connexin 43 channels. However, when PI(4,5)P2 levels were restored through overexpression of PI(4)P5-K, this effect was attenuated. Furthermore, overexpression of PI(4)P5-K alone, reduced closure of connexin 43 channels. These data are supported by the fact that PI(4)P5-Kγ localises to adherens junctions in A431 epithelial cells [125]. Worthy of note, PI(4)P5-Kγ localisation to the junction, much like the previously described localisation of Rab 13, only occurs in polarised cell types, but is vesicular and cytoplasmic in non-polarised cell types. This work demonstrated a key role for levels of PI(4,5)P2 in the gating

of connexin channels. However, these findings were rather crude, in that they force the event of PI(4,5)P2 generation or depletion.

The physiological significance of these studies was inferred when it was shown that connexin 43 binds to the tight junction protein ZO-1, bringing with it the PI(4,5)P2 lipase, PLCβ3. PLCβ3, when activated through stimulation of Gαq, inhibited gap junction communication [120]. Interestingly, knock-down of ZO-1 mediated defects in gap junction communication, but had no effect on agonist induced calcium responses. This result may suggest that the interaction between ZO-1 and PLCβ3 is not significant to levels of PI(4,5)P2 at the junction, but simply an effect upon gross connexin 43 biology. The authors propose that this complex represents an endogenous system of regulating PI(4,5)P2 levels at gap and presumably tight junctions. Although the effect of PI(4,5)P2 depletion, through a number of methods, was shown to inhibit gap junction communication, the significance of PI(4,5)P2 depletion upon tight junction read-outs was not assessed. However, evidence for a role for PLCβ at tight junctions can be drawn from a study by Ward *et al.*, where the activity of PLCβ is shown to be directly linked to the permeability function of tight junctions in MDCK cells [126]. In this study, it was shown that the activity of PLCβ causes changes in the underlying actin cytoskeleton and that this modulation altered the permeability of tight junctions. Given that ZO-1 also co-ordinates and binds actin, the existence of this complex is highly possible. This change in the actin cytoskeleton may alter other properties of the tight junction as well. A previously mentioned study in Caco-2 cells supports this theory, in demonstrating that PLCγ activity is the component that confers

EGF-mediated protection of tight junctions treated with acetaldehyde [127]. This activity was closely related to association of F-actin at junctional interfaces. The roles of PI(4,5)P2 activity and its effects on the actin cytoskeleton, in concert with proteins such as WASP, profilin, GAP43, MARCKS and Rac1 are well documented [100, 128-130]. Should OCRL1 be key to formation and function of this complex, or even located within it, another potential method for removal of PI(4,5)P2, and its many downstream functions including closure of gap junctions can be envisaged.

There is also pre-existing evidence for another inositol 5-phosphatase, SHIP-1, in regulation of cell-cell junctions. SHIP-1 functions as a 5-phosphatase to PI(3,4,5)P3, the product of PI3K activity. Overexpression of SHIP-1 in MDCK cells leads to a phenotype that resembles an epithelial to mesenchymal transition (EMT) [131]. During EMT, epithelial cells lose contact with one another in a monolayer and adopt more motile and independent behaviour, much unlike the nature of epithelial cells. Cells overexpressing SHIP-1 lost cortical actin, developed stress fibers and became highly motile. Upon over-expression of a phosphatase-null mutant of SHIP-1, these phenotypes were not observed. However HGF stimulation, which induces EMT-like behaviour in normal, untransfected MDCK cells, did not cause EMT expressing this mutant. This is another piece of work that is highly suggestive of a role for phosphoinositides at intercellular junctions.

Other junctional proteins, especially those containing PDZ domains, have strong links to phosphoinositides. Two studies, one looking at syntenin and

the other, looking at Par proteins and other PDZ containing proteins reveal that PDZ domains have a high affinity for phosphoinositides [132, 133]. Interestingly, many PDZ domains, including at least one in each of ZO-1, Par 3 and syntenins bind PIPs. In a recent paper by Wu *et al.*, these domains are suggested to be phosphoinositide signalling integrators [132]. Much like pleckstrin homology domains, PDZ domains seem to be modules that recognise a combination of phosphoinositide and protein. However, the high occurrence of PDZ domains in junctional proteins is suggestive that phosphoinositides are integral to their function [134]. This is further highlighted by an experiment where the second PDZ domain of Par3, which binds phosphoinositides, is shown to be required for epithelial cell polarisation. In a very neat model, it is shown that Par3 also binds to PTEN through its third PDZ domain. By doing so, Par 3 integrates the signalling action of PTEN activity on PI(3,4,5)P3 to generate PI(4,5)P2, thus facilitating its binding to the membrane [132]. Syntenins are interesting examples of junctional proteins with PDZ domains that bind to PI(4,5)P2. Syntenin-1 interaction with PI(4,5)P2 has been shown to be important in receptor cargo recycling whereas syntenin-2 has been found to play a role in organisation and localisation of PI(4,5)P2 to nuclear speckles [21, 133].

Many proteins, designated to be junctional in localisation, actually shuttle between the nucleus and junction [135]. It is now well established that PI(4,5)P2 exists in nuclear speckles within the nucleus, at sites involved in pre-mRNA processing [14, 136]. In addition to syntenin-2, ZO-1 and ZO-2 have also been found to target nuclear speckles and their PDZ domains have been shown to

interact with phosphoinositides [132, 137, 138]. The full physiological extent of nuclear PI(4,5)P2 has not yet been elucidated, however for a long time nuclear speckles and the PI(4,5)P2 were thought to regulate the expression of specific mRNAs [139]. This has been verified recently through regulation of a poly(A) polymerase, Star PAP [140]. Nuclear speckles containing PI(4,5)P2 have previously been found to co-localise with pre-mRNA splicing factors, but the significance of this colocalisation had not been found. The existence of nuclear PLCβ has also been established and characterised. So far, only SHIP-2 has been found to be localised to nuclear speckles, but it is not clear if this is the only 5-phosphatase active on nuclear PI(4,5)P2 [141].

One of the most recent and important findings was that of Martin-Belmonte and colleagues, in which they demonstrate the importance of segregation of PI(4,5)P2 and PI(3,4,5)P3 between apical and basal membranes, respectively, in 3D MDCK culture [123]. Previous work had shown the necessity of PI(3,4,5)P3 in formation of the basolateral plasma membrane, but now it seems that this concentration of basolateral PI(3,4,5)P2 is only important relative to apical PI(4,5)P2 [142]. Phosphoinositide segregation is brought about through specific recruitment of PI(3,4,5)P3 3-phosphatase, PTEN, to apical membranes. PTEN recruitment causes the generation and concentration of PI(4,5)P2 at apical membranes, which in turn recruits Annexin A2, a calcium and PI(4,5)P2 binding protein with actin polymerisation activity. Annexin A2 recruits the RhoGTPase Cdc42 to the apical membrane, where presumably both proteins act in concert to facilitate the subapical actin remodelling required for lumen formation characteristic of MDCK 3D cysts [123].

Furthermore, apical localisation of Cdc42 brings aPKC/Par6 to the apical surface, establishing the polarity of the MDCK cyst. This paper highlights that PI(4,5)P2, the preferred substrate of OCRL1, is a key determinant of the apical plasma membrane. Interestingly, the segregation of phosphoinositides seems to be a conserved model for polarity between species, as regulated PTEN activity and localisation is also shown to be required for apical membrane morphogenesis in Drosophila photoreceptor epithelial cells [143]. Furthermore, the demonstration of apical to basolateral segregation of PI(4,5)P2 and PI(3,4,5)P2 adds to the view that phosphoinositides are general determinants of membrane identity. Should OCRL1 play a role in reducing the levels of PI(4,5)P2 at either the apical or basolateral membrane at key stages of cyst formation, a phenotype related to the organisation of junctions and epithelial polarity may become apparent upon OCRL1 loss. This may occur through increased levels of PI(4,5)P2 at either membrane, causing mistargetting of PI(4,5)P2-binding proteins. On the other hand, the excess PI(4,5)P2 may be converted to PI(3,4,5)P3 by PI3K family members at aberrant sites, perhaps uncompensated by PTEN activity. Testing for a role for OCRL1 in this model system would be quite appealing if evidence for OCRL1 at junctions were to be found.

This thesis comprises of three chapters of results. In Chapter 3, I will present data from experiments testing changes in PI(4,5)P2 upon OCRL1 depletion. To do this, we have created a construct that seeks to target PLCδ-PH to internal membranes, and possibly redistributes from the plasma membrane to intracellular sites of PI(4,5)P2 elevation. We have also investigated whether

endogenous Annexin A2, a known PI(4,5)P2 binding protein, translocates upon OCRL1 depletion. In Chapter 4, data will be presented from work assessing the effect of depletion of OCRL1 on the PLC pathway and intracellular calcium handling. Finally, in Chapter 5 work on OCRL1 in polarised cells will be presented. In this chapter we provide evidence for a potential new site for OCRL1 activity- intercellular junctions, and a novel binding partner, tight junction protein zona occludens 1 (ZO1).

Chapter 2:
Material and methods

2: Materials and Methods

Materials and antibodies

All materials were obtained from Sigma unless otherwise stated. Sheep polyclonal antibody against OCRL1 was a kind gift from Dr. Martin Lowe. Rabbit anti-ZO-1 was a kind gift from Prof. Karl Matter. Mouse anti-E-cadherin was a kind gift from Dr. Patric Turowski. Transferrin-alexa 555, donkey anti-sheep HRP, mouse anti-sheep CY2, mouse anti-sheep CY3 and mouse antibody to EEA1 were kind gifts from Dr. Clare Futter. Anti-Annexin A2, donkey anti-mouse CY3, TRITC- and FITC-phalloidin were a kind gift from Prof. Stephen Moss. Sheep polyclonal anti-TGN46 was a kind gift of Dr. Vas Ponnambolam.

Molecular biology

Plasmids: EGFP-OCRL1 (Isoform b, 893 amino acids), EGFP-INPP5B (a kind gift from Dr. Martin Lowe), GFP-AKT-PH, GFP-Grp1-PH (a kind gift from Dr. Tamas Balla).

GFP-POP consisted of the CMV immediate early promoter, followed by GFP, the first 175 amino acids of rat PLC∂1 which include its PH domain, a linker (GAGARS) then the PH domain of human OSBP (residues 87-185) carrying R109E and R110E mutations and followed by KNS*. POP was derived from a

similar construct containing two copies of the mutated PH domain of OSBP (pTL352, ref [144]), replacing the last 150 base pairs of GFP and first of these PH domains with the analogous sequence from GFP-PLC∂ PH (pTL335 ref [144]) from a PCR product using CAAAATACTCCAATTGGCG (19mer 5'→3', within GFP) and GGGAAGATCTAGCTCCTGCACCCTGGATGTTGAGCTCC-TTC (43mer 3'→5', coding for linker and the last 19 base pairs of the PLC∂1 PH domain). The PCR product was digested with Mfe1 and Bgl2, inserted between these sites in the vector, and checked by sequencing.

OCRL1 amino-terminus-GFP consisted of the first CMV immediate early promoter, followed by GFP, and then the first 501 amino acids of OCRL1 which include its PH-like domain and half of the inositol 5-phosphatase domain. This construct was created through digestion of GFP-OCRL1 (a gift from Dr. Martin Lowe) with restriction enzymes EcoRI and SmaI.

OCRL1 carboxy-terminus-GFP consisted of the first CMV immediate early promoter, followed by GFP, and then the amino acids 501 to 893 of OCRL1 which include half of the inositol 5-phosphatase domain, ASH domain and RhoGAP homology domain. This construct was created through digestion of GFP-OCRL1 (gift from Dr. Martin Lowe) with restriction enzymes EcoRI and BspEI, followed by addition of Klenow enzyme and dNTPs to the restriction mixture, to fill-in the over-hanging sticky-ends.

GFP-POP with a *PHO5* promotor was created for visualisation within yeast. This was created by digestion of *PHO5*>GFP-Scs2/VAP chimera[145] with MfeI

and Sac2 and insertion of POP sequence from CMV>GFP-POP, also digested with MfeI and Sac2.

Mammalian cell culture and transfection

HeLa, Caco-2, MDCK and primary porcine retinal epithelial cells were grown at 37ºC and 5% CO2 in DMEM containing 10% foetal calf serum (FCS), 100µg/ml streptomycin and 100µg/ml penicillin (regular medium). HLE-B3 cells were grown at 37ºC and 5% CO_2 in MEMα containing 20% FCS supplemented with 2mM glutamine, 100µg/ml streptomycin and 100µg/ml penicillin. Lowe Syndrome patient skin fibroblasts, designated Lowe B and Lowe 2 were a kind gift from Dr. William O'Brien, University of Texas Medical Branch . Lowe B and Lowe 2 cells were cultured at 37ºC and 5% CO2 in DMEM containing 20% foetal calf serum (FCS), 100µg/ml streptomycin and 100µg/ml penicillin.

For visualisation of GFP-tagged constructs, cells at 70-80% confluence were transfected with 0.4µg plasmid DNA in 35mm glass bottom dishes (MatTek Corporation) with 10µl Lipofectamine 2000 (Invitrogen). DNA/lipofectamine complexes were made in serum-free conditions and incubated with cells in 2ml regular medium. After 6 hours of incubation, cells were washed with PBS and replaced in regular medium overnight. GFP-tagged constructs were analysed 24 hours after transfection.

Yeast cell culture

Wild-type or deletion strains were obtained from freezer stocks of the yeast deletion collection (Mat a, based on parental strain BY4741). Yeast were grown overnight at 30 °C and on the day of experiment, split back to log phase of growth then examined with a confocal microscope system (AOBS SP2; Leica) at room temperature (63x NA 1.4 objective) using LCS software (Leica) for acquisition.

RNAi interference

Cells were transfected according to manufacturer's instructions. Briefly, non-targetting, Allstars negative control siRNA (Catalogue number 1027281, Qiagen), Annexin A11 siRNA sequence CUGCCGAAUGCCGUUCCUA (Qiagen), which has shown to be defective (Dr. Rebecca Longbottom, UCL Institute of Ophthalmology, personal communication) or pooled OCRL1 siRNA sequences CUUUCCGGUACCUUCGUUCUU, AAAGCCUUAGUCUUCUUC-GUU, UUUGAUGAGACCCUCCCGCUU, UAUCGACACUGAUCCUUUCUU (SmartPool, Dharmacon) were made into complexes with 5μl Oligofectamine (Invitrogen) in serum-free medium. Oligofectamine/siRNA complexes were added to cells grown to 40-50% confluence in 2ml regular medium minus penicillin/streptomycin on 35mm glass bottom dishes (MatTek Corporation). Cells were treated twice with siRNA, at 24 hours and 48 hours then left for a further 24 hours in regular medium to recover. Cells treated with siRNA for calcium experiments were treated only once with siRNA, at 24 hours. Final siRNA concentrations were 100nM and cells were analysed either 48 hours (in some calcium experiments) or otherwise 72 hours post-transfection.

Percoll based sub-cellular fractionation

Cells grown to approximately 90-100% confluence in 35mm tissue culture dishes were washed twice with HBSS followed by trypsinisation and re-suspension in complete medium. Cells were centrifuged at 100 x g and resuspended in 1ml homogenisation buffer (10mM HEPES, 200mM sucrose, 3mM imidazole, pH 7.2). Cells were homogenised by passing the samples through a ball-bearing homogeniser set with a clearance of 10μM x 20 times. An in situ gradient was formed by mixing the 1ml homogenate with 5ml 36% Percoll solution in homogenisation buffer to form an average density of 1.08g/ml. Samples were centrifuged at 50,000 x g for 90 minutes in a S80 AT3-0051 rotor (Sorvall RC M150 GX). The resulting gradient was then split into 6 x 1ml aliquots. Triton X-100 (final 1%) and EGTA (5mM) was added to each aliquot and mixed. Samples were centrifuged at 100,000 x g for 120 minutes and the supernatant removed. Protein in the supernatant was precipitated by addition of an equal volume of acetone and left on ice for 10 minutes. Samples were then centrifuged at 16,000 x g at 4ºC. The resulting supernatant was aspirated and precipitated protein was re-suspended in boiled 2x sample buffer.

Immunoprecipitation

Cells were washed three times in PBS. In cases where DSP was used to cross-link proteins, cells were incubated for 30 mins in 1mM DSP in cross-

linking solution (10mM triethanolamine, 250mM sucrose, 2mM $CaCl_2$, pH 7.4) at room temperature. Cells were then washed three times for 15 mins in blocking solution (10mM triethanolamine, 250mM sucrose, 2mM $CaCl_2$, 50mM ethanolamine, pH 7.4) at room temperature. Cells were then scraped, centrifuged at 1,000 x g and re-suspended in 250μl lysis buffer (10mM HEPES, 142.5 mM KCl, 0.2% NP-40, 2.5mM sodium pyrophosphate, 1mM β-glycerol phosphate, 1mM sodium orthovanadate, 100μM $CaCl_2$, pH 7.4). In the case of immunoprecipitations performed without DSP, cells were lysed directly after three washes in PBS. All lysis steps and subsequent washes were performed in the presence of protease inhibitor cocktail (Sigma). Lysates were then incubated with pre-clearing Protein G beads in lysis buffer and left to rotate for 30 mins at 4°C. After three washes in lysis buffer, the washed beads were centrifuged at 7,500 x g and pre-cleared lysates were added to beads pre-coated (overnight) with stated antibodies. Lysate and bead mixes were then placed on a rotator and incubated at 4°C for two hours. Lysate and bead mixes were then centrifuged at 7,500 x g and the supernatants were saved. Beads used for the immunoprecipitation were then washed and centrifuged at 7,500 x g six times. After washing steps, sample buffer was added to the beads. 2x sample buffer was also added to supernatants (1:1). Bead and supernatant samples were then boiled for ten minutes and stored at -20°.

Sample preparation and SDS-PAGE and Western blotting

For studies of Annexin A2 secretion, cells were placed in serum-free conditions for 24 hours. Medium was collected and precipitated with 150μl

TCA for 15 minutes at 4°C, centrifugation at 16,000 x g for 5 minutes and two ice-cold washes with acetone. Excess acetone was then evaporated at 95°C and resuspended in 50μl 2x sample buffer. Cells were washed twice with HBSS and then incubated for 2 minutes with 5mM EGTA in PBS at 4ºC to liberate Annexin A2 adhering to the extracellular surface and then subjected to TCA precipitation as above. Whole cell lysates were prepared by addition of boiling 2x sample buffer in the presence of protease inhibitors directly to plates washed once with PBS. Samples were run on 10% acrylamide minigels for 90 minutes at 150V at 4ºC. Proteins were transferred by wet blotting for 45 mins at 300 Amps to PVDF membranes, blocked in 1x PBS in 0.05% Tween20 supplemented with 5% powdered milk (Marvel) and incubated either with mouse anti-Human α-tubulin, rabbit anti-Human ZO1, sheep anti-Human OCRL1, mouse anti-Human β-actin or mouse anti-Human Annexin A2 primary antibodies (dilutions in range 1 in 1000 to 5000). For ZO-1 Western blots, SDS-PAGE gels were transferred to nitrocellulose through wet blotting for 3 hours at 350 Amps at 4ºC. Nitrocellulose membranes were then treated with Amidon Black solution for 5 minutes and destained in 20% methanol/7.5% acetic acid. Primary antibody incubations were for one hour at room temperature or overnight at 4ºC. PVDF membranes were then washed with PBS/Tween20 three times before a one hour incubation at room temperature with relevant HRP-conjugated secondary antibodies raised in Goat (Dako). After 6 washes with PBS/Tween20, PVDF membranes were visualised with ECL (Amersham Biosciences) using Fuji medical x-ray film.

Labelling of early endosomes

Cells were grown to 50% confluence in 2ml regular medium minus penicillin/streptomycin on 35mm glass bottom dishes (MatTek Corporation). On the day of experiment, cells were washed once with PBS, placed in serum-free medium for one hour and fed 5ng transferrin conjugated to alexa-555 for 45 minutes, before one wash with PBS and fixation with freshly-made 4% paraformaldehyde (PFA).

Immunofluorescence microscopy

Cells were first washed with PBS and subsequently either fixed with 4% PFA at room temperature for 20 mins or with methanol for 5 mins at -20ºC. After fixation with methanol, cells were washed three times with PBS and then left in PBS for 15 minutes. Cells fixed by 4% PFA were then permeabilised by 0.2% Triton X-100 in PBS. Blocking of the cells was carried out in PBS in the presence of 0.5mg/ml bovine serum albumin and 0.2% Triton X-100 for 20 minutes. Primary antibodies were incubated with the cells in PBS in the presence of 0.2% Triton X-100 overnight and washed three times. Secondary antibodies (Invitrogen, unless stated) were then incubated in PBS plus 0.2% Triton X-100 and cells were washed three times, before one wash with water and mounting in Vectashield (Vector Laboratories, Inc) for imaging on a confocal microscopy system (AOBS SP2; Leica) at room temperature (63x NA 1.4 objective) using LCS software (Leica) for acquisition.

Calcium imaging

Cells at approximately 90-100% confluence in 96 well plates were washed twice in regular extracellular media (ECM) containing 121mM NaCl, 5.4 KCl, 0.8mM MgCl2, 1.8mM CaCl2, 6mM NaHCO3, 5.5mM D-glucose and 25mM Hepes (pH7.3). Cells were then loaded in the dark with 2μM Fluo-4 dye in the presence of pluronic acid (0.1%) for 45 minutes. Cells were washed twice and left in ECM at room temperature. Either 10μM or 100μM histamine (final concentrations) made up in regular ECM or regular ECM alone was added to cells. Changes in calcium levels reported through Fluo-4 intensity were then recorded using a high-throughput 96-well plate fluorescence reader, FLIPR (Molecular Devices, USA). After 10 minutes stimulation, 1μM thapsigargin (final concentration) in calcium free ECM plus 10mM BAPTA, or calcium free ECM plus 10mM BAPTA alone was added to cells and imaged using FLIPR for a further 5 minutes. Data were then normalised based upon baseline fluorescence values of Fluo-4. Subsequent analysis was then performed using Microsoft Excel spreadsheets, mean values calculated and error bars represent standard deviations of 3 or 4 replicates. Data are expressed in arbitrary units.

Calcium switch assay and TER measurement

HCE cells were washed three times in PBS and then treated with trypsin-EDTA for 30 minutes, to break apart the majority of cell-cell junctions. Cells

were then re-suspended in regular DMEM (containing 10% FBS, 100µg/ml streptomycin and 100µg/ml penicillin) and incubated at room-temperature for 15 minutes. Cells were then centrifuged at 1,000 x g for 5 minutes and supernatants were removed carefully. Cells were then resuspended in low calcium Sigma Spinner culture medium (containing 2mM L-glutamine, 1mM Na-pyruvate and 10% dialysed FCS (Sigma)). Cells were then re-centrifuged and re-suspended in fresh Sigma Spinner culture medium and plated in excess, onto an 8-well ECIS 8W10E slide. After cells had become adherent to the bottom of the wells, excess cells were removed through careful aspiration and Sigma Spinner culture media was exchanged for fresh medium. Cells were then left in this low calcium media overnight at 37ºC. The next day, the low calcium medium was removed and regular DMEM was added. After 15 minutes, measurement of the impedance and TER across the HCE monolayer was started and carried out for 6 hours.

Chapter 3:
OCRL1 and regulation of PI(4,5)P2 localisation

3: OCRL1 and regulation of PI(4,5)P2 localisation

PI(4,5)P2 is most abundant at the plasma membrane. Much of the work carried out with regard to PI(4,5)P2 has focussed upon its wide range of roles that it coordinates from the cell periphery, such as regulation of membrane trafficking, the actin cytoskeleton and membrane channels. However, there are reports in the literature that provide support for a role of PI(4,5)P2 on internal membranes such as the TGN, even though such reports are rare and experiments to support this are technically difficult for many different reasons [13, 72]. These reports do however suggest that there is a physiologically relevant pool of PI(4,5)P2 on internal membranes, and one hypothesis is that OCRL1 plays a pivotal role in maintaining low levels of PI(4,5)P2 at some of these sites. Should an increased pool of PI(4,5)P2 at internal membranes occur upon depletion of OCRL1, it is important to know specifically to which membranes OCRL1 is targeted. For this reason, experiments were carried out to re-confirm the specific subcellular localisation of OCRL1 in HeLa cells, in particular studying its targeting to early endosomes, by co-localisation of OCRL1 with fluorescently-tagged transferrin fed to HeLa cells over a period of forty-five minutes. The punctate pattern of internalised transferrin revealed significant regions of co-localisation with OCRL1 (Figure 3.1.1, white arrows). Targeting of OCRL1 to early endosomes was further confirmed by immunofluorescence studies, however there was only limited colocalisation of OCRL1 with EEA1. This suggests that OCRL1 is present on only a specific subset of early endosomes (Figure 3.1.2). Apart from endosomes, OCRL1

has been predominantly localised to the TGN[42, 52, 146]. We confirmed these data by comparing the localisation of OCRL1 with the resident TGN glycoprotein TGN46. Strong perinuclear localisation of TGN46 and OCRL1 was found in HeLa cells (Figure 3.1.3). These results are supported by recent data showing that OCRL1 is targeted to these sites by its ability to bind members of the Rab GTPase family that are known to localise to the TGN and endosomes [52]. In fact, a large scale screen revealed that OCRL1 has an extremely broad Rab binding specificity, binding a total of 16 Rab GTPases that target to these sites [45].

3.1: Confirmation of subcellular localisation of OCRL1 in HeLa cells

Figure 3.1.1: Colocalisation of OCRL1 with transferrin

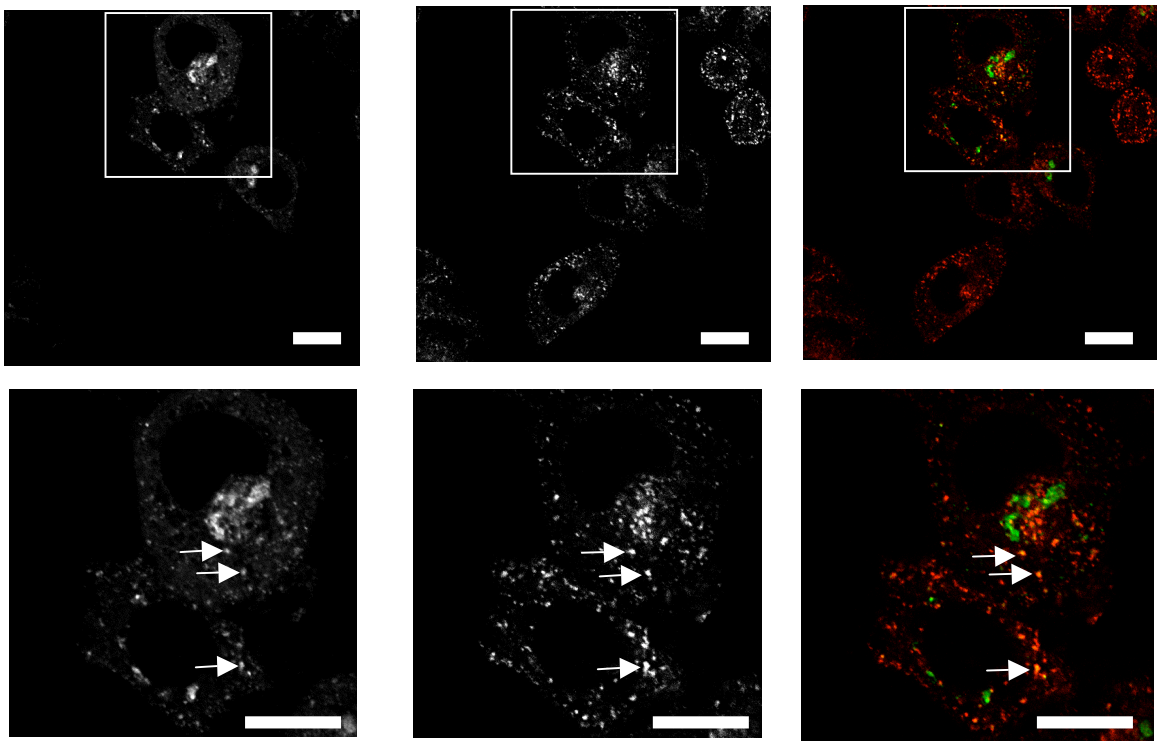

Figure 3.1.1 legend: OCRL1-EGFP positive puncta co-localise with internalised transferrin, indicating that OCRL1 is localised to early endosomes. HeLa cells were transfected with 0.4µg OCRL1-EGFP 24 hours prior to feeding with transferrin-alexa555 (a gift from Dr. Clare Futter, UCL) for 45 minutes. Top panel: left: OCRL1-EGFP; middle: Transferrin-alexa 555; right: Overlay – OCRL1 green, Transferrin red, co-localisation yellow. Bottom panel: enlarged images of the boxed area indicated in the top panel. Arrows highlight regions of co-localisation. Single confocal sections. (Scale bar 10µm)

.

Figure 3.1.2: OCRL1 is targeted to early endosomes

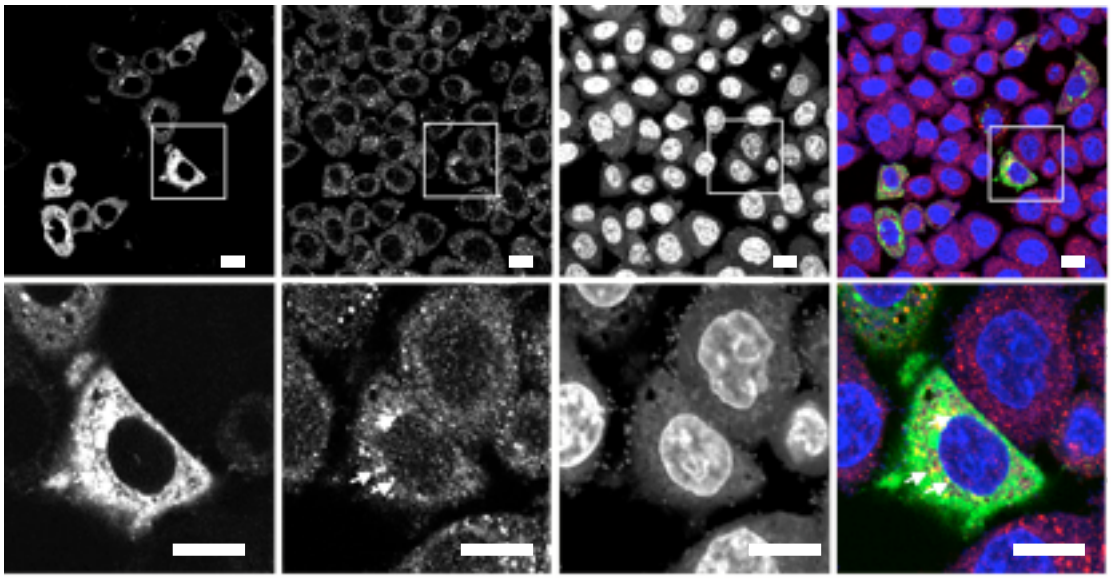

OCRL-EGFP EEA1 DAPI Overlay

Figure 3.1.2. legend: OCRL1-EGFP positive puncta co-localise with antibodies specific to early endosome antigen 1 (EEA1), indicating that OCRL1 is localised to early endosomes. HeLa cells were transfected with 0.4µg OCRL1-EGFP 24 hours prior to fixation and immunostaining. Top panel: left: OCRL1-EGFP; second: EEA1 immunostain; third: DAPI stain; right: overlay - OCRL1 green, EEA1 red, co-localisation yellow, DAPI blue. Bottom panel: enlarged image of boxed area indicated in top panel. Arrows highlight regions of co-localisation. Single confocal sections. (Scale bar 10µm)

.

Figure 3.1.3: OCRL1 protein is targeted to the TGN

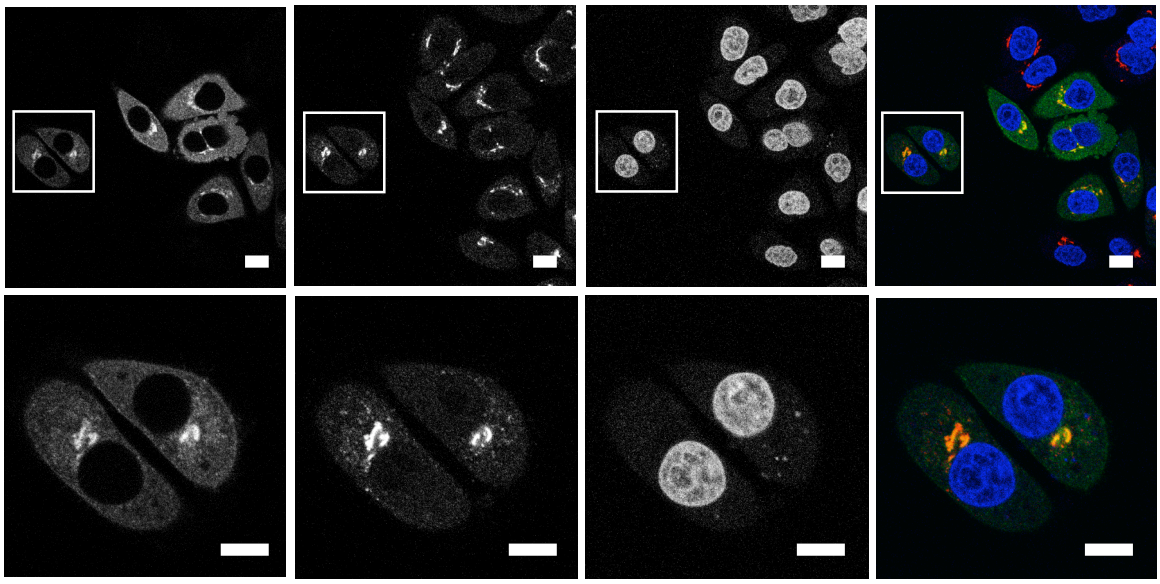

OCRL-EGFP TGN46 (Red) DAPI (Blue) Overlay

Figure 3.1.3. legend: OCRL1-EGFP positive puncta co-localise with antibodies specific to TGN46, indicating that OCRL1 is localised to the trans-Golgi network. HeLa cells were transfected with 0.4µg OCRL1-EGFP 24 hours prior to fixation and immunostaining. Top panel: left: OCRL1-EGFP; second: TGN46 immunostain; third: DAPI stain; right: Overlay – OCRL1 green, TGN46 red, co-localisation yellow. Bottom panel: zoom image of white box indicated in top panel. Single confocal sections. (Scale bar 10µm)

3.2: Effect of OCRL depletion on Annexin A2 distribution

The discovery that some patients with Dent's disease, a renal proximal tubulopathy without central nervous or ocular phenotypes, have mutations in OCRL1 suggests that there may be a common mechanism between the disorders [80]. Recent data has shown that in cells with inactive CLCN5, the proton/chloride antiporter mutated in Dent's Disease, Annexin A2 translocates from the cytosol to the plasma membrane [78]. Translocation of Annexin A2 coincided with it being detected at the extracellular face of the plasma membrane. This discovery was interpreted to indicate that extracellular Annexin A2 might nucleate calcium oxalate deposition, a known mechanism for nephrocalcinosis and nephrolithiasis, which are common to both Dent's disease and Lowe syndrome.

These discoveries provide a potential link between the two disorders, in that cells derived from Lowe Syndrome patients contain elevated levels of PI(4,5)P2, a known calcium-enhanced binding partner of Annexin A2 [36, 147]. The potential links between OCRL1 and Annexin A2 are further supported by the shared targeting of both proteins to sites within the endosomal trafficking pathway and shared binding partners such as Rac1 and clathrin-adaptor AP-2 [73, 74]. Annexin A2 is also proposed to be important in central nervous system function and lens differentiation [148, 149]. For the above reasons, the effect of OCRL1 depletion upon the localisation of Annexin A2 was investigated.

OCRL1 can be efficiently depleted from both HeLa and HLE-B3 cells. In a representative experiment (taken from three separate experiments) depletion of 60% OCRL1 from HeLa cells (Figure 3.2.1) was associated with a striking translocation of Annexin A2 from the cytosol to limiting membranes (Figure 3.2.2). Annexin A2 seems to accumulate at the plasma membrane to a higher degree in cells depleted of OCRL1, is less prevalent in the cytosol and is possibly present more on internal membranes. This membrane pool is likely to be a small percentage of the overall amount of Annexin A2, which is a very highly expressed protein in epithelial and endothelial cells, at an estimated 0.5% of total cellular protein in most transformed cell lines such as HeLa cells (Professor Stephen Moss, personal communication). In order to achieve these results cells had to be fixed in methanol, which tends to not preserve the cytoplasm. Fixation in paraformaldehyde did not show the same effect, possibly due to better preservation of the cytoplasm.

A more physiologically relevant cell line to study in which to study the effects of OCRL1 depletion is HLE-B3, a cell line derived from human lens epithelium, a tissue known to be severely affected in Lowe Syndrome [150]. A similar effect was produced in HLE-B3 cells, again showing an increased general re-distribution of Annexin A2 to the plasma membrane from the cytosol, and some cells display accumulations on internal membranes and vesicles (Figure 3.2.3). The redistribution of Annexin A2 to membranes upon OCRL1 depletion was present in every cell. This observation was unanticipated as depletion of OCRL1 was not 100%. This observation is

suggestive of an increase in intercellular calcium handling. This is discussed in detail in Chapter 6.

To confirm these findings further, a biochemical analysis of Annexin A2 redistribution upon OCRL1 depletion from HeLa cells was undertaken. Analysis by Western blot shows that total Annexin A2 levels are unchanged upon OCRL1 depletion (data not shown). This indicates that the higher prevalence of Annexin A2 at membranes is not due to an up-regulation of Annexin A2 expression, but a translocation event. This was confirmed by fractionation of HeLa cells on Percoll gradients, which separate membranes and cellular material based on density. Percoll fractionation of OCRL1 depleted HeLa cells revealed increased of Annexin A2 in dense membrane fractions, in comparison to mock oligofectamine treated controls (Figure 3.2.4). This result is in agreement with the redistirubution of Annexin A2 to membranes in OCRL1 depleted cells (Figures 3.2.2 & 3).

Annexin A2 has also been reported to be secreted in some cellular environments [151]. The tendency for Annexin A2 to accumulate at membranes suggested that upon OCRL1 depletion, Annexin A2 may translocate across the membrane as it does in cells lacking CLCN5 function, and even be secreted. Incubation of cells with 5mM EGTA, a calcium chelator, strips calcium binding proteins from the cell surface. Upon this treatment, data indicate that Annexin A2 levels at the extracellular face of the plasma membrane after OCRL1 siRNA treatment are unaffected, in comparison with mock oligofectamine treated HeLa cells (Figure 3.2.4., first lane). The

appearance of a band positive for Annexin A2 in a lane that was left blank suggests that over-flow from either EGTA-stripped membranes or fraction one occurred. This means that the redistribution of Annexin A2 to the extracellular face of the membrane cannot be fully determined from the current data (Figure 3.2.4). However, a much clearer effect was that Annexin A2 was found to be elevated in the medium of cells treated with OCRL1 siRNA, showing that Annexin A2 is lost from these cells (Figure 3.2.5). Here, the tubulin control shows that the recovered Annexin A2 is not associated with cells. This is consistent with the finding that Annexin A2 is shed from cells in exosomes [152].

Overall these results show that depletion of OCRL1 leads to translocation of Annexin A2 from the cytoplasm to the plasma membrane, which it crosses. The mechanism by which this event occurs has not yet been fully investigated.

Figure 3.2.1: OCRL1 can be efficiently depleted from cells upon siRNA transfection

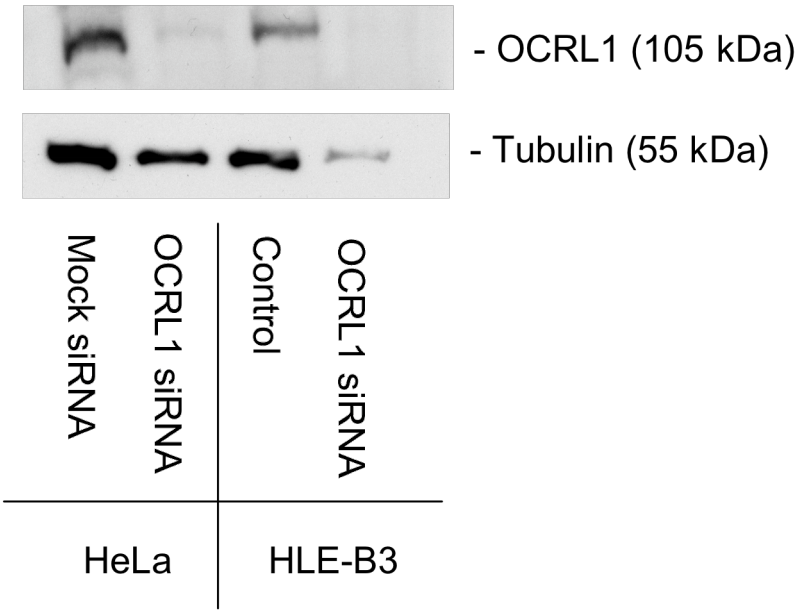

Figure 3.2.1. legend: HeLa and HLE-B3 cells were treated with OCRL1 siRNA or oligofectamine alone 72 hours prior to analysis of OCRL1 and α-tubulin expression levels by Western Blot. AIDA densitometry reveals that relative OCRL1 expression is reduced by 60% in comparison to mock oligofectamine control. The effect of OCRL1 siRNA in HLE-B3 is not statistically relevant due to a loss of HLE-B3 cell viability upon treatment with siRNA.

Figure 3.2.2: Immunofluorescence studies reveal that Annexin A2 is re-distributed upon OCRL1 depletion in epithelial cell line, HeLa

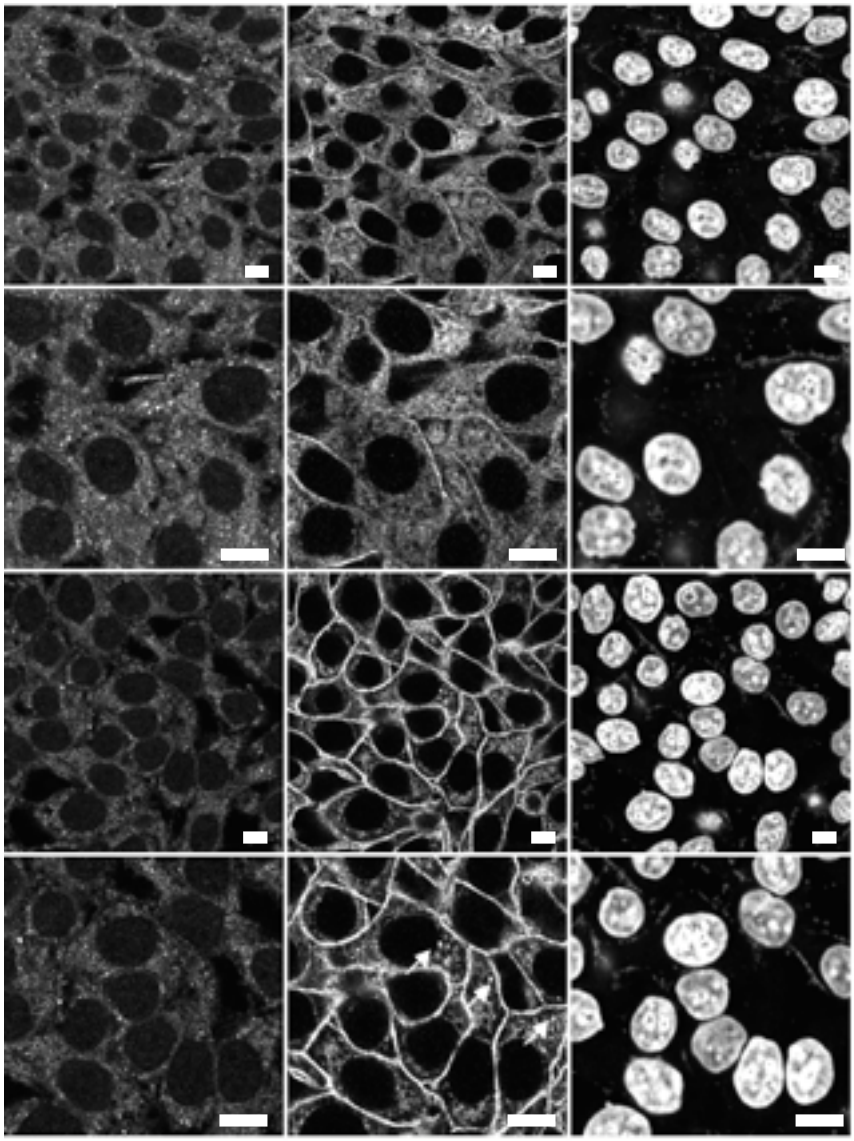

Figure 3.2.2. legend: HeLa cells were treated with oligofectamine alone (1st and 2nd rows) or OCRL1 siRNA (3rd and 4th rows). 72 hours later cells were fixed with methanol at -20ºC for 5 minutes, and immunostained with antibodies specific to OCRL1 (left column), Annexin A2 (middle column) and

stained with DAPI (right column). The bottom two rows are zoomed images from the top rows. White arrows highlight internal membranes positive for Annexin A2. Single confocal sections. (Scale bar 10μm).

The effect of OCRL1 depletion with siRNA on the OCRL1 immunostain seems to be very weak, especially when compared to western blot analyses, which show an approximate 60% reduction in protein levels. This discrepancy is due to high background staining by this batch of immunoaffinity purified OCRL1 primary antibody, which is associated with the appearance of three non-specific bands on Western blots.

Figure 3.2.3: Effect of OCRL1 depletion on Annexin A2 distribution in human lens epithelial cell line, HLE-B3

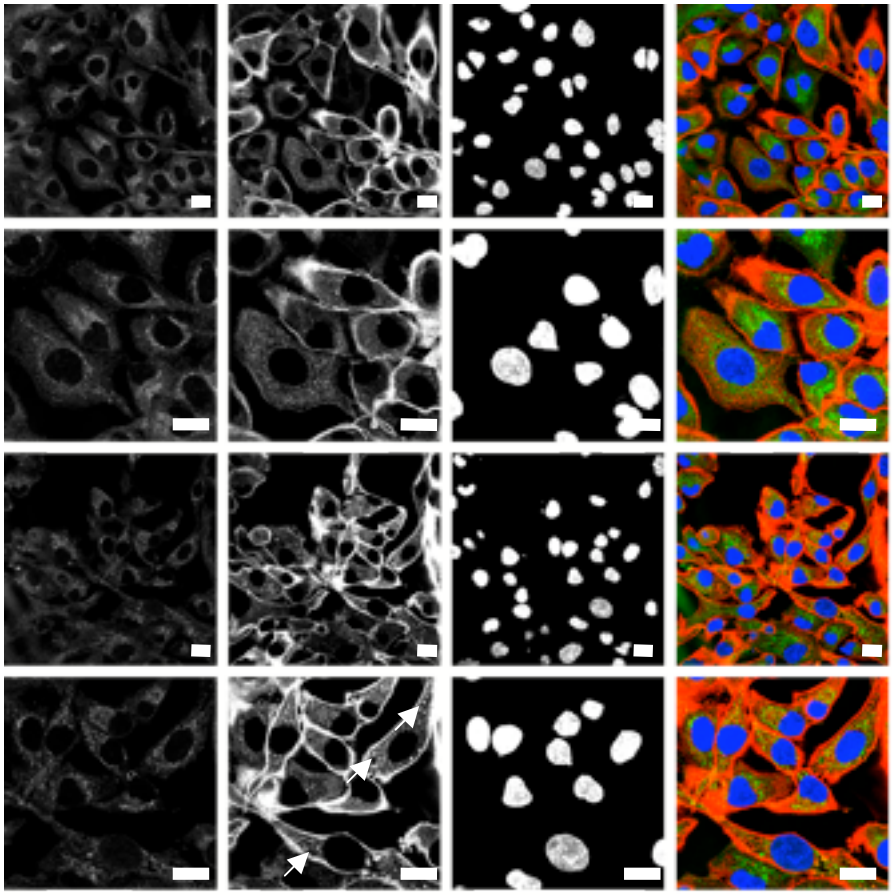

Figure 3.2.3. legend: HLE-B3 cells were treated 72 hours prior to fixation with methanol at 20ºC with mock oligofectamine (top panel) or OCRL1 siRNA (bottom panel) and immunostained with antibodies specific to OCRL1 and Annexin A2. Nuclei were stained with DAPI. White arrows indicate sites of Annexin A2 accumulation at internal membranes. Single confocal sections.

In a similar fashion to Figure 3.2.2., there is only a small change in the OCRL1 immunostain upon depletion of OCRL1. (Scale bar 10μm).

Figure 3.2.4: Percoll fractionation to examine Annexin A2 re-distribution upon OCRL1 depletion from HeLa cells

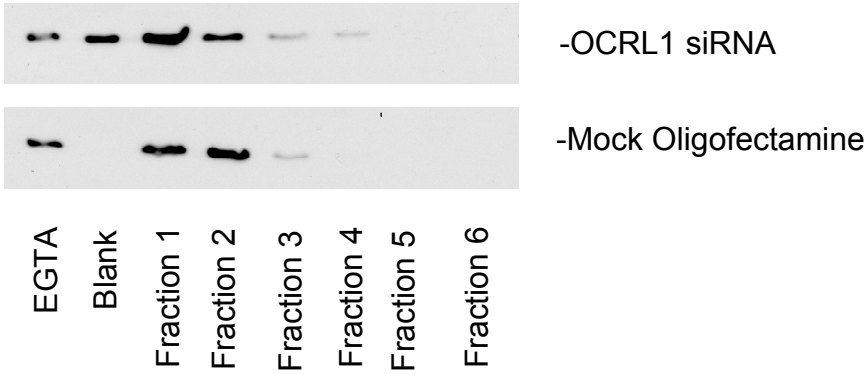

Figure 3.2.4. legend: HeLa cells were treated with either oligofectamine or OCRL1 siRNA for 72 hours. Cells were washed twice with HBSS and were incubated for 2 minutes with 5mM EGTA, a calcium chelator that served to strip Annexin A2 from the extracellular plasma membrane. From these EGTA treated cells, lysates were prepared and separated by Percoll density gradient centrifugation. The EGTA stripped solution and each fraction were then precipitated with TCA and probed by Western Blot for Annexin A2.

Figure 3.2.5: Annexin A2 is found in the extracellular medium upon OCRL1 depletion from HeLa cells

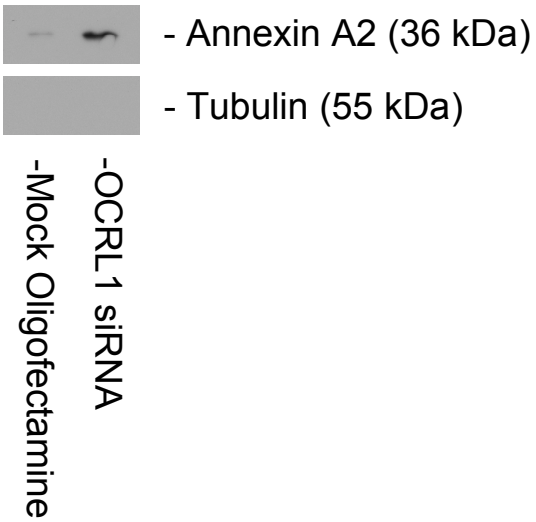

Figure 3.2.5. legend: HeLa cells were treated with either OCRL1 siRNA or oligofectamine alone for 72 hours. Cells were placed in serum-free medium at 48 hours and medium was removed and precipitated after 72 hours. Precipitates were then analysed for Annexin A2 and α-tubulin levels by Western blot. The tubulin blot demonstrates that the precipitates did not include dead cells. A similar result was obtained in two experiments.

3.3: Effect of OCRL1 depletion on the localisation of different phosphoinositides using PH domains

The preferred substrate of OCRL1 has been reported to be PI(4,5)P2 and accordingly PI(4,5)P2 levels are elevated in cells lacking expression of OCRL1 [36, 38]. However, the location within cells of this PI(4,5)P2 is unknown. There are reports of PI(4,5)P2 pools residing at other sites in the cell other than the plasma membrane, such as the nucleus, and within Golgi stacks [13]. The increased levels of PI(4,5)P2 raise another interesting possibility, that there is an impact on levels of other phosphoinositides. For example, a loss of PI(4,5)P2 5-phosphatase activity as a result of OCRL1 depletion may lead to a reduction in PI(4)P or an elevation in PI(3,4,5)P3 levels. Again these changes may coincide with a change in the normal distribution of these phosphoinositides within the cell. To address this possibility, analysis of living cells transiently expressing GFP-PH domain chimeras specific to different phosphoinositides was undertaken. A plethora of phosphoinositide binding domains have been discovered, some of which bind one particular phosphoinositide. One such domain is the PH domain of PLCδ1, which recognises PI(4,5)P2 with high specificity. Another PH domain, that of oxysterol binding protein (OSBP) recognises a pool of PI(4)P that resides at the Golgi apparatus. These domains were expressed as GFP fusions in HeLa cells, and showed the expected distributions (Figure 3.3.1).

Previous results showing a re-distribution of Annexin A2 to the plasma membrane and intracellular compartments suggested that PI(4,5)P2 may

accumulate at these sites upon OCRL1 depletion (Figure 3.2.2). In yeast, intracellular pools of PI(4,5)P2 are tightly regulated by the activity of proteins belonging to the synaptojanin family, which are able to dephosphorylate the phosphoinositide at the 5' position of the myo-inositol ring. Upon inactivation of multiple synaptojanin-like proteins in yeast, PI(4,5)P2 accumulates at internal membranes [72]. Other evidence of the presence of PI(4,5)P2 at internal membranes comes from an immuno-electron microscopic study using the purified PH domain of PLCδ . This method was effective in showing that PI(4,5)P2 is greatly concentrated at the plasma membrane, but is also present at lower levels in the Golgi, endosomes and also the nucleus [13].

OCRL1 is localised to the TGN and endosomes and therefore PI(4,5)P2 may be at these sites at low levels in normal cells, and accumulate there upon OCRL1 depletion. Classically, the localisation of PI(4,5)P2 is reported in living cells using a GFP chimera of the PH domain of PLCδ1. The localisation of GFP-PLCδ-PH upon OCRL1 depletion in HeLa cells was therefore analysed. The localisation of GFP-PLCδ-PH in mock transfected cells reveals a plasma membrane distribution thought to be driven principally by the high abundance of PI(4,5)P2 at this membrane (Figure 3.3.2., top panel). Upon RNAi mediated depletion of OCRL1, no significant difference in the localisation of GFP-PLCδ-PH was observed with the majority of cells showing a purely plasma membrane accumulation. However in a subset of the cells, GFP-PLCδ-PH showed signs of accumulating at intracellular sites within the cell (Figure 3.3.2., bottom panel). Given that the PLCδ1-PH domain has other factors driving its accumulation at the plasma membrane such as anionic charge this

observation suggests that PI(4,5)P2 might be accumulating on internal membranes in cells lacking OCRL1 [71].

Despite claims that the PLCδ1-PH domain localises to the plasma membrane based on its affinity for PI(4,5)P2 alone, there are other, non-phosphoinositide dependent mechanisms, such as an affinity for anionic charge that play a part in targeting to the plasma membrane [71]. Therefore, the signal of PI(4,5)P2 as reported by PLCδ-PH is contaminated by non-phosphoinositide, plasma membrane-specific factors. For this reason, we investigated whether a fusion of PLCδ-PH to a protein loosely targeted to an intracellular site within the cell (here the TGN) may reveal previously unobserved PI(4,5)P2. We have created a construct that expresses a mutant version of the OSBP PH domain fused to PLCδ-GFP. In previous work by Levine and Munro in 1998 and 2002, it was shown that the PH domain of OSBP binds tightly to the TGN [144, 153]. This is also shown in Figure 3.3.1 (right panel). This interaction was shown to be dependent on a phosphoinositide determinant and a protein determinant, now thought to be Arf1[23]. Upon mutation of two critical arginine residues to glutamic acid residues, the ability of OSBP-PH (RR->EE) to localise to the TGN is greatly reduced due to a loss of phosphoinositide binding ability [144], although there is weak targeting that is still detected using a dimeric construct with two PH domains in tandem.

By fusing the mutated OSBP-PH domain to GFP-PLCδ-PH, the weak Golgi targeting may be sufficient to allow PI(4,5)P2 at the Golgi to compete with PI(4,5)P2 at the plasma membrane for binding to the PLCδ-PH, and so detect

PI(4,5)P2 at the TGN in living cells. This fusion protein (given the acronym GFP-POP, from PLC∂-OSBP[EE] PH dimer) may be more likely to report intracellular accumulations of PI(4,5)P2, which potentially arise upon OCRL1 depletion. Alternatively, if OCRL1 depletion causes PI(4,5)P2 accumulation at the plasma membrane, redistribution of GFP-POP from intracellular sites to the plasma membrane may occur. Therefore, analysis of the abundance of GFP-POP at the plasma membrane, the cytosol and intracellular compartments, was carried out to detect potential changes in sub-cellular PI(4,5)P2 accumulation with knockdown of OCRL1.

In mock siRNA treated HeLa cells, GFP-POP exhibited a largely plasma membrane and cytosolic localisation with weak intracellular accumulations sometimes observed (Figure 3.3.3., top panel). Upon depletion of OCRL1 with siRNA a redistribution of GFP-POP from the cytosol and plasma membrane to intracellular sites was suggested upon initial analysis (Figure 3.3.3., bottom panel,). Strong accumulation of GFP-POP at perinuclear sites within OCRL1 siRNA-treated HeLa cells was not seen as readily in cells treated with mock siRNA, although some punctate distribution of GFP-POP was seen. Further characterisation based on the ratio of GFP-POP localisation between the plasma membrane, cytosol and internal membrane compartments upon OCRL1 depletion was required and three separate experiments revealed a statistically significant difference (Figure 3.3.4).

However, upon assessment of a large number of cells, different clones of HeLa cells and further categorisation of the strength of accumulations of GFP-

POP on internal membranes, these results were irreproducible. We began to find that a higher percentage of control siRNA treated cells exhibited strong accumulations on internal membranes, and the significance of the initial set of results was reduced. We decided to further characterise whether there were any undesired effects of over-expression of GFP-POP in these cells. Immunofluorescent studies of control and OCRL1 siRNA treated cells transiently expressing GFP-POP revealed that over-expression caused strong relocalisation of endogenous OCRL1 to a perinuclear site (Figure 3.3.5). Furthermore, in control siRNA and OCRL1 siRNA treated cells the localisation and possibly the detectable levels of TGN46, a protein highly enriched at the trans-Golgi network was adversely affected (Figure 3.3.6). In GFP-POP expressing cells, the normal perinuclear distribution of TGN46 was lost and a much lower level of fluorescence was detected. This result is similar to, though less strong than, the effect of over-expressing GFP-OSBP-PH on TGN46 and indicates that the GFP-POP construct is binding to and thereby sequestering, ARF1 on the TGN, leading to dispersal of that organelle [23, 153].

It is possible that loss of OCRL1 has effects on levels and localisations of phosphoinositides other than PI(4,5)P2. Increases in PI(4,5)P2 may reflect a decrease in PI(4)P. Also, since PI(4,5)P2 is the substrate for PI3K family members and OCRL1 can dephosphorylate PI(3,4,5)P3, there may be an increase in PI(3,4,5)P3 levels. Further studies were carried out analysing the distribution of a GFP chimera of the AKT-PH domain often used to report PI(3,4,5)P3 [11, 154]. However, no significant changes in GFP-AKT-PH or GFP-Grp1-PH localisation upon OCRL1 depletion were observed (Figure 3.3.7). It

is worth bearing in mind that differences in GFP-AKT-PH or GFP-Grp1-PH localisation may only be achieved upon stimulating cells to synthesise PI(3,4,5)P3, for example with platelet-derived growth factor, PDGF [155].

Figure 3.3.1: Use of PH domains to visualise two different phosphorylated phosphoinositide populations

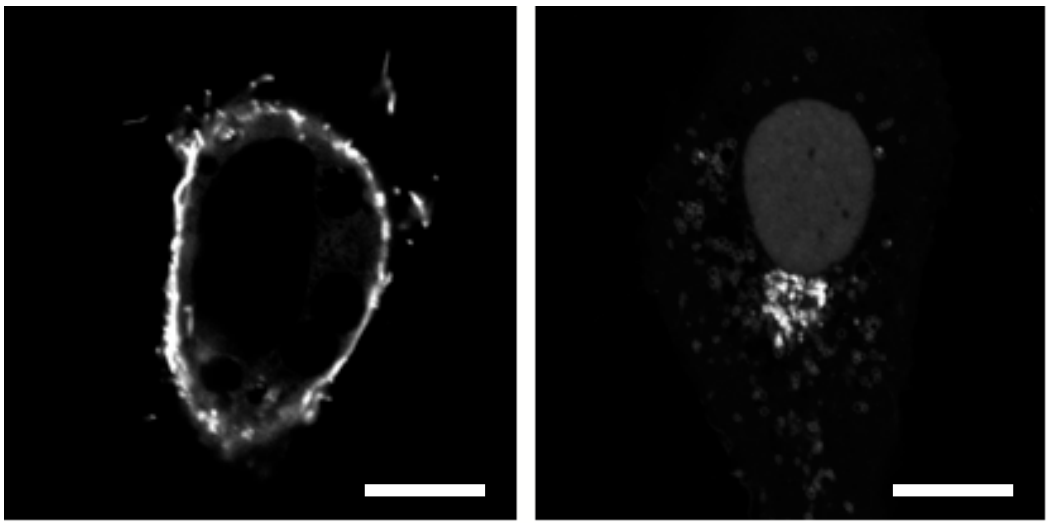

GFP-PLCδ-PH GFP-OSBP-PH

Figure 3.3.1. legend: HeLa cells transiently expressing GFP-PLCδ-PH and GFP-OSBP-PH. HeLa cells were transfected with DNA encoding either expressing GFP-PLCδ-PH (left panel) GFP-OSBP-PH (right panel), 24 hours prior to analysis by confocal microscopy. Single confocal sections. Scale bar (10μm).

Figure 3.3.2: Effect of OCRL1 depletion on intracellular localisation of GFP-PLCδ-PH in living HeLa cells

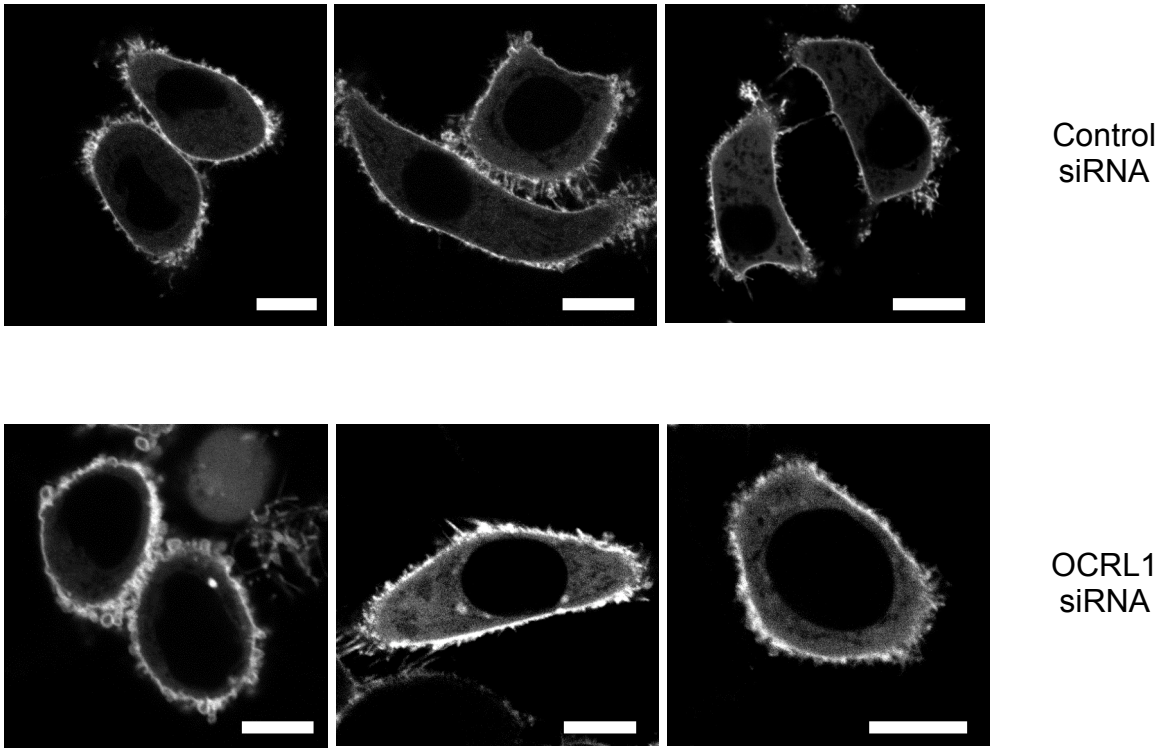

Figure 3.3.2. legend: HeLa cells expressing GFP-PLCδ-PH. Cells were treated with either mock siRNA (top panel) or OCRL1 siRNA (bottom panel), 48 hours prior to analysis by confocal microscopy, and transfected with GFP-PLCδ-PH 24 hours prior to imaging. Single confocal sections. Scale bar (10μm).

Figure 3.3.3: Effect of OCRL1 depletion on intracellular localisation of GFP- POP in living HeLa cells

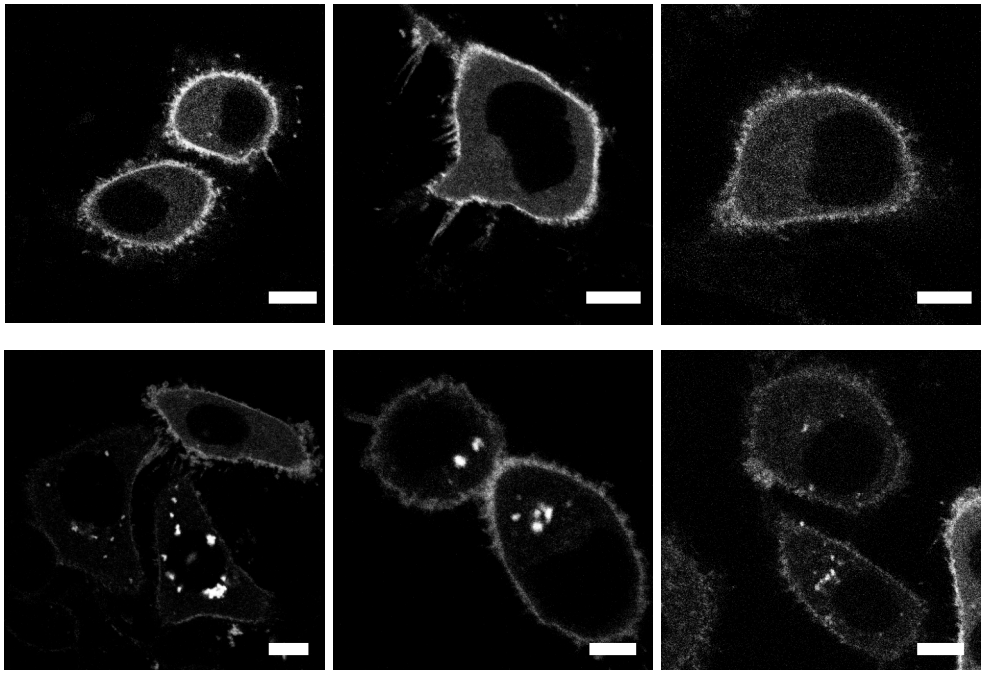

Figure 3.3.3. legend: Representative images of living HeLa cells transiently expressing GFP-POP for 24 hours after either mock siRNA (top panel) or OCRL1 siRNA (bottom panel) treatment for 48 hours. Single confocal sections. Scale bar (10μm).

Figure 3.3.4: Quantification of change in localisation of GFP-POP upon OCRL1 depletion

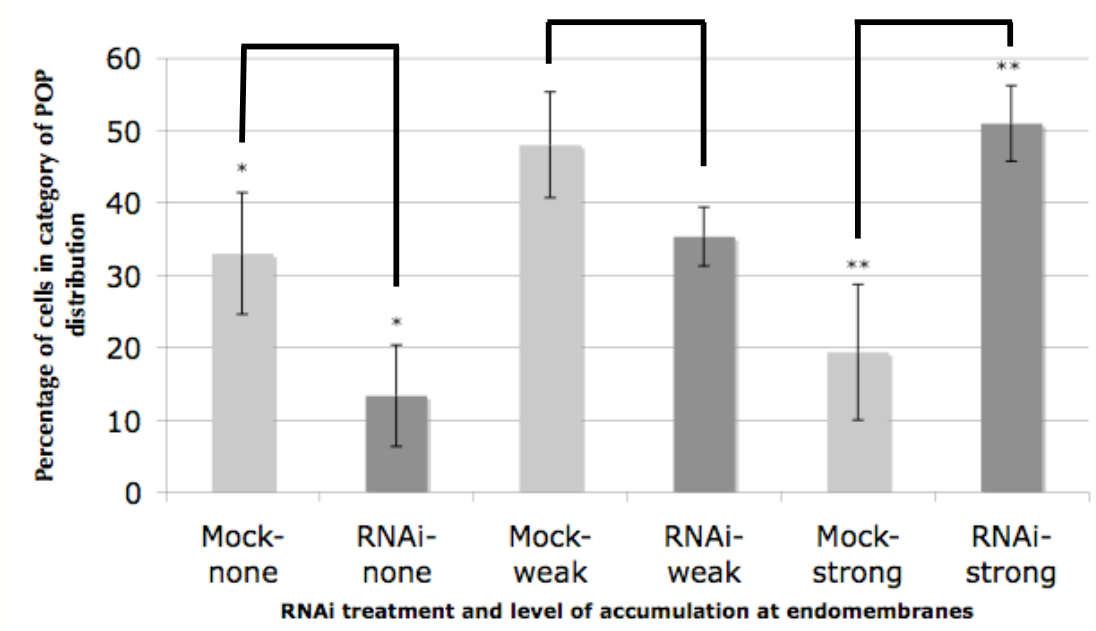

Figure 3.3.4 legend: Three separate categories were coded based on accumulation of GFP-POP at internal membranes. These categories were: none, weak and strong internal membrane accumulation. Three separate experiments were performed; control siRNA (n=70) and OCRL1 siRNA (n=70) treated cells were coded to be indistinguishable, and assigned to these categories by a third party. *p=<0.05. **p=<0.02.

Figure 3.3.5: OCRL1 localisation in HeLa cells over-expressing GFP-POP

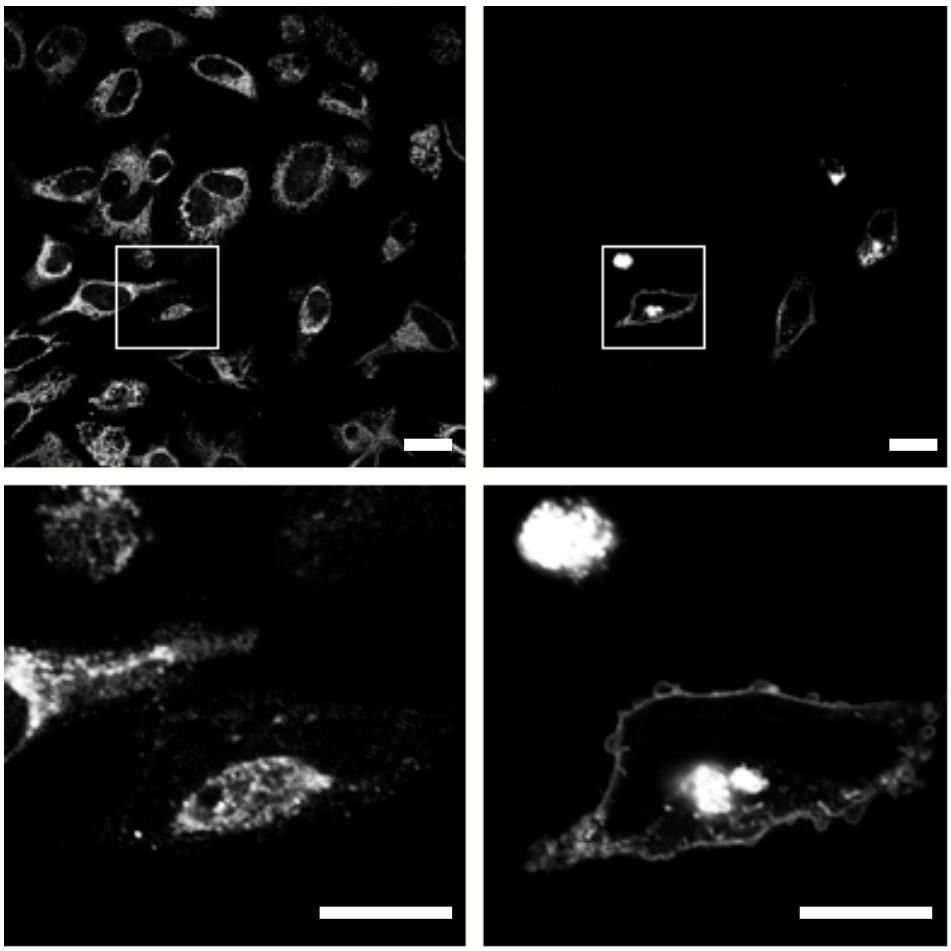

OCRL1 GFP-POP

Figure 3.3.5 legend: Control siRNA treated HeLa cells were transiently transfected with DNA encoding GFP-POP. After 24 hours of over-expression, cells were fixed with 4% paraformaldehyde, permeabilised and blocked in 1mg/ml BSA and stained for OCRL1. The lower two panels are enlarged images taken from the white boxes in the upper panels. Single confocal sections. Scale bar (10μm).

Figure 3.3.6: TGN46 localisation in HeLa cells over-expressing GFP-POP

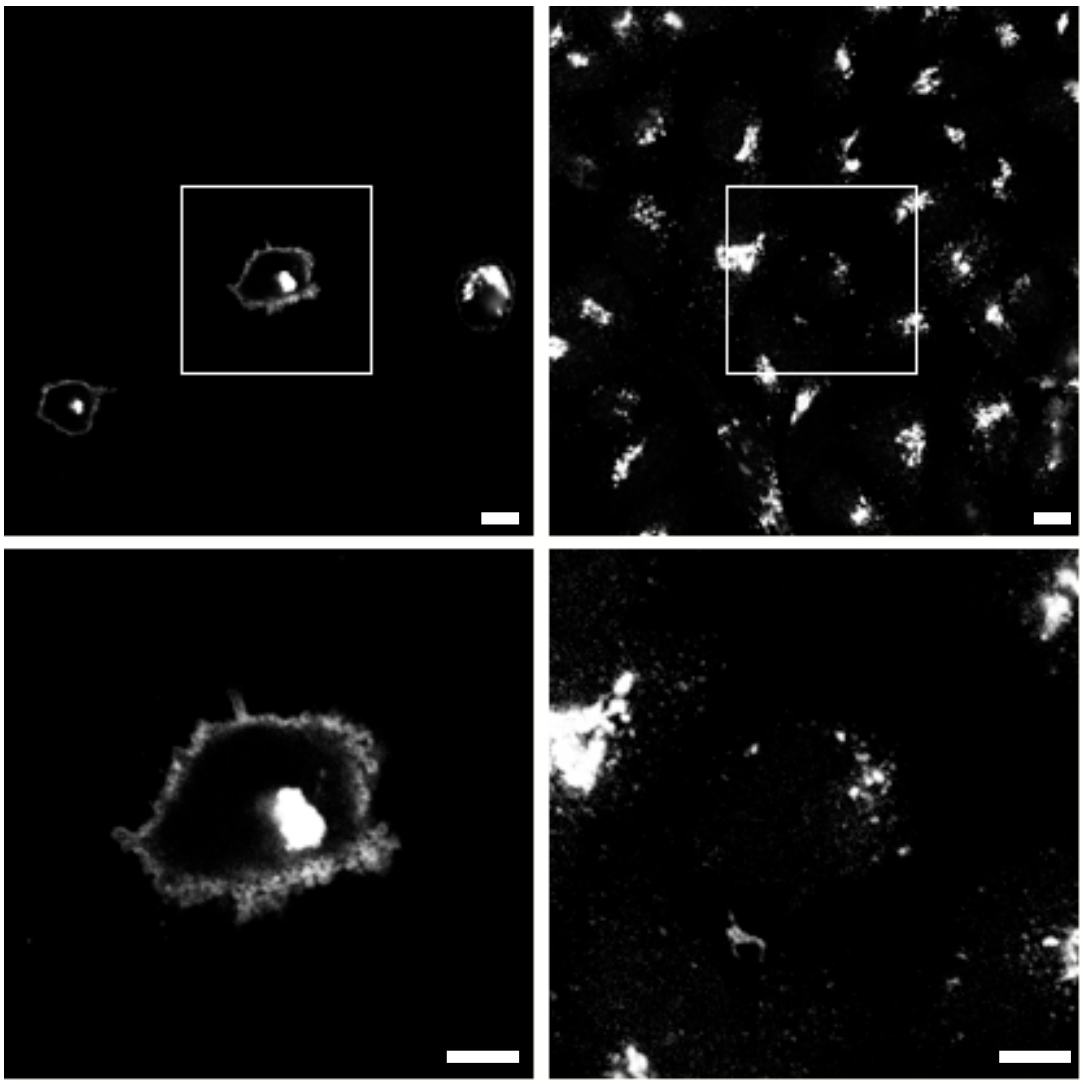

GFP-POP TGN46

Figure 3.3.6 legend: Control siRNA treated HeLa cells were transiently transfected with DNA encoding GFP-POP. After 24 hours of over-expression, cells were fixed with 4% paraformaldehyde, permeabilised and blocked in 1mg/ml BSA and stained for TGN46. The lower two panels are enlarged images taken from the white boxes in the upper panels. Single confocal sections. Scale bar (10μm).

Figure 3.3.7: PI(3,4,5)P3 localisation in HeLa cells over-expressing PH domains of GFP-AKT or GFP-Grp1 upon OCRL1 depletion

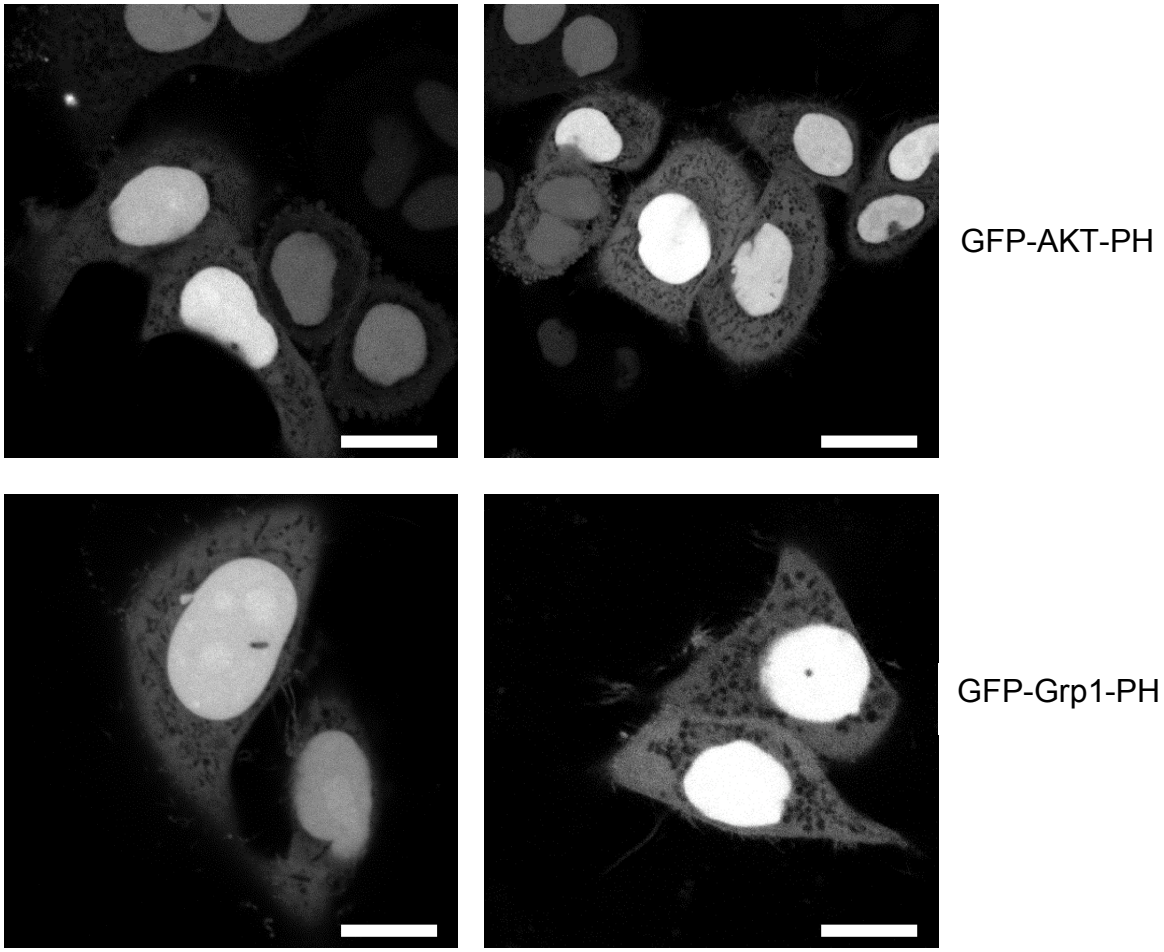

Figure 3.3.7 legend: HeLa cells were treated with non-targetting, negative control siRNA or OCRL1 siRNA for 72 hours. Cells were transiently transfected with DNA encoding GFP-tagged PH domains of AKT (top row) or Grp1 (bottom row) after 48 hours of siRNA treatment. After 24 hours of over-expression, living cells visualised using a Leica confocal microscope at room temperature. No differences were seen with either construct. Single confocal sections. Scale bar (10μm).

3.4: PI(4,5)P2 localisation studies in Saccharomyces Cerevisiae

In a previous study in yeast it was shown that the PLCδ-PH domain can target internal membranes upon inactivation of multiple members of the synaptojanin family [72]. These data provide evidence that PI(4,5)P2 can accumulate at internal membranes in yeast mutants. The results achieved in this thesis with GFP-POP in mammalian cells (Figure 3.3.2) suggested that our novel construct may be able to visualise changes in PI(4,5)P2 levels and localisation in yeast. In the aforementioned study, only upon inactivation of the entire complement of synaptojanin-like family members did GFP-PLCδ-PHx2 accumulate at internal membranes.

S.cerevisiae do not express OCRL1, however the synaptojanin family proteins share the same highly conserved inositol polyphosphate 5-phosphatase domain [33, 156]. Given the suggested propensity of GFP-POP in the OCRL1 RNAi experiments to bind PI(4,5)P2 on internal membranes, we decided to compare GFP-POP with GFP-PLCδ-PH in wild-type yeast and mutants with single deletion of either Inpp51, Inpp52, Inpp53 or Inpp54. We decided to test whether POP detects a previously unappreciated internal pool of PI(4,5)P2 in the single deletion mutants.

Upon comparison of GFP-PLCδ-PH and GFP-POP in wildtype yeast, two clear differences were observed (Figure 3.4.1). Firstly, the expression levels of GFP-POP were much lower than that of GFP-PLCδ-PH. Fluorescence

levels varied a great amount between cells within an experiment, as the expression vector used produces a variable copy number. However, on average, expression levels of GFP-PLCδ-PH in yeast were much higher than GFP-POP cells. Secondly, a clearer localisation to the cell periphery above the cytoplasmic background was reproducibly seen for GFP-POP in comparison to GFP-PLCδ-PH. Interestingly, in some of the yeast, an internal GFP-POP positive punctum was visible, in close proximity but not adjoining, the nucleus and vacuole.

It is well known that yeast contain a higher level of inositol phosphates in comparison to mammalian cells, which would compete for the GFP-PLCδ-PH interaction with PI(4,5)P2. For this reason, a dimer of the PLCδ-PH domain is often used for visualisation of PI(4,5)P2 in yeast [72, 144]. One factor not considered originally in the design of POP, is that in theory this novel hetero-dimeric construct would bind, in addition to the desired sites of co-incidence, any membrane receptors of both PH domains. The increased plasma membrane targeting of POP over PLCδ-PH may be caused by additional, yet weak, affinity of mutant OSBP-PH for the plasma membrane. This is likely to be because of a residual interaction by mutant OSBP-PH with anionic phospholipids such as phosphatidic acid (Dr. Tim Levine, unpublished observation).

Upon deletion of each synaptojanin homologue, GFP-POP localisation to the plasma membrane was diminished (Figure 3.4.2). Given that the majority of PI(4,5)P2 resides at the plasma membrane, this result was surprising. The

most plausible explanation for this is that loss of plasma membrane targeting of GFP-POP is due to increased cytosolic I(1,4,5)P3, with increased phospholipase C action occurring when PI(4,5)P2 is turned over less by phosphatases. To test this, we decided to look at PLC1 deletion mutants. In yeast there is only one PLC family member, therefore these yeast are unable to hydrolyse PI(4,5)P2 to I(1,4,5)P3 and (1,2)-diacylglycerol. Due to the loss of I(1,4,5)P3 formed from PI(4,5)P2 hydrolysis, and possibly an increase in plasma membrane PI(4,5)P2, we expected to see an increase in the plasma membrane targeting of GFP-POP and GFP-PLCδ-PH. As expected, the plasma membrane localisation of GFP-POP was enhanced in ∆plc1 yeast, in comparison to wildtype yeast (Figure 3.4.3, top and bottom right panels). However, the localisation and intensity of GFP-PLCδ-PH in wildtype and mutant yeast seemed to be very comparable (Figure 3.4.3, top and bottom left panels). This result suggested that GFP-POP may be better than GFP-PLCδ-PH as a reporter for PI(4,5)P2 in yeast.

To further this study we would like to look at double ∆plc1/∆inp51-54 yeast expressing GFP-PLCδ-PH or GFP-POP: if our hypothesis is correct then it may be that deletion of PLC1 recovers plasma membrane recruitment of GFP-POP.

Figure 3.4.1: Comparison of GFP-POP and GFP-PLCδ-PH in wildtype S.cerevisiae

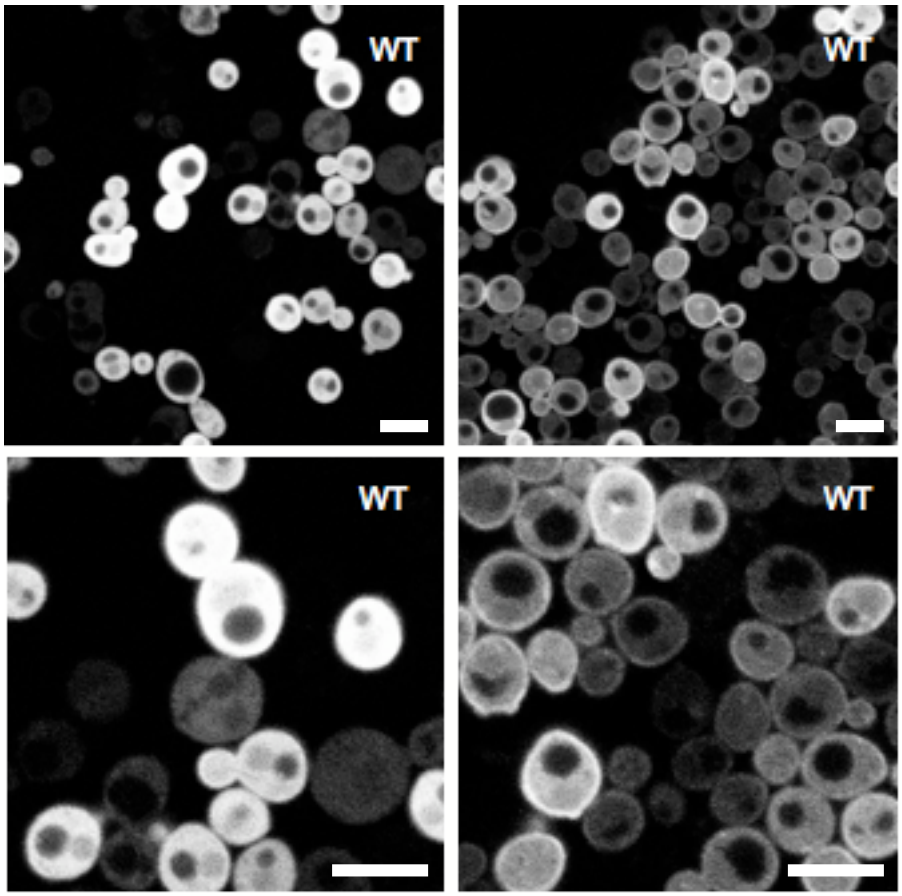

GFP-PLCδ-PH GFP-POP

Figure 3.4.1 legend: GFP-tagged proteins (PLCδ-PH and POP) were visualised in live wild-type cells growing in log phase at 30°C. Confocal images of cells were taken immediately after plating onto a glass slide and spread gently by application of a coverslip. Images from the top row have been enlarged and are shown in the bottom row. Single confocal sections. Scale bar (10μm).

Figure 3.4.2: Effect of deletion of synaptojanin-like proteins in yeast on localisation of GFP-POP

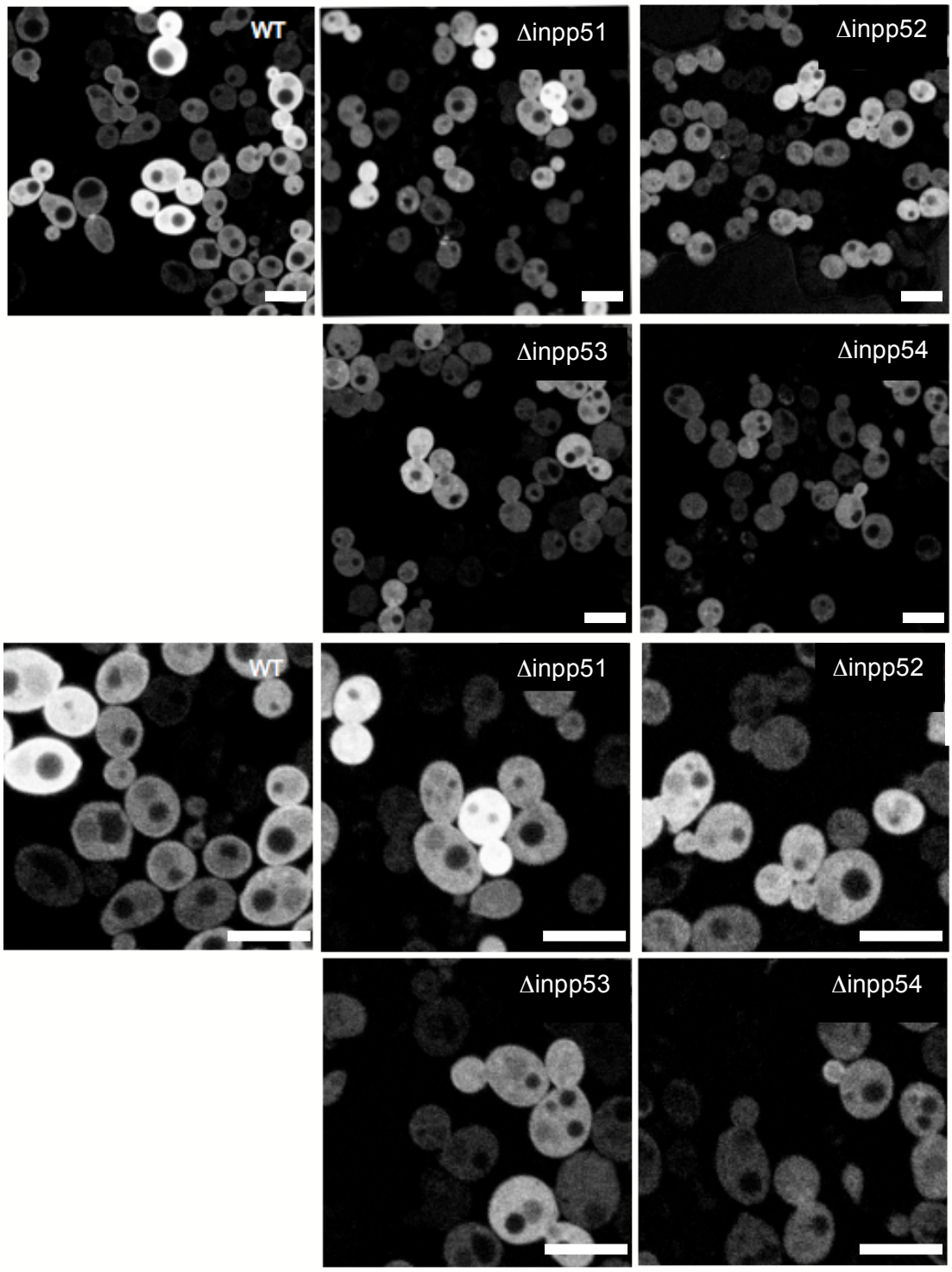

(2x magnification)

Figure 3.4.2 legend: GFP-POP was visualised in wild-type and mutant yeast (synaptojanin-like family member deleted is labelled in the top right hand corner) growing in log phase at 30°C. Confocal images of cells were taken immediately after plating onto a glass slide and spread gently by application of a coverslip. Images from the top two rows have been enlarged and are shown in the bottom two rows. Single confocal sections. Scale bar (10μm).

Figure 3.4.3: Effect of PLC1 deletion on localisation of GFP-PLCδ-PH and GFP-POP

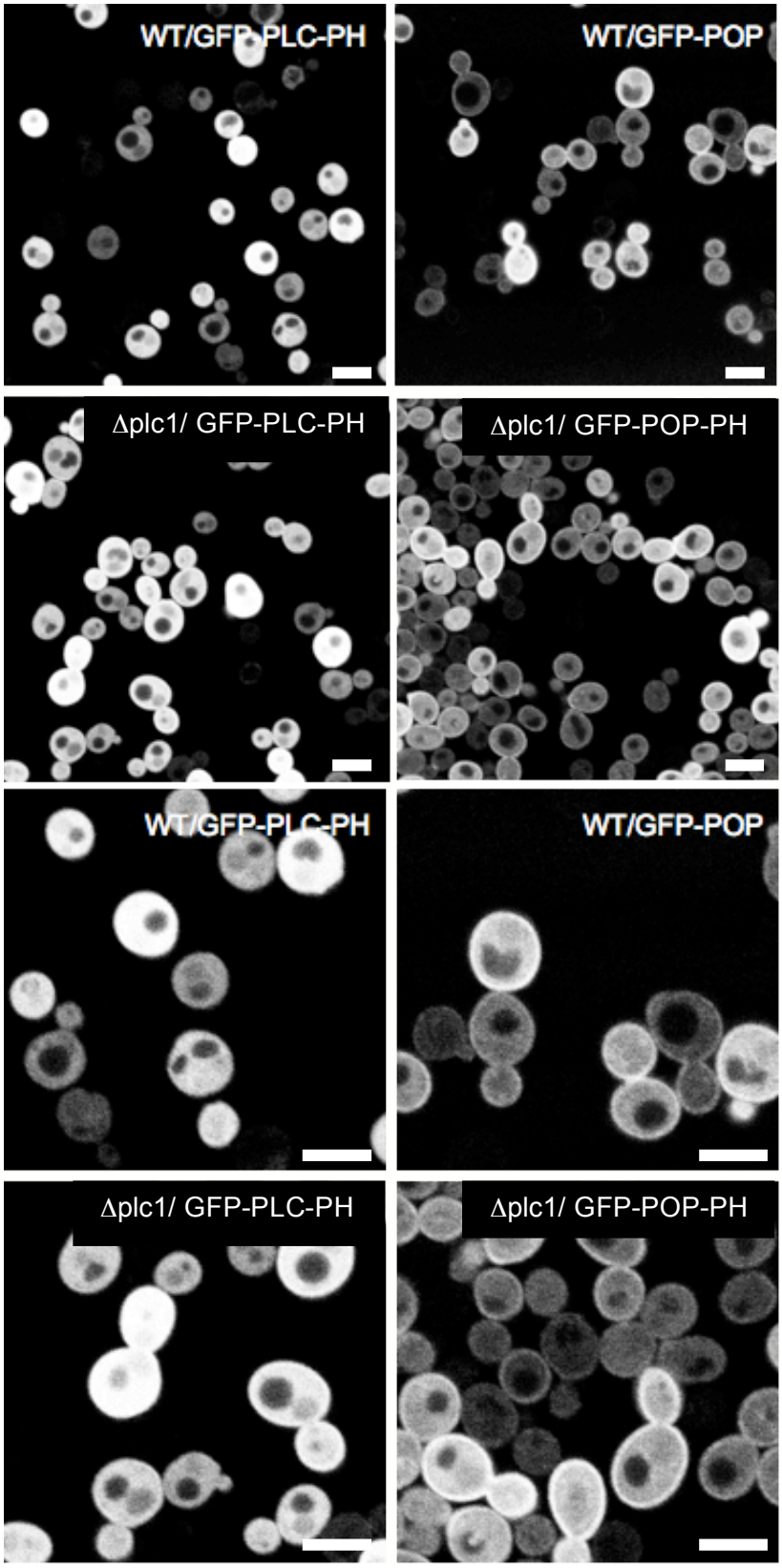

(2x magnification)

Figure 3.4.3 legend: GFP-tagged proteins (PLCδ-PH and POP) were visualised in live wild-type and PLC1 delete cells growing in log phase at 30°C. Confocal images of cells were taken immediately after plating onto a glass slide and spread gently by application of a coverslip. Images from the top two rows have been enlarged and are shown in the bottom two rows. Single confocal sections. Scale bar (10μm).

Chapter 4:
OCRL1 and Calcium Signalling

4: OCRL1 and calcium signalling

Cells taken from Lowe Syndrome patients have elevated levels of PI(4,5)P2 [36]. Regulation of the level and localisation of PI(4,5)2 is integral to many cell signalling pathways. Upon stimulation of G-protein mediated PLC family members, PI(4,5)P2 is readily hydrolysed to IP3 and DAG. The IP3 generated from this event causes the release of calcium stores into the cytosol, through the IP3 receptor [157]. IP3-sensitive calcium stores include organelles such as the endoplasmic reticulum and Golgi apparatus, the latter of which OCRL1 localises to.

If OCRL1 5-phosphatase activity regulates a signalling pool of PI(4,5)P2, cells without OCRL1 may exhibit a difference in intracellular calcium handling. It is possible that elevated PI(4,5)P2 levels as a result of OCRL1 loss has a knock-on effect on the speed and magnitude of calcium store release, through an increase in substrate availability for PLC family members. It is also possible that OCRL1 functions to dampen the IP3 signal by dephosphorylating IP3 to inositol(1,4)-bisphosphate (IP2). This means that IP3 may persist in the cytosol of a cell lacking OCRL1, which may change the kinetics of calcium levels in the cytosol. In support of this hypothesis, inositol polyphosphate 5-phosphatases specific to PI(4,5)P2 have been shown to have very important roles in calcium signalling [26, 85].

Furthermore, our previous results are intricately linked to this hypothesis. We have demonstrated a change in localisation of Annexin A2 upon OCRL1 depletion. Previous work has shown that Annexin A2 binding to PI(4,5)P2 is enhanced by the presence of calcium. Therefore the altered distribution of Annexin A2 upon OCRL1 loss may be due to a change in calcium levels as well as PI(4,5)P2 levels and localisation. Also, it is possible that Annexin A2 redistribution corresponds to a functional role, tightly linked to regulation of intracellular calcium levels. Annexin A2 has been shown to be an effective inhibitor of G-protein mediated PLC activation [158]. Therefore Annexin A2 redistribution may represent a homeostatic inhibition of uncontrolled IP3-mediated calcium signalling in OCRL1 depleted cells.

All these ideas suggest that OCRL1 plays a negative role in calcium signalling by keeping PI(4,5)P2 and IP3 levels down. Conversely, loss of OCRL1 function may lead to a reduction in the ability of the cell to release calcium stores upon stimulation. It has been shown that PI(4,5)P2 has an inhibitory effect upon the IP3 receptor [86]. Therefore, should PI(4,5)P2 levels be elevated at sites containing the IP3 receptor, or increased PI(4,5)P2 levels at the plasma membrane be in apposition to internal membranes containing the IP3 receptor, an inhibition of calcium signalling would be anticipated. This suggests that OCRL1 might play a positive role in calcium signalling in the cell. Only upon PLC stimulation and subsequent hydrolysis of PI(4,5)P2 would this inhibition be relieved, with IP3 competing with PI(4,5)P2 for the IP3 receptor. IP3 has a much greater binding affinity than PI(4,5)P2 for the IP3 receptor and would therefore have the dominating interaction upon IP3

generation. Many other receptors and channels important in calcium signalling have been shown to be affected by PI(4,5)P2 and it was felt a study of OCRL1 and calcium signalling was warranted [87].

Histamine and ATP are known stimuli for G-protein coupled PLC activation and can be used for analysis of the IP3-sensitive calcium response. To investigate the effect of OCRL1 depletion upon calcium signalling in HeLa cells, two different concentrations of histamine were used: one submaximal dose (10μM) and one maximal dose (100μM). In comparison to mock siRNA treated HeLa cells, a greater increase in intracellular calcium levels was observed upon stimulation with both concentrations of histamine after 48 hours and 72 hours treatment with OCRL1 siRNA (Figure 4.1.1 and Figure 4.1.3, filled bars). Little or no difference was observed in the kinetics of calcium levels in the cytosol, with peaks of calcium levels being achieved within the same time-frame, regardless of cell treatment (Figure 4.1.2 and Figure 4.1.4).

Treatment of cells with a sarco/endoplasmic reticulum calcium ATPase (SERCA) pump inhibitor, thapsigargin, causes the release of intracellular stored calcium. Histamine treatment of cells was followed by application of thapsigargin, in order to deplete residual levels of calcium in stores. A higher calcium concentration in the cytosol was observed in OCRL1 depleted cells in comparison with mock siRNA treated cells after treatment with thapsigargin (striped bars; Figure 4.1.1 and Figure 4.1.3). This indicated that it was possible that total store calcium was elevated in OCRL1 siRNA treated cells,

or an increase in the store-operated calcium influx pathway through the plasma membrane. To test these findings further, cells were treated with thapsigargin alone as a measure of IP3-independent changes in cytosolic calcium. Clear differences in cytosolic calcium levels between mock siRNA treated and OCRL1 siRNA treated cells were observed, with OCRL1 depleted cells comparatively showing an approximate 2-fold increase in cytosolic calcium (Figures 4.2.1-4.2.2). This result indicates one of two things; either total store calcium in cells depleted of OCRL1 is higher, leading to higher levels of calcium release into the cytosol, or more calcium is entering the cell from the extracellular medium upon thapsigargin treatment, through capacitative calcium entry. The two phases of calcium elevation are representative of the initial IP3-dependent release of calcium stores, and then a second wave representative of store-operated calcium entry. These data suggest that the increased level of cytosolic calcium in OCRL1 RNAi treated cells upon thapsigargin alone suggests that the differences observed upon histamine treatment between control and OCRL1 siRNA treated cells (Figures 4.1.1-.4.1.4) may not be IP3-dependent, but due to increases in total store calcium or calcium entry from the extracellular medium.

To test these theories, we analysed calcium signalling in these cells in the presence of an extracellular calcium chelator, BAPTA. Upon stimulation with thapsigargin in the presence of BAPTA, we found that there was no difference to the change in cytoplasmic calcium between control siRNA and OCRL1 siRNA treated cells (Figure 4.3.1, *left hand pair of bars*). Thapsigargin treatment causes the ER stores of calcium to become depleted into the

cytoplasm. Upon calcium entry into the cytoplasm, different channels become activated, such as plasma membrane calcium ATPases (PMCAs) and store-operated calcium channels (SOCs). In this experiment, upon ER calcium release, the cell extrudes cytoplasmic calcium through the plasma membrane, where it is chelated by the BAPTA in the extracellular medium. This process activates and primes SOCs at the plasma membrane, but no calcium can enter the cell through the plasma membrane, as it has been buffered out. However, upon addition of excess calcium to the extracellular medium, we can monitor the calcium entry back through the plasma membrane. We hypothesised that OCRL1 may alter levels of PI(4,5)P2 at the plasma membrane, where it may regulate plasma membrane SOCs. Upon re-addition of calcium to the extracellular medium, we saw a rapid rise in cytosolic calcium in both populations of cells, indicative of calcium entry through plasma membrane channels. We observed that cells depleted of OCRL1 allowed more calcium to enter from the extracellular medium (Figure 4.3.1, *right hand pair of bars*). This elevated level of calcium was maintained and formed a sustained plateau, in a similar pattern to control siRNA treated cells. It is noteworthy that the shape of both graphs was very similar, the difference being the amplitude of response to re-addition of calcium (Figure 4.3.2).

In previous studies, OCRL1 has been shown to translocate to the plasma membrane, either to plasma membrane clathrin coated pits, or to membrane ruffles upon growth factor treatment. The latter study suggested that OCRL1 moves to the plasma membrane upon certain stimuli that evoke calcium signalling (namely EGF treatment), perhaps in order to reduce PI(4,5)P2

levels or pools, to switch off the PLC/IP3 signalling cascade. For this reason, we decided to look at whether OCRL1 changes its distribution upon histamine treatment. We found that OCRL1 translocated to the plasma membrane and distributed itself in a non-linear pattern of punctate dots as soon as one minute after histamine treatment. Furthermore, this localisation to the plasma membrane became stronger as time passed, and was particularly prominent at later time points such as ten minutes, and even as long as one hour post-stimulation (Figure 4.4). OCRL1 localisation to the plasma membrane in the time period of one minute to ten minutes was of particular importance, as this is the period after histamine stimulation in which levels of calcium in the cytosol begin to reduce. This is the period in which OCRL1 depleted cells display a higher level of calcium in the cytosol. Given our theory that increased calcium levels in the cytosol of OCRL1 depleted cells seems to be due to flow from the extracellular medium, this observation seems to fit in with the kinetics of the calcium measurements. It seems that OCRL1 may translocate to the plasma membrane after stimulation in order to regulate capacitative calcium entry and turn off IP3 generation.

To further our findings that OCRL1 loss affects calcium signalling, we decided to look at skin fibroblasts taken from two different Lowe Syndrome patients (these cells were designated the names, Lowe B and Lowe 2). These cells may provide more meaningful insights into the effect of OCRL1 in calcium signalling, as RNAi treatment only looks at short-term, transient downstream consequences of OCRL1 loss. We found that these fibroblasts responded best to ATP rather than histamine and assessed responses of the these cells

to three difference doses of ATP, 10μM, 50μM and 100μM. Unfortunately there seemed to be no consistency between Lowe B and Lowe 2 cells, however both were consistently different from control skin fibroblasts.

At the lowest dose of 10μM ATP there were clear differences in the way Lowe Syndrome fibroblasts responded in comparison to contol traces. (Figure 4.5.1). Control fibroblast traces show cytosolic calcium levels rapidly reaching a peak within the first minute of stimulation. Calcium levels then fall rapidly, traces displaying a plateau at 200 seconds, indicative of capacitative calcium entry, and finally fall down to base level again 600 seconds post stimulation. (Figure 4.5.1, red line trace) However, the initial response of Lowe B cells to 10μM ATP is much less in amplitude and speed. (Figure 4.5.1, green line trace) Lowe B fibroblasts only reach approximately half the peak calcium level of control fibroblasts and much slower, at 300 seconds (Figure 4.5.2). The cytosolic calcium level then fails to drop back down to zero during the 20 minute period of measurement. In comparison, the response of Lowe 2 cells is very different to both Lowe B and control fibroblast responses. Lowe 2 fibroblasts achieve a peak calcium level in the cytosol within the first minute post stimulation, a little higher than control fibroblasts, however this level is only slightly reduced in the time period after. A very high calcium level is maintained in the cytosol, indicating that either the cell is failing to pump out calcium from the cytosol, or is allowing too much calcium to enter through plasma membrane channels. The failure of Lowe Syndrome fibroblasts to reduce cytosolic calcium back down to resting levels is clearly observed when comparing control, Lowe B and Lowe 2 calcium levels at the 600 second time

point (Figure 4.5.2, light grey bars). Whereas control fibroblast calcium levels are nearly back down to resting levels, Lowe B levels are a bit higher and Lowe 2 levels are significantly raised, remaining so even up to 20 minutes post stimulation.

This trend was reproducible with a higher dose of 50μM ATP (Figures 4.5.3 and 4.5.4). Again, within one minute, peak levels of calcium in the cytosol were observed in control and Lowe 2 cells, with Lowe 2 displaying a slightly higher peak calcium level than control fibroblasts. However, Lowe B cells exhibited a much lower average calcium level and in a much slower fashion, reaching its peak at approximately 300 seconds post stimulation. (Figure 4.5.3). Like responses to 10μM ATP, Lowe 2 cells maintained a significantly high level of cytosolic calcium in comparison to control cells, clearly observed when comparing calcium levels at the 600 second time point (Figure 4.5.4, light grey bars) . Again, when looking at the final values 20 minutes post-stimulation, control responses are back down to basal values, whereas Lowe B and Lowe 2 cells maintain a higher level of cytosolic calcium.

At a maximal dose of 100μM ATP, we saw the strongest responses, however the pattern of differences between Lowe Syndrome fibroblasts and control fibroblasts was slightly different (Figures 4.5.5 and 4.5.6). Again, sharp responses to ATP were seen with control and Lowe 2 fibroblasts, both peaking within one minute. However the highest peak calcium level was observed with control fibroblasts, suggesting that a dose of 10-50μM ATP is maximal for Lowe 2 fibroblasts, perhaps representing a heightened sensitivity

to agonist in Lowe 2 fibroblasts. A much-weakened response was observed with Lowe B fibroblasts, with low peak calcium levels and an average line trace that at some time-points dipped lower than resting values (Figure 4.5.5). Again, a very high level of cytosolic calcium was maintained in Lowe 2 fibroblasts up to 20 minutes post stimulation, whereas control and Lowe B fibroblast cytosolic calcium returned back to resting levels. This again has been shown by plotting calcium levels of the three cell types at the 600 second time-point post stimulation with a ATP. It is noteworthy that in wild-type cells the shape of calcium response was very similar at every concentration of ATP stimulation. However, these characteristic sharp peaks, troughs and returns to basal levels were unseen in Lowe Syndrome fibroblasts. In Lowe Syndrome fibroblasts, acute peaks of cytosolic calcium upon ATP stimulation were not observed. Interestingly, if calcium levels were elevated above basal levels upon ATP stimulation, it was persistent within the cytoplasm. This is suggestive of a failure to extrude calcium out of the cell, or buffer it back into internal organelles such as the ER, Golgi or lysosomes.

To further elucidate the mechanism of the differences observed between Lowe Syndrome fibroblasts and control fibroblasts, we assessed the responses of these cells to an IP3-independent stimulus for calcium release, thapsigargin. (Figures 4.5.7 and 4.5.8). Control and Lowe 2 responses to thapsigargin were very similar, with a peak calcium level in the cytosol observed within 2 minutes and then slowly reducing as time passed (Figure 4.5.7, red and blue line traces, respectively). Interestingly, the response of Lowe B to thapsigargin was the most intriguing (Figure 4.5.7, green line

trace). Given the poor responses of Lowe B cells to ATP, a weak response to thapsigargin may have been expected. Surprisingly, the initial response to thapsigargin was very similar to control and Lowe 2 fibroblasts and as time passed, the level of cytosolic calcium continued to rise, producing a second peak in cytosolic calcium which is maintained all the way through to the final time point measured at 20 minutes post stimulation. This difference is clearly observed when plotting the cytosolic calcium levels at the 600 second time point (Figure 4.5.8, grey bars), with a significantly higher value in Lowe B cells. Furthermore, when comparing the peak calcium level to the 600 second time point in all measurements, we notice a consistent reduction in the ratio between the two. Beneath each graph of response kinetics, the ratio of peak to 600 second time points is consistently lower with loss of OCRL1 activity, be it through OCRL1 depletion or in Lowe Syndrome patient fibroblasts. This suggests that cells lacking OCRL1 either fail to buffer out the initial increase in cytoplasmic calcium through efflux mechanisms, and/or a sustained, unregulated level of SOC entry.

These data show that Lowe Syndrome cells handle calcium levels very differently to control fibroblasts. Taking data from responses to thapsigargin, Lowe B cells contain a similar level of store calcium to Lowe 2 and control fibroblasts (Figures 4.5.7-4.5.8). However, at later time points when capacitative calcium entry occurs, the cytosolic calcium level is higher and maintained at this level. However Lowe B cells respond in a much weaker fashion to extracellular agonist in comparison to other cells, suggesting that the signalling pathway to calcium store release may have been attenuated in

some manner, perhaps by downregulating the receptor for ATP. The reason for this downregulation could be suggested from the observed heightened ATP responses to Lowe 2 cells (Figure 4.5.1-4.5.6, blue line traces), which seem to have a heightened sensitivity to ATP leading to greater calcium responses in comparison to control traces. It may be possible that the way in which cells from Lowe Syndrome patients have adapted to OCRL1 loss affects the severity of their condition. Hypersensitive calcium responses to agonist would be highly detrimental to many physiological processes, however without details of the patients these cells have been taken from, these results cannot be tallied to the severity of Lowe Syndrome. It may be the case that there is so much variability that we need to test a higher number of different cell lines, from control and Lowe Syndrome patients, in order to obtain a typical phenotype.

4.1: Effect of OCRL1 depletion on calcium signalling in HeLa cells

Figure 4.1.1. Relative changes in Fluo-4 fluorescence after application of 10μM histamine and 1μM thapsigargin

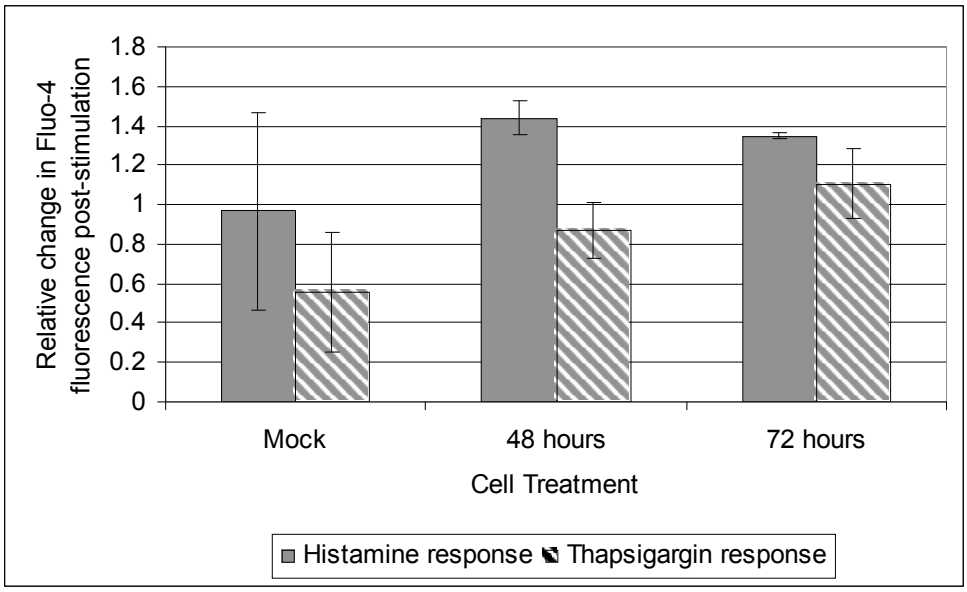

Figure 4.1.1 legend: HeLa cells were treated with mock siRNA for 72 hours or OCRL1 siRNA for 48 or 72 hours. Cells were loaded with Fluo-4 AM 45 minutes prior to stimulation. Cells were stimulated with 10μM histamine and imaged for 10 minutes. After 10 minutes cells were then stimulated with 1 μM thapsigargin and imaged for 5 minutes. All experiments were done at room temperature. Each bar is representative of 3 wells. All data are expressed as relative arbitrary values, normalised against basal Fluo-4 fluorescence before stimulation. Error bars are standard deviations.

Figure 4.1.2. Kinetics of relative change in Fluo-4 fluorescence after application of 10μM histamine and 1μM thapsigargin

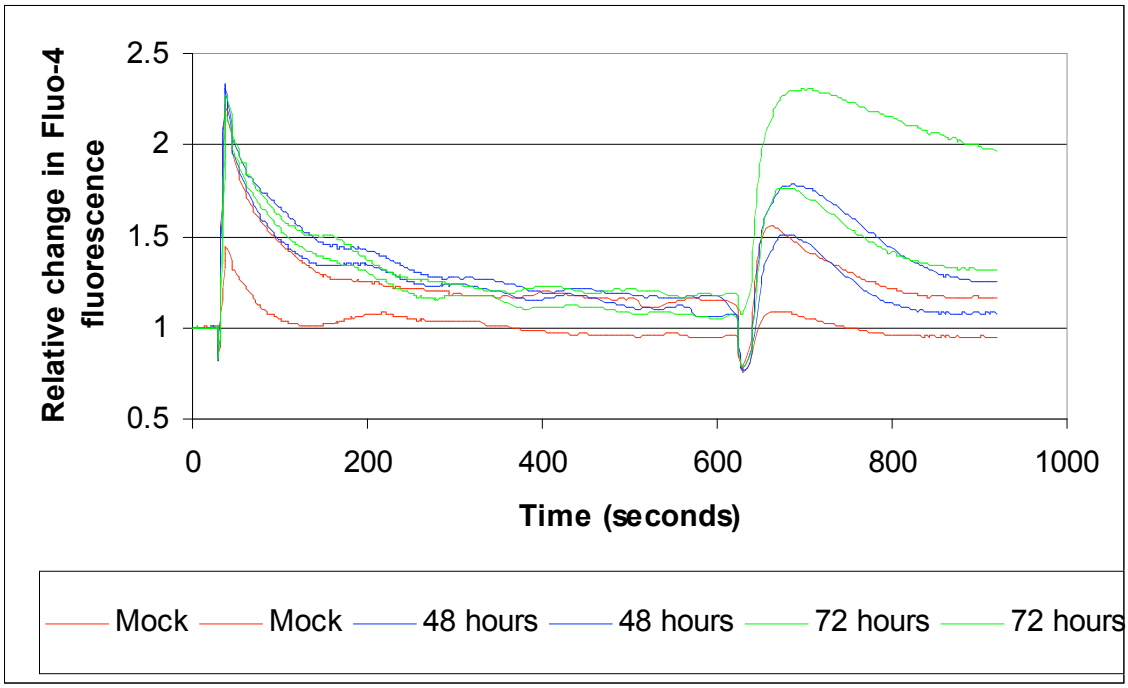

Figure 4.1.2. legend: HeLa cells were treated with mock siRNA for 72 hours or OCRL1 siRNA for 48 or 72 hours. Cells were loaded with Fluo-4 AM 45 minutes prior to stimulation. Cells were stimulated with 10μM histamine and imaged for 10 minutes. After 10 minutes cells were then stimulated with 1 μM thapsigargin and imaged for 5 minutes. All experiments were done at room temperature. Two examples of each cell treatment are represented on the graph, choice was made based on highest basal Fluo-4 fluorescence. All data are expressed as relative arbitrary values, normalised against basal Fluo-4 fluorescence before stimulation.

Figure 4.1.3. Relative changes in Fluo-4 fluorescence after application of 100μM histamine and 1μM thapsigargin

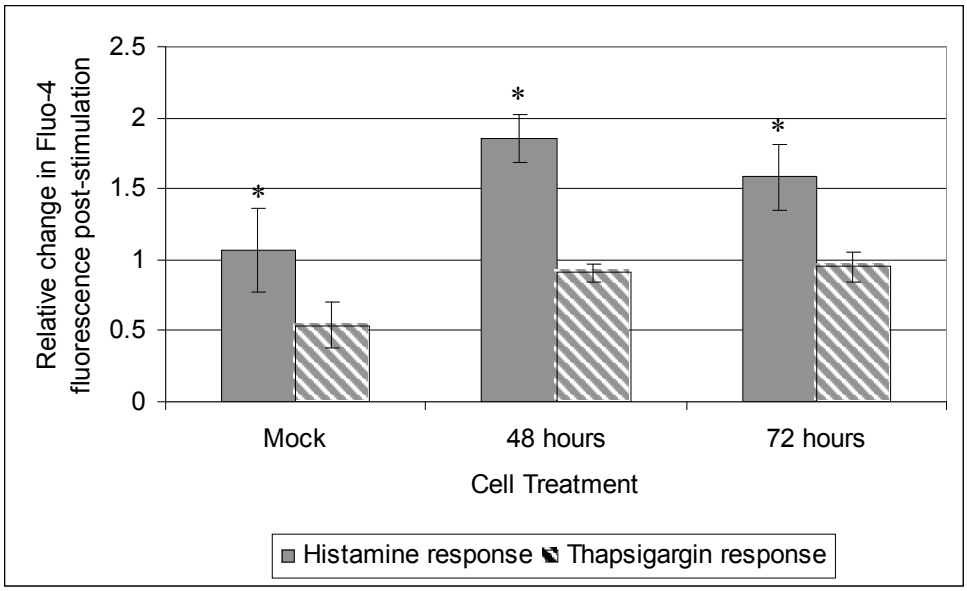

Figure 4.1.3. legend: HeLa cells were treated with mock siRNA for 72 hours or OCRL1 siRNA for 48 or 72 hours. Cells were loaded with Fluo-4 AM 45 minutes prior to stimulation. Cells were stimulated with 100μM histamine and imaged for 10 minutes. After 10 minutes cells were then stimulated with 1 μM thapsigargin and imaged for 5 minutes. All experiments were done at room temperature. Each bar is representative of 3 wells. All data are expressed as relative arbitrary values, normalised against basal Fluo-4 fluorescence before stimulation. Error bars are standard deviations. * T-tests comparing siRNA treated cells with controls produce p values < 0.05.

Figure 4.1.4. Kinetics of relative change in Fluo-4 fluorescence after application of 100µM histamine and 1µM thapsigargin

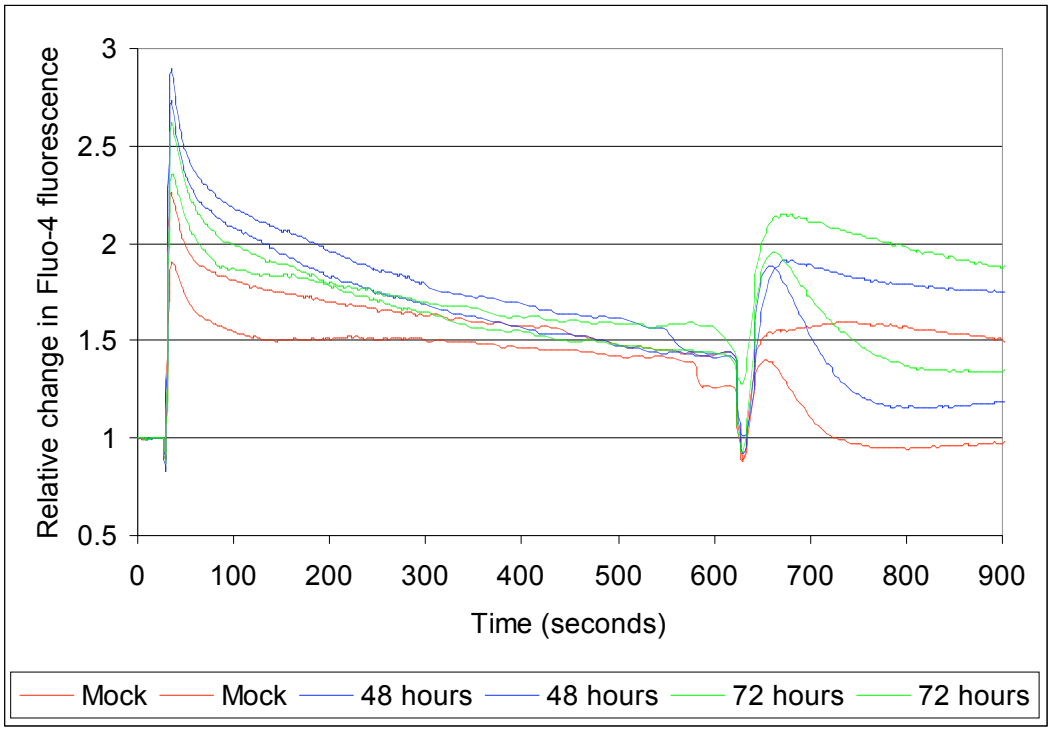

Figure 4.1.4. legend: HeLa cells were treated with mock siRNA for 72 hours or OCRL1 siRNA for 48 or 72 hours. Cells were loaded with Fluo-4 AM 45 minutes prior to stimulation. Cells were stimulated with 100µM histamine and imaged for 10 minutes. After 10 minutes cells were then stimulated with 1 µM thapsigargin and imaged for 5 minutes. All experiments were done at room temperature. Two examples of each cell treatment are represented on the graph, choice was made based on highest basal Fluo-4 fluorescence. All data are expressed as relative arbitrary values, normalised against basal Fluo-4 fluorescence before stimulation.

4.2: Effect of OCRL1 loss on total store calcium in HeLa cells

Figure 4.2.1. Measurement of total store calcium by cell response to thapsigargin alone

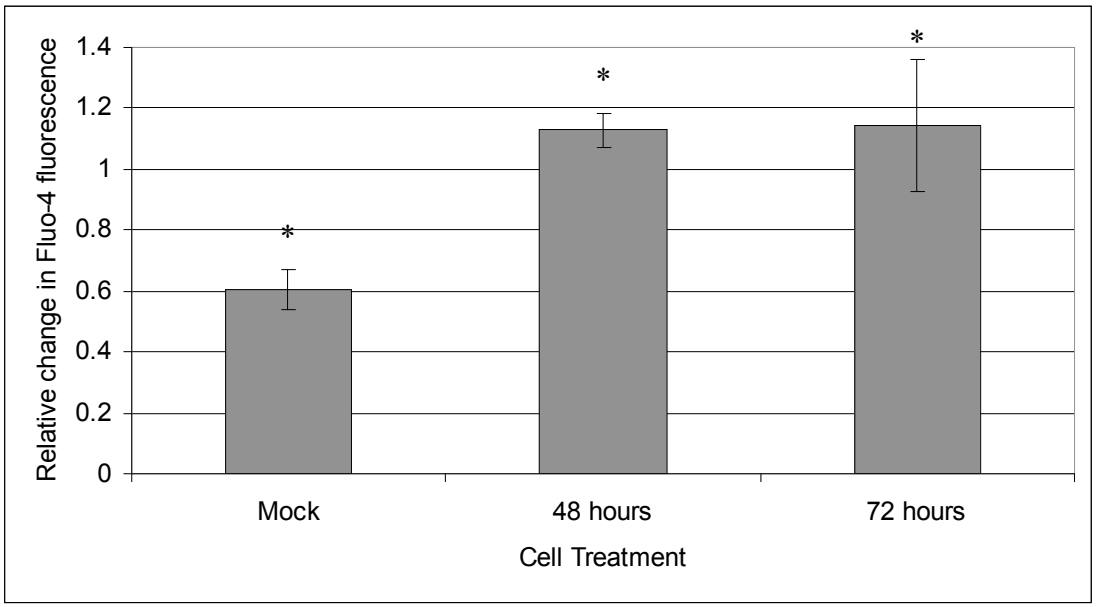

Figure 4.2.1. legend: HeLa cells were treated with mock siRNA for 72 hours or OCRL1 siRNA for 48 or 72 hours. Cells were loaded with Fluo-4 AM 45 minutes prior to stimulation. Cells were mock stimulated with buffer and imaged for 10 minutes. After 10 minutes cells were then stimulated with 1 μM thapsigargin and imaged for 5 minutes. All experiments were done at room temperature. Each bar is representative of 3 wells. All data are expressed as relative arbitrary values, normalised against basal Fluo-4 fluorescence before stimulation. Error bars are standard deviations. * T-tests comparing siRNA treated cells with controls produce p values < 0.05.

Figure 4.2.2. Kinetics of total store calcium release

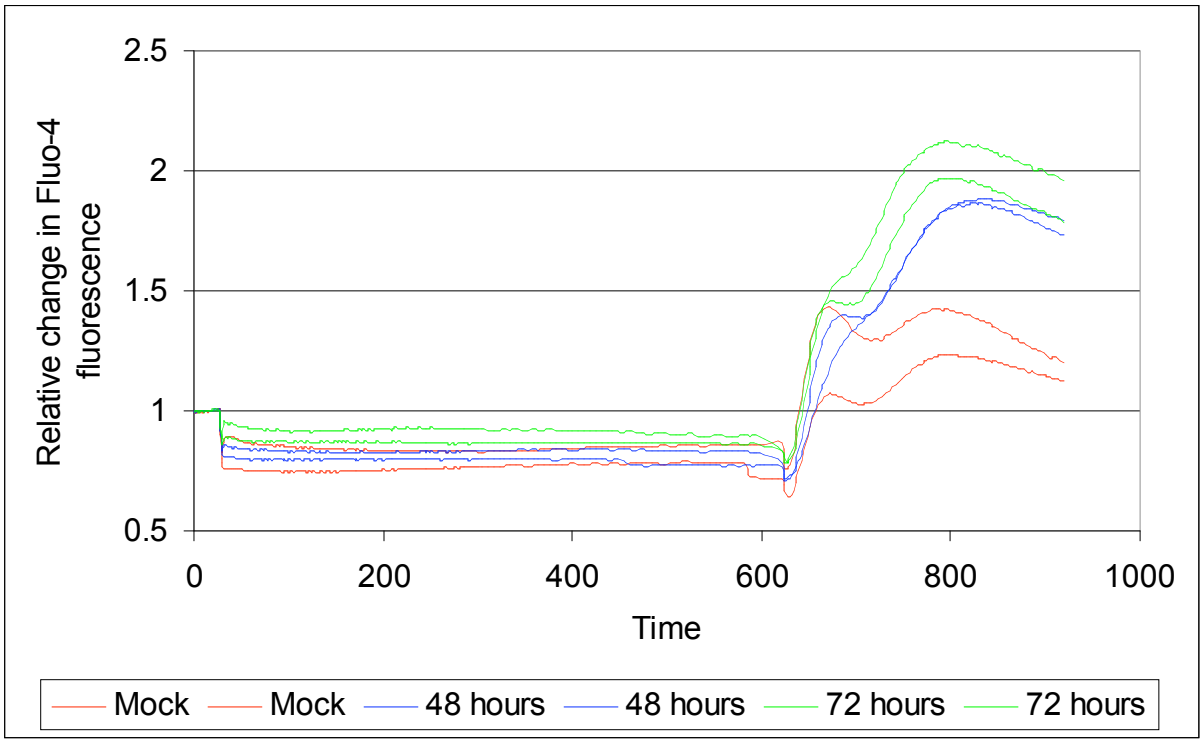

Treatment	Peak/Plateau ratio
Control siRNA	0.87
OCRL1 siRNA (48)	0.64
OCRL1 siRNA (72)	0.53

Figure 5.2.2. legend: HeLa cells were treated with mock siRNA for 72 hours or OCRL1 siRNA for 48 or 72 hours. Cells were loaded with Fluo-4 AM 45 minutes prior to stimulation. Cells were mock stimulated with buffer and imaged for 10 minutes. After 10 minutes cells were then stimulated with 1 μM thapsigargin and imaged for 5 minutes. All experiments were done at room temperature. Two examples of each cell treatment are represented on the graph, choice was made based on highest basal Fluo-4 fluorescence. All data are expressed as relative arbitrary values, normalised against basal Fluo-4 fluorescence before stimulation.

4.3: Elucidating the origin of elevated cytosolic calcium in OCRL1 depleted cells

Figure 4.3.1: Measurement of cytosolic calcium after thapsigargin treatment and calcium add-back in calcium-free conditions

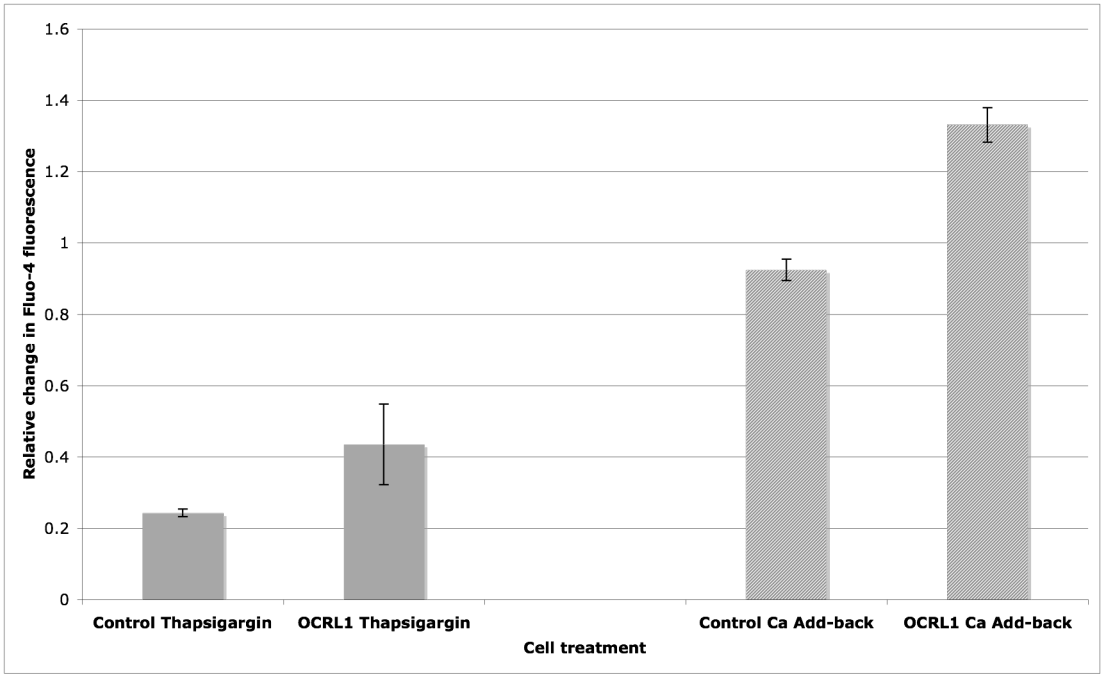

Figure 4.3.1. legend: HeLa cells were treated with mock siRNA for 72 hours or OCRL1 siRNA for 72 hours. Cells were loaded with Fluo-4 AM 45 minutes prior to stimulation. Cells were stimulated with 1 μM thapsigargin, in the presence of 10mM BAPTA and imaged for 10 minutes. After 10 minutes, regular extracellular medium with 50mM $CaCl_2$, was applied to cells and monitored for 5 minutes. All experiments were done at room temperature. Three examples of each cell treatment are represented on the graph. All data are expressed as relative arbitrary values, normalised against basal Fluo-4 fluorescence before stimulation.

Figure 4.3.2: Kinetics of change of Fluo-4 fluorescence after thapsigargin treatment and calcium add-back in calcium-free conditions

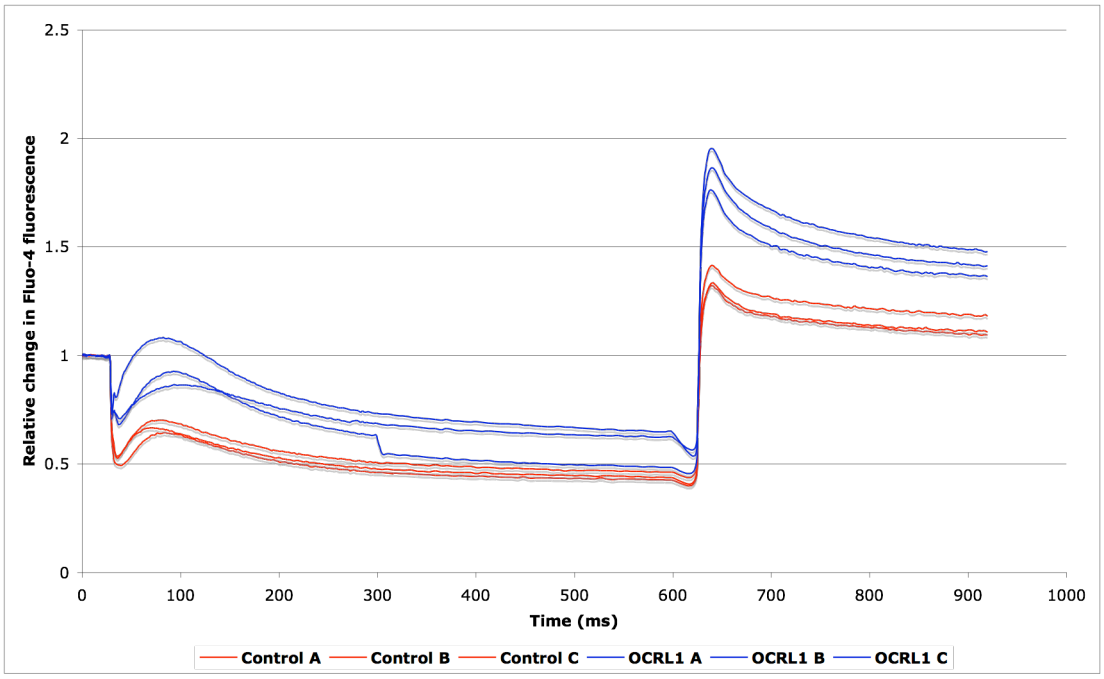

Figure 4.3.2. legend: HeLa cells were treated with mock siRNA for 72 hours or OCRL1 siRNA for 72 hours. Cells were loaded with Fluo-4 AM 45 minutes prior to stimulation. Cells were stimulated with 1 μM thapsigargin, in the presence of 20mM BAPTA and imaged for 10 minutes. The reduction in fluorescence upon application of BAPTA represents the chelation of free calcium. After 10 minutes, regular extracellular medium with 50mM $CaCl_2$, was applied to cells and monitored for 5 minutes. All experiments were done at room temperature. Three examples of each cell treatment are represented on the graph. All data are expressed as relative arbitrary values, normalised against basal Fluo-4 fluorescence before stimulation.

4.4: OCRL1 localisation after histamine treatment

Figure 4.4: Localisation of GFP-OCRL1 upon histamine stimulation

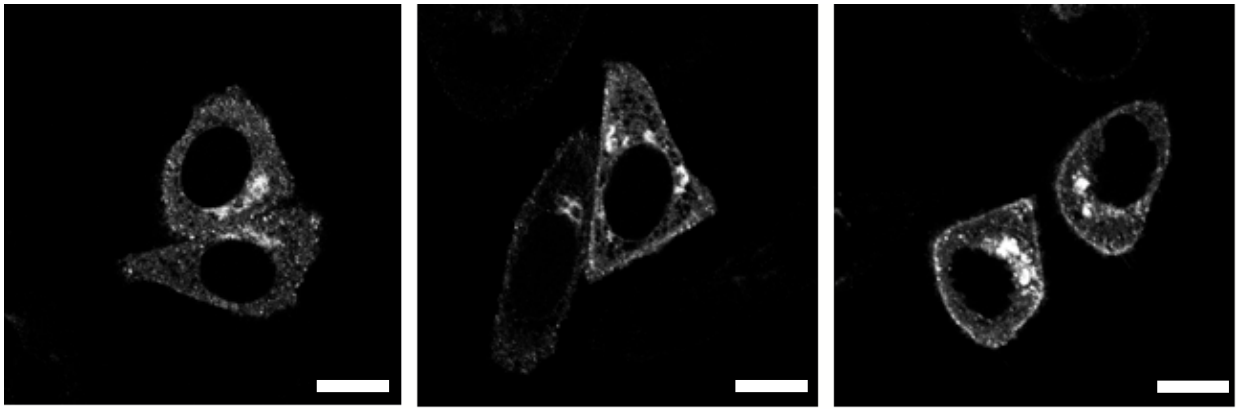

1 minute 10 minutes 1 hour

Figure 4.4 legend: HeLa cells were transfected with 0.4μg GFP-OCRL1 DNA using lipofectamine, grown for 16 hours and treated with 100μM histamine for either 1 minute (left panel), 10 minutes (middle panel) or 1 hour (right panel). Cells were then fixed using 4% PFA and visualised using a Leica confocal microscope. All experiments were undertaken at room temperature. Single confocal sections. Scale bar (10μm).

4.5: Calcium signalling in Lowe Syndrome patient skin fibroblasts

Figure 4.5.1: Response of Lowe Syndrome fibroblasts to 10μM ATP

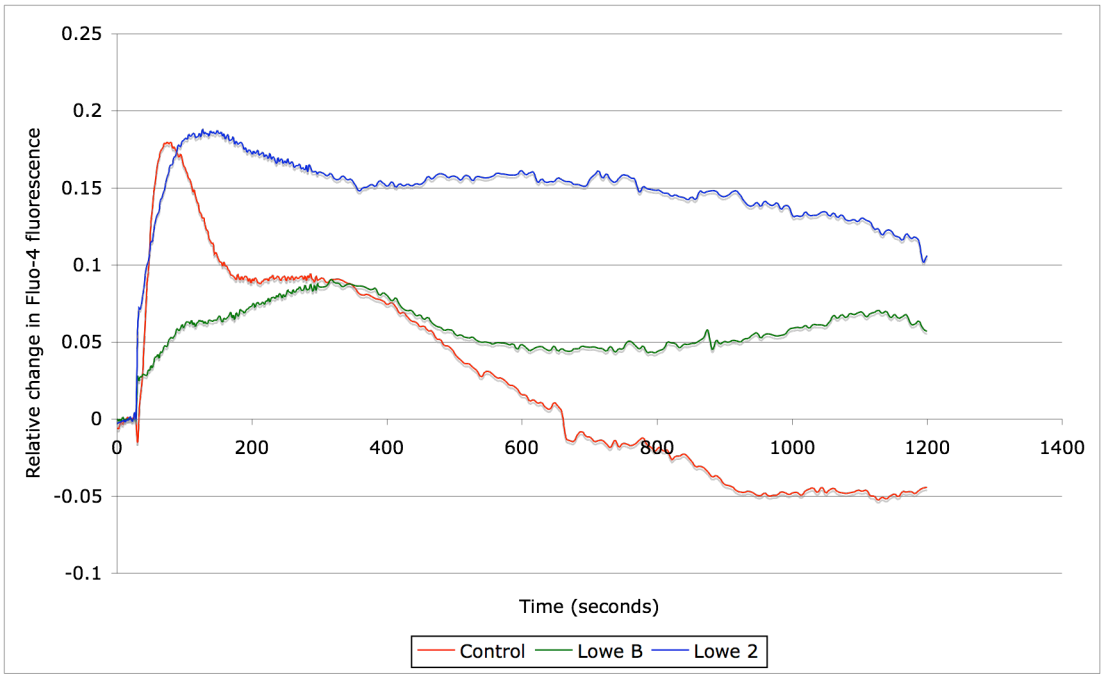

Cell type	Peak/600 sec ratio
Control	3.42
Lowe B	1.8
Lowe 2	1.17

Figure 4.5.1. legend: Fibroblasts were plated at 100% confluence one day before experiments. Cells were loaded with Fluo-4 AM 45 minutes prior to stimulation. Cells were mock stimulated with buffer or 10μM ATP and imaged for 20 minutes. All experiments were done at room temperature. Line traces represent six independent tests on the graph. All data are expressed as relative arbitrary values, normalised against basal Fluo-4 fluorescence before stimulation and with mock stimulated cell responses deleted from final values.

Figure 4.5.2: Analysis of response of Lowe Syndrome fibroblasts to 10μM ATP

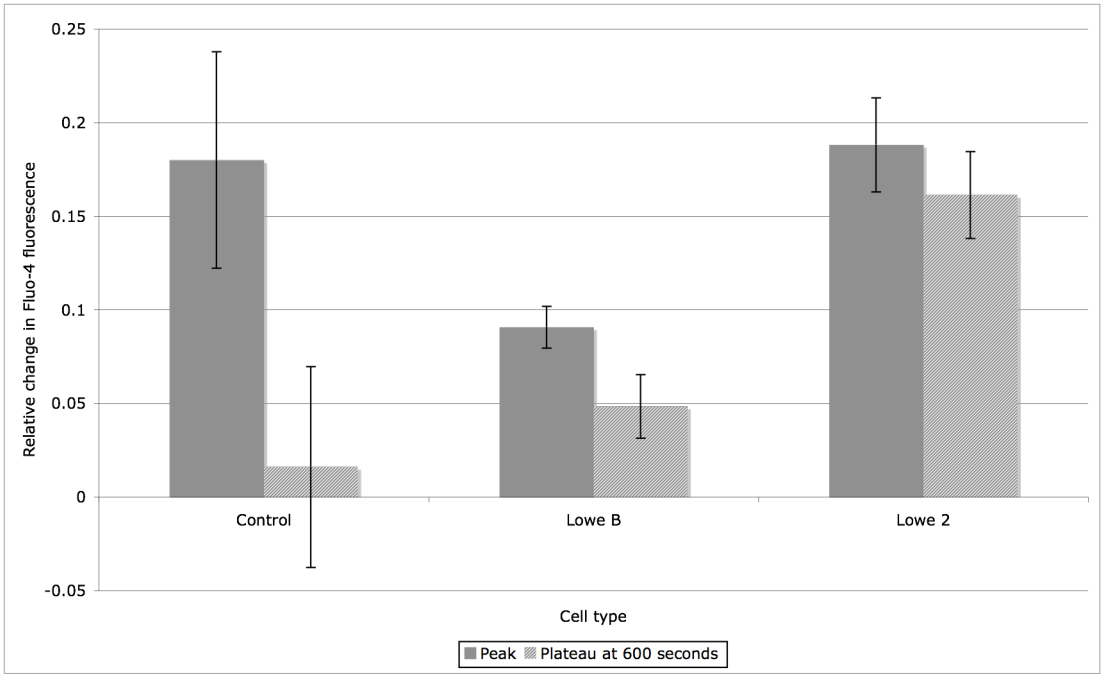

Figure 4.5.2. legend:. Fibroblasts were plated at 100% confluence one day before experiments. Cells were loaded with Fluo-4 AM 45 minutes prior to stimulation. Cells were mock stimulated with buffer or 10μM ATP and imaged for 20 minutes. All experiments were done at room temperature. Data are plotted for the peak calcium level in the cytosol (dark grey bars) and level of calcium at the 600 second time-point post stimulation (light grey bars). These data are representative of six independent experiments. All data are expressed as relative arbitrary values, normalised against basal Fluo-4 fluorescence before stimulation and with mock stimulated cell responses deleted from final values. Error bars are standard deviations.

Figure 4.5.3: Response of Lowe Syndrome fibroblasts to 50μM ATP

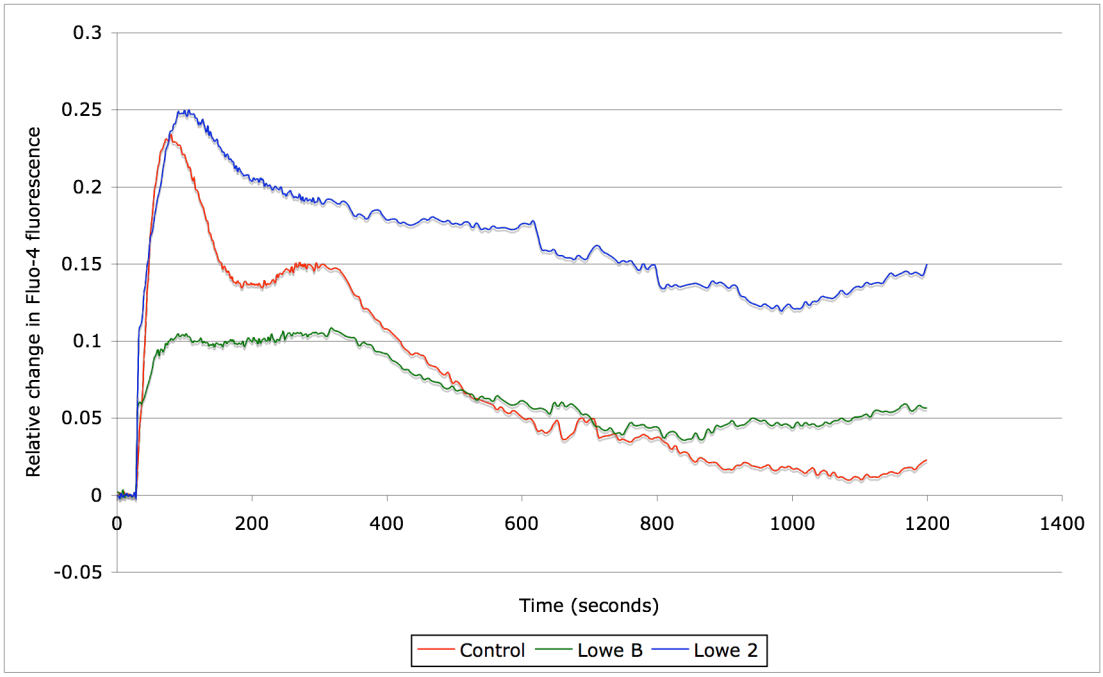

Cell type	Peak/600 sec ratio
Control	4.8
Lowe B	1.83
Lowe 2	1.41

Figure 4.5.3. legend: Fibroblasts were plated at 100% confluence one day before experiments. Cells were loaded with Fluo-4 AM 45 minutes prior to stimulation. Cells were mock stimulated with buffer or 50μM ATP and imaged for 20 minutes. All experiments were done at room temperature. Line traces represent six independent tests on the graph. All data are expressed as relative arbitrary values, normalised against basal Fluo-4 fluorescence before stimulation and with mock stimulated cell responses deleted from final values. Error bars are standard deviations.

Figure 4.5.4: Analysis of response of Lowe Syndrome fibroblasts to 50μM ATP

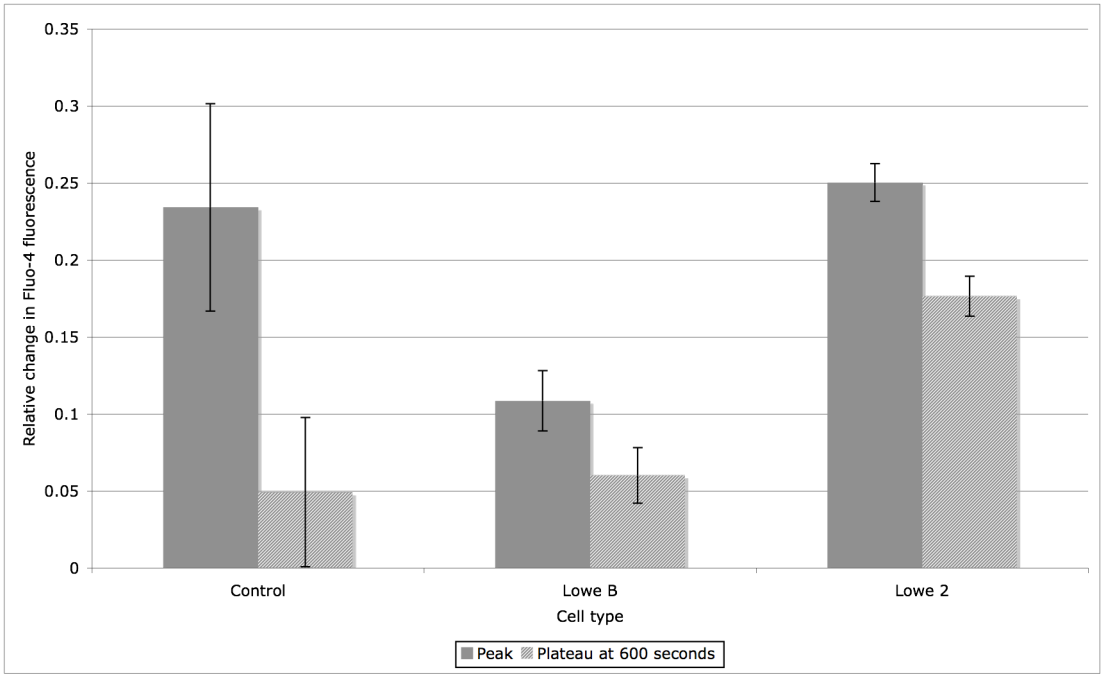

Figure 4.5.4. legend:. Fibroblasts were plated at 100% confluence one day before experiments. Cells were loaded with Fluo-4 AM 45 minutes prior to stimulation. Cells were mock stimulated with buffer or 50μM ATP and imaged for 20 minutes. All experiments were done at room temperature. Data are plotted for the peak calcium level in the cytosol (dark grey bars) and level of calcium at the 600 second time-point post stimulation (light grey bars). These data are representative of six independent experiments. All data are expressed as relative arbitrary values, normalised against basal Fluo-4 fluorescence before stimulation and with mock stimulated cell responses deleted from final values. Error bars are standard deviations.

Figure 4.5.5: Response of Lowe Syndrome fibroblasts to 100μM ATP

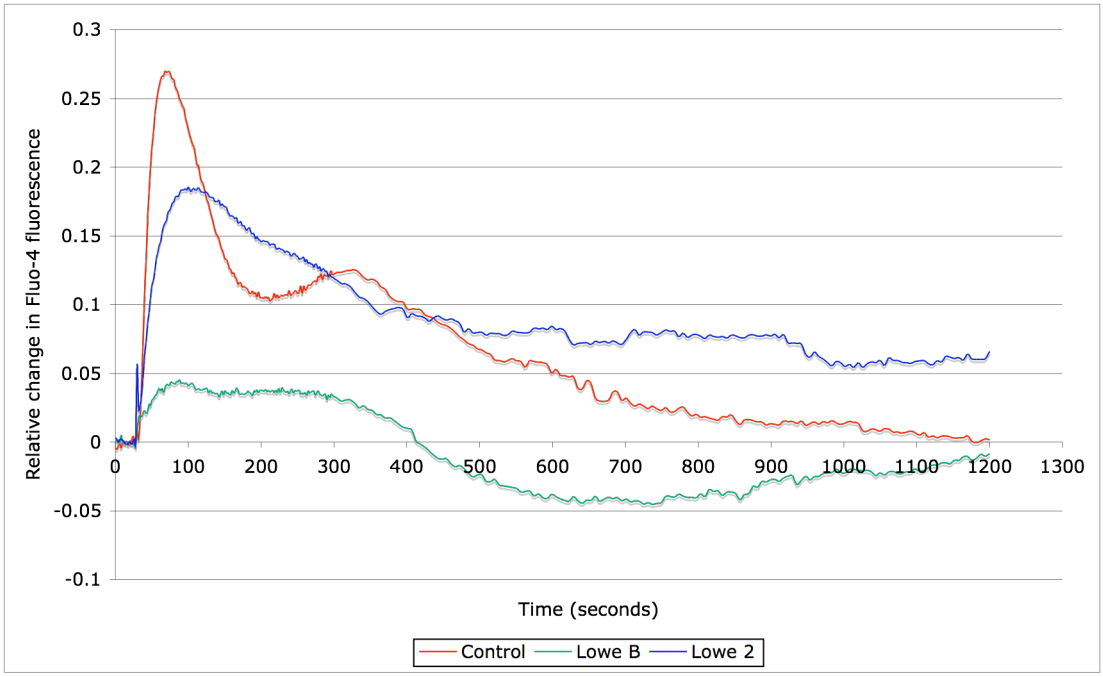

Cell type	Peak/600 sec ratio
Control	5.44
Lowe B	2
Lowe 2	2.06

Figure 4.5.5. legend: Fibroblasts were plated at 100% confluence one day before experiments. Cells were loaded with Fluo-4 AM 45 minutes prior to stimulation. Cells were mock stimulated with buffer or 100μM ATP and imaged for 20 minutes. All experiments were done at room temperature. Line traces represent six independent tests on the graph. All data are expressed as relative arbitrary values, normalised against basal Fluo-4 fluorescence before stimulation and with mock stimulated cell responses deleted from final values. Error bars are standard deviations.

Figure 4.5.6: Analysis of response of Lowe Syndrome fibroblasts to 100μM ATP

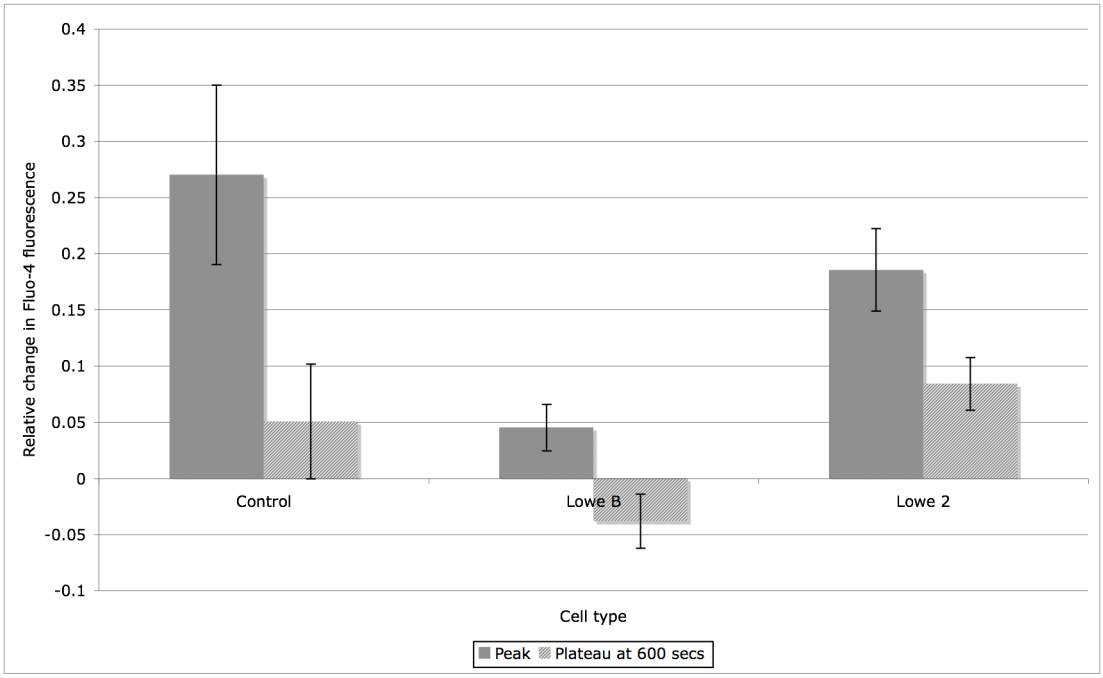

Figure 4.5.6. legend:. Fibroblasts were plated at 100% confluence one day before experiments. Cells were loaded with Fluo-4 AM 45 minutes prior to stimulation. Cells were mock stimulated with buffer or 100μM ATP and imaged for 20 minutes. All experiments were done at room temperature. Data are plotted for the peak calcium level in the cytosol (dark grey bars) and level of calcium at the 600 second time-point post stimulation (light grey bars). These data are representative of six independent experiments. All data are expressed as relative arbitrary values, normalised against basal Fluo-4 fluorescence before stimulation and with mock stimulated cell responses deleted from final values. Error bars are standard deviations.

Figure 4.5.7: Response of Lowe Syndrome fibroblasts to thapsigargin

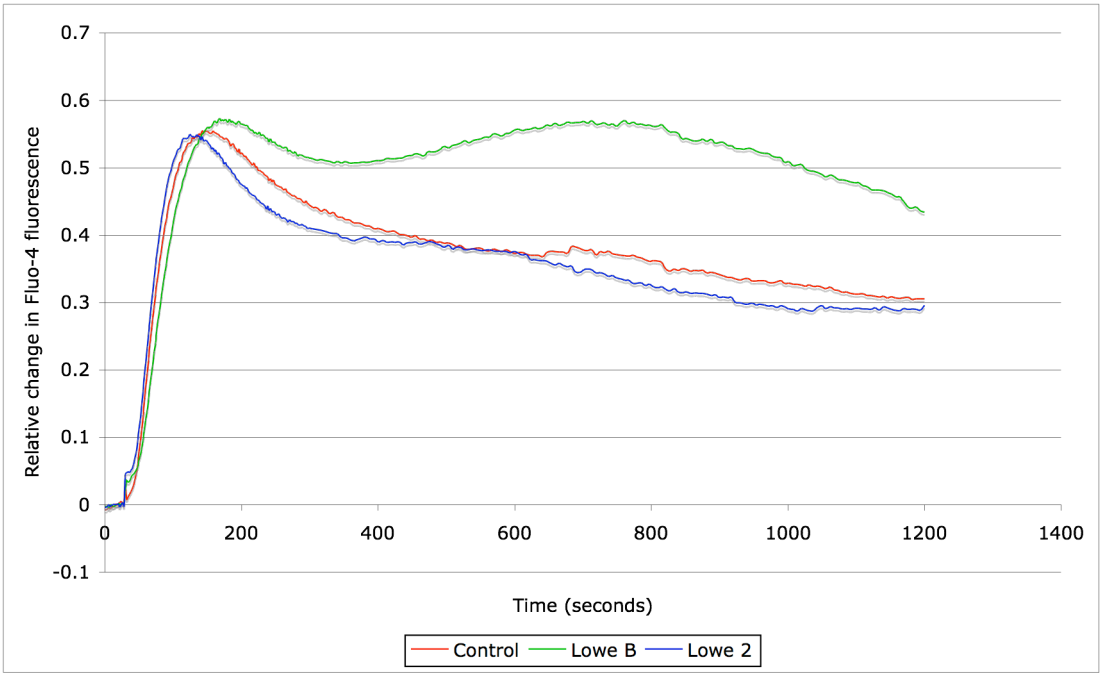

Cell type	Peak/600 sec ratio
Control	1.48
Lowe B	1.06
Lowe 2	1.45

Figure 4.5.7. legend: Fibroblasts were plated at 100% confluence one day before experiments. Cells were loaded with Fluo-4 AM 45 minutes prior to stimulation. Cells were mock stimulated with buffer or 1μM thapsigargin and imaged for 20 minutes. All experiments were done at room temperature. Line traces represent six independent tests on the graph. All data are expressed as relative arbitrary values, normalised against basal Fluo-4 fluorescence before stimulation and with mock stimulated cell responses deleted from final values. Error bars are standard deviations.

Figure 4.5.8: Analysis of response of Lowe Syndrome fibroblasts to thapsigargin

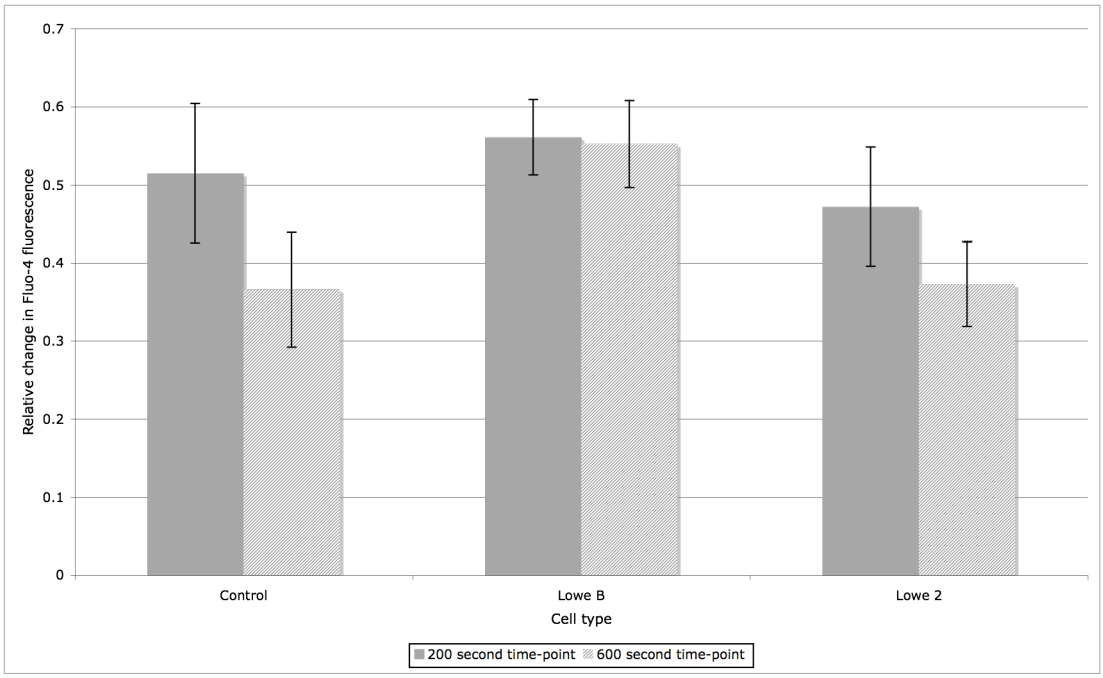

Figure 4.5.8. legend:. Fibroblasts were plated at 100% confluence one day before experiments. Cells were loaded with Fluo-4 AM 45 minutes prior to stimulation. Cells were mock stimulated with buffer or 100μM ATP and imaged for 20 minutes. All experiments were done at room temperature. Data are plotted for the peak calcium level in the cytosol (dark grey bars) and level of calcium at the 600 second time-point post stimulation (light grey bars). These data are representative of six independent experiments. All data are expressed as relative arbitrary values, normalised against basal Fluo-4 fluorescence before stimulation and with mock stimulated cell responses deleted from final values. Error bars are standard deviations.

Chapter 5:
OCRL1 and polarised cells

5: OCRL1 and polarised cells

Oculocerebrorenal syndrome of Lowe manifests itself in dysfunction of a very few cell types, the most affected being neurons and/or glia, lens cells (epithelial and fiber cells) and renal proximal tubular epithelial cells. Thus the symptoms suffered by Lowe Syndrome patients arise from the dysfunction of polarised cells. These cells, upon contacting one another, form distinct apical and basolateral domains connected through three major types of intercellular junction: gap junctions, adherens junctions and tight junctions. Intercellular junctions regulate and are regulated by a wide array of cellular processes, such as cell signalling, membrane trafficking, transcription and apoptosis [88, 89, 135]. Furthermore, all three of these types of junction have been shown to be regulated, in part, by the levels and localisation of phosphoinositides, and so might be affected by loss of OCRL1.

We set upon testing whether the subcellular localisation of OCRL1 in a polarised cell type matches that observed in non-polarised cell lines such as HeLa and COS-7 [52]. Most of our experiments used two well-characterised polarised cell lines to assess the role of OCRL1: Caco-2 and Madin-Darby canine kidney (MDCK) cells. The Caco-2 epithelial cell line is derived from a human colonic adenocarcinoma and upon reaching confluency forms a tightly packed monolayer complete with each of the three aforementioned types of cell-cell junction. These desired cellular properties are also present in the MDCK cell line. MDCK cells form a much more regular cobblestone-patterned epithelial monolayer. However, due to the canine origin of these cells, any

experiments with them on OCRL1 must be treated with caution. Recent studies showed that the OCRL1 knockout mouse does not develop the phenotype observed in humans [41]. A current theory for this lack of phenotype is that other species compensate for OCRL1 loss with an alternatively spliced version of INPP5B, as discussed in the introduction of this thesis. Thus at this stage it is not clear which (if any) non-human species are likely to reproduce the salient features of Lowe Syndrome upon loss of OCRL1. For this reason we used the Caco-2 cell line in the majority of our work.

Intercellular junction formation occurs in a specific temporal manner. Initiation of cell-cell contact leads to the formation of a primordial, “spot-like” adherens junction, a platform upon which cell polarisation and other types of intercellular junction form [94-96]. These primordial junctions then fuse with one another, through interaction with F-actin filaments to form “belt-like” adherens junctions [101, 159]. This process occurs alongside the formation of tight junctions, apical to the newly forming “belt-like” adherens junction. These two junctions then go on to mature separately, using a great number of proteins involved in actin reorganisation, membrane trafficking and signal transduction [88, 103, 109, 111, 112, 114, 121]. Therefore, to carry out a full and thorough investigation of a possible role for OCRL1 at intercellular junctions it was important to look at more than one time point during junction formation. For this reason we undertook a time-course experiment, fixing cells at different confluencies in order to assess OCRL1 localisation at different stages of intercellular junction maturation.

In Caco-2 cells, a limited and weak co-localisation of OCRL1 and ZO-1 was observed when cells were plated at low confluency. (Figure 5.1.1), and was quantified using line-scan analysis (Figure 5.1.2). This showed that relatively low proportion of total OCRL1 at cell-cell junctions in Caco-2 cells was present specifically at the level of the tight junction. The majority of OCRL1 still localised to the cytoplasm and internal membranes, as in non-polarised cells such as HeLa and COS-7. The partial co-localisation with ZO-1 was lost upon allowing cells to grow to a greater density (Figure 5.1.3). This suggests that the junctional recruitment of OCRL1 only occurs at early time points in the maturation of the epithelial monolayer. The level of junctional and plasma membrane localised OCRL1 was clearer when looking at MDCK cells growing at very low densities (Figure 5.1.4). There were a great number of cells with endogenous OCRL1 localised to intercellular junctions, however in some instances it was also highly abundant at parts of the plasma membrane making no contact with other cells (Figures 5.1.4, white arrows). Interestingly, a high level of fluorescence was detected in the nucleus. Furthermore, in a similar fashion to that observed in Caco-2 cells, the junctional recruitment of OCRL1 reduced with increased cell density (Figure 5.1.5).

We decided to further the investigation of OCRL1 localisation in polarised cells by looking at OCRL1 distribution in primary cells. Using primary porcine retinal pigment epithelial cells (harvested by Jennifer Williams, UCL), we found a very similar localisation to that seen in MDCK cells, with OCRL1 highly abundant in the nucleus and the plasma membrane (Figure 5.1.6). In a similar fashion to the staining pattern of OCRL1 in MDCK cells, plasma

membrane staining of OCRL1 in primary porcine retinal pigment epithelial cells was highly, but not fully, co-incident with cell-cell junctions.

These results show that OCRL1 in polarised epithelial cells localises to tight junctions, with some cell types also showing nuclear targeting. Both these sites, the plasma membrane and nucleus, have been shown to contain high levels of PI(4,5)P2. These data place OCRL1 at locations within the cell that contain its preferred substrate and suggest that recruitment to tight junctions is temporally regulated in a manner related to epithelial maturation.

5.1: Subcellular localisation of OCRL1 in polarised cell types

Figure 5.1.1: OCRL1 localisation in Caco-2 cells at low density

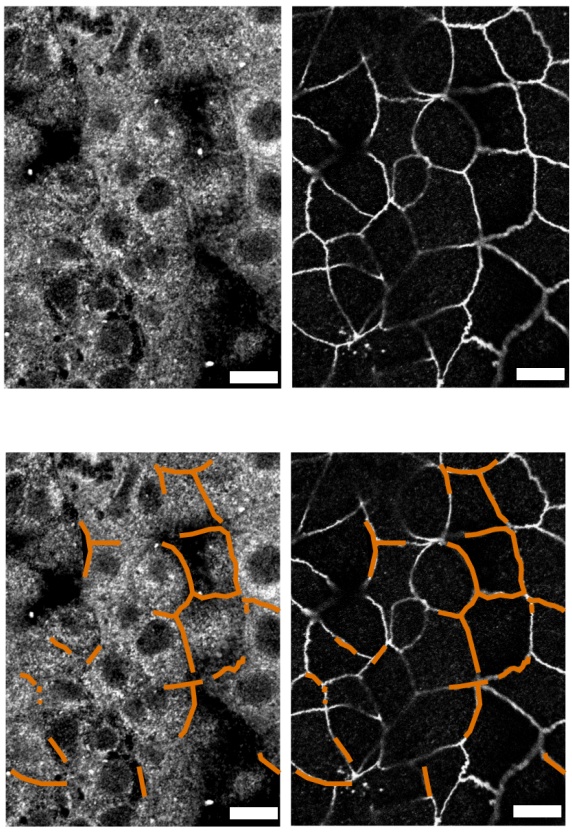

OCRL1 ZO-1

Figure 5.1.1 legend: Cells were plated onto 35mm tissue culture plastic dishes and allowed to grow to low density (40% confluency). Cells were then fixed with 4% paraformaldehyde, permeabilised, blocked and processed for OCRL1 and ZO-1 immunostaining. Images were then taken with a Leica confocal microscope. The top pair of images represent the staining of OCRL1 and ZO-1 in Caco-2 cells. Regions of colocalisation between OCRL1 and ZO-1 have been highlighted in the bottom pair of images, by overlaying orange lines. Single confocal sections. Scale bar (10μm).

Figure 5.1.2: Line-scan analysis of Figure 5.1A showing ZO-1 colocalisation with OCRL1

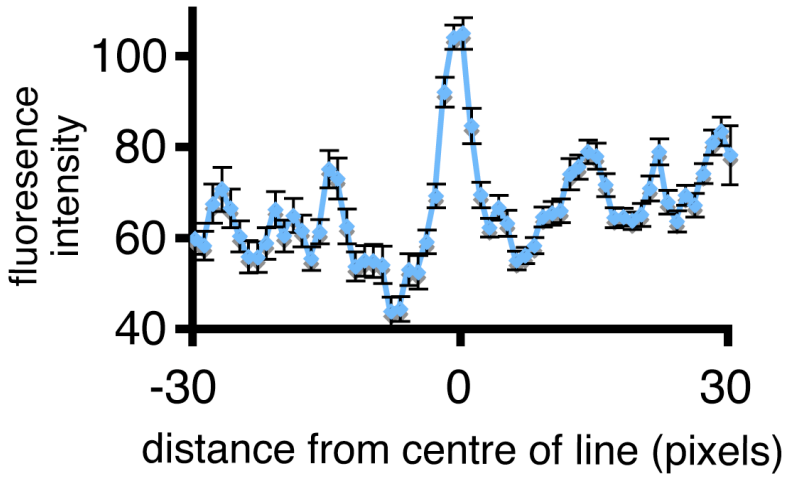

Figure 5.1.2 legend: Image processing of Figure 5.1.1. This graph shows the mean of 12 line scans (± s.e.m.) of OCRL1 fluorescence measured 30 pixels either side of cell junctions highlighted in orange in Figure 5.1.1.

Figure 5.1.3: Loss of specific junctional localisation of OCRL1 upon growth to medium density

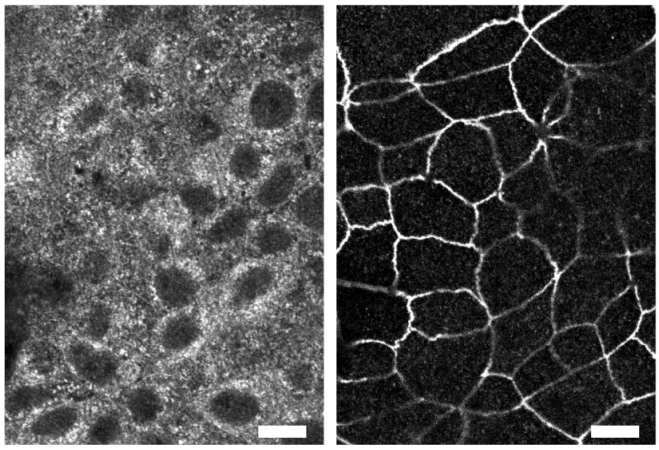

OCRL1 ZO-1

Figure 5.1.3 legend: Cells were plated onto 35mm tissue culture plastic dishes and allowed to grow to medium density (70% confluency). Cells were then fixed with 4% paraformaldehyde, permeabilised, blocked and processed for OCRL1 and ZO-1 immunostaining. Images were then taken with a Leica confocal microscope. Image consists of 3 compressed confocal sections in the plane of the tight junction.

Figure 5.1.4: Localisation of OCRL1 in MDCK cells grown at low density

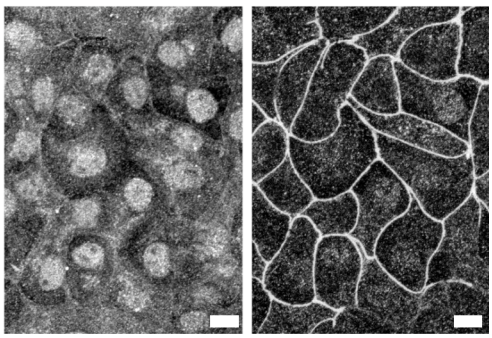

OCRL1 ZO-1

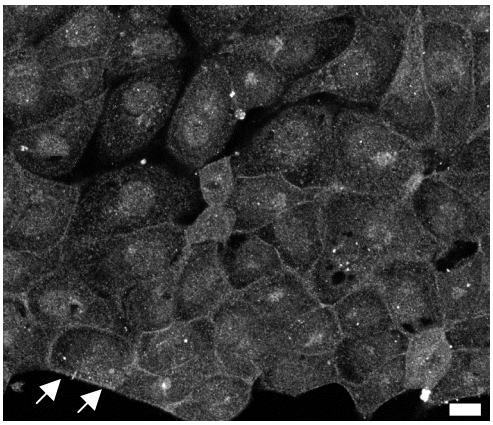

OCRL1

Figure 5.1.4 legend: Cells plated onto 35mm tissue culture dishes and allowed to grow to low density (40% confluency). Cells were then fixed with 4% PFA, permeabilised, blocked and processed for OCRL1 and ZO-1 immunostaining. Single sections were then taken with a Leica confocal microscope. Upper panels show colocalisation of OCRL1 and ZO-1 staining. OCRL1 also shows a strong nuclear localisation in MDCK cells. The bottom panel shows immunofluorescence of MDCK cells, stained with OCRL1 specific antibody only, demonstrating that the junctional localisation seen is not an artefact of cross-reaction of antibodies. Arrows indicate plasma membrane staining of OCRL1 at non-contacting cell edges. Scale bar (10μm)

Figure 5.1.5: Loss of ZO-1 colocalisation with OCRL1 in MDCK cells grown to medium density

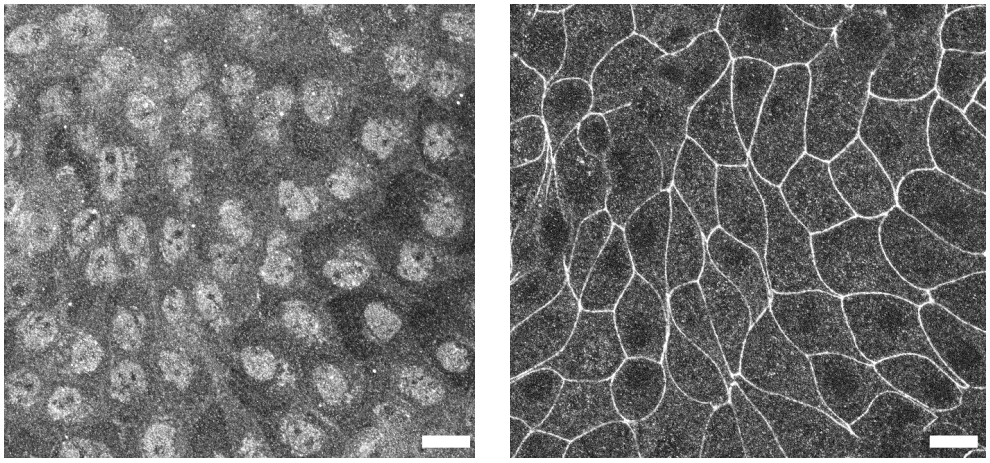

OCRL1 ZO1

Figure 5.1.5 legend: Cells were plated onto 35mm tissue culture plastic dishes and allowed to grow to medium density (70% confluency). Cells were then fixed with 4% paraformaldehyde, permeabilised, blocked and processed for OCRL1 and ZO-1 immunostaining. Three confocal sections were then taken with a Leica confocal microscope. Scale bar (10μm).

Figure 5.1.6: Localisation of OCRL1 in primary porcine retinal pigment epithelial cells

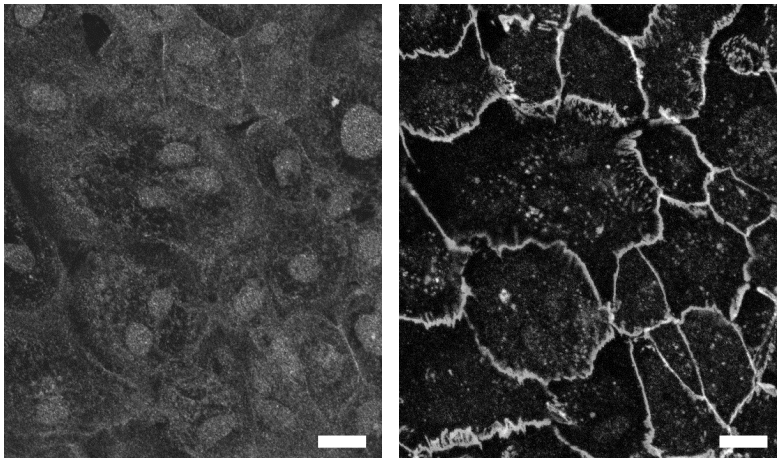

OCRL1 ZO1

Figure 5.1.6 legend: Cells were plated onto 35mm tissue culture plastic dishes and allowed to grow to full confluency (100% coverage on the dish). Cells were then fixed with 4% paraformaldehyde, permeabilised, blocked and processed for OCRL1 and ZO-1 immunostaining. Images were then taken with a Leica confocal microscope. Image comprises of three compressed confocal sections. Scale bar (10μm).

5.2: Over-expression studies

We transfected these polarised cell types with GFP-tagged OCRL1, to see whether over-expressed OCRL1 matches the observed endogenous localisation of OCRL1. Caco-2 and MDCK cells expressing OCRL1-GFP partially colocalised with ZO-1 at the tight junction (Figure 5.2.1). However it did not match the endogenous localisation of OCRL1 observed in Figures 5.1.1-.6. Interestingly the perinuclear distribution of OCRL1 normally seen in non-polarised cells was more evident upon over-expression. This may represent a mechanism where increased levels of OCRL1 are kept away from the plasma membrane to prevent undesired cellular effects. Interestingly there were examples where overexpression of OCRL1 led to pleiomorphic effects, with the formation of multinucleate cell syncytia, as observed by ZO-1 immunostaining and DNA staining (Figure 5.2.2). Within these syncytia, we observed some ZO-1 in a punctate vesicular distribution (Figure 5.2.2, white arrows), however at this stage the significance of this is unclear.

We decided to elucidate which determinants within OCRL1 target tight junctions. To do so, we expressed GFP-tagged chimeras of the amino- and carboxy-terminal halves of OCRL1 (as shown in Figure 5.2.3). We first expressed these proteins in HeLa cells and observed their localisations. The amino-terminal half of OCRL1 was cytoplasmic (Figure 5.2.4, left panel). However, the carboxy-terminus of OCRL1 localised strongly to internal membranes, and interestingly also entered the nucleus (Figure 5.2.4, right

panel). Regarding the punctate targeting, the pattern was consistent with targeting to TGN and/or endosomes, but a double labelling experiment has not been performed. Regarding the nuclear localisation of GFP-OCRL1-carboxy terminus, this has been found before with the expression of a GFP-tagged chimera of the Rho-GAP domain of OCRL1 [42]. In that study, GFP-OCRL1-RhoGAP displayed a highly nuclear and cytoplasmic localisation. However, upon activation of RhoGTPases Cdc42 and Rac1 (known binding partners of OCRL1) GFP-OCRL1-RhoGAP moved into plasma membrane ruffles.

Taking into consideration the past finding that the RhoGAP homology domain of OCRL1 has the propensity to move to the plasma membrane, our hypothesis was that the carboxy-terminus of OCRL1 would mediate the junctional localisation of OCRL1. To test this, we over-expressed each half of OCRL1 in Caco-2 cells. The GFP-OCRL1-amino-terminus was again cytoplasmic, and was limited to the basal cytoplasm of the cell (Figure 5.2.5). In contrast, a low proportion of GFP-OCRL1-carboxy terminus was seen at intercellular junctions (Figure 5.2.6). This maps the ability of OCRL1 to target intercellular junctions to the carboxy-terminal half. This, alongside the RhoGAP domain study by Faucherre *et al.* in 2003, suggests that OCRL1 has the propensity to move to the plasma membrane/intercellular junction in a stimulus dependent manner, perhaps through modulation of RhoGTPase proteins. Intercellular junction formation and function is known to be highly dependent on the activation of specific Rho GTPases such as Rho, Rac1 and Cdc42 [104, 105, 160-162].

These data suggest that OCRL1 may be recruited to sites where its preferred substrate, PI(4,5)P2, exists. Other studies looking at lipid phosphatase activity show that OCRL1 is more active when in complex with Rab GTPases, perhaps through changes in the configuration of OCRL1 structure [44]. This work demonstrated that OCRL1 activity is controlled and regulated through specific recruitment. It may be possible that this proposed mechanism applies to OCRL1 activity at intercellular junctions. Much like the specific recruitment of OCRL1 to clathrin-coated pits at the plasma membrane during endocytosis, OCRL1 may be temporally recruited to junctions and activated to reduce PI(4,5)P2 levels. [54].

The closely related homologue of OCRL1, INPP5B, is the only other inositol polyphosphate 5-phosphatase containing a RhoGAP homology domain in the human genome. Interestingly, previous studies have shown an effect of INPP5B loss on adherens junctions in sertoli cells, suggesting a role for this protein at intercellular junctions [163]. Given that INPP5B shares 45% homology with OCRL1, and its suggested compensatory role in the mouse model of OCRL1, we decided to look at GFP-tagged INPP5B in Caco-2 cells [41]. Upon transfection we found that INPP5B also weakly targets tight junctions, as shown by colocalisation with tight junction marker ZO-1 (Figure 5.2.7). This indicates that OCRL1 and INPP5B may have similar functions at intercellular junctions. This supports a theory that Lowe Syndrome arises not because of differences in the functions of OCRL1 and INPP5B but relatively different levels of INPP5B and OCRL1 transcript. If there were a difference in the ratio

of INPP5B to OCRL1 transcript in polarised cells, in comparison to non-polarised cells, this theory would be validated.

Figure 5.2.1: Localisation of GFP tagged OCRL1 in MDCK and Caco-2 cells

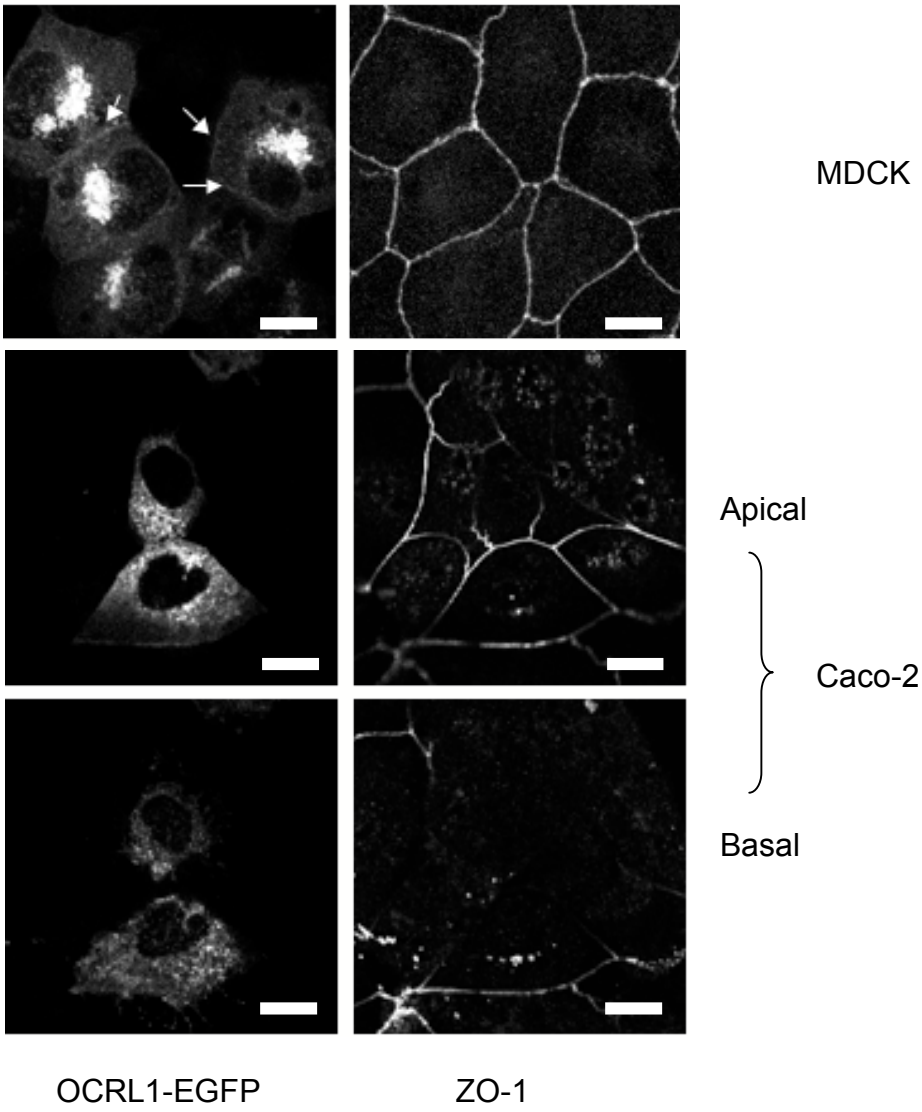

Figure 5.2.1 legend: Cells were plated onto 35mm tissue culture plastic dishes at medium density (70% confluency). Cells were transfected with 0.4μg GFP-OCRL1 DNA and left for 24 hours. Cells were fixed with 4% PFA, permeabilised, blocked and processed for ZO-1 immunostaining. Images were then taken with a Leica confocal microscope. White arrows indicate sites where OCRL1 co-localises with ZO-1. Single confocal sections. Scale bar (10μm). MDCK above, Caco-2 apical section middle, Caco-2 basal section below.

Figure 5.2.2: Over-expression of OCRL1 can lead to polynuclear syncytia

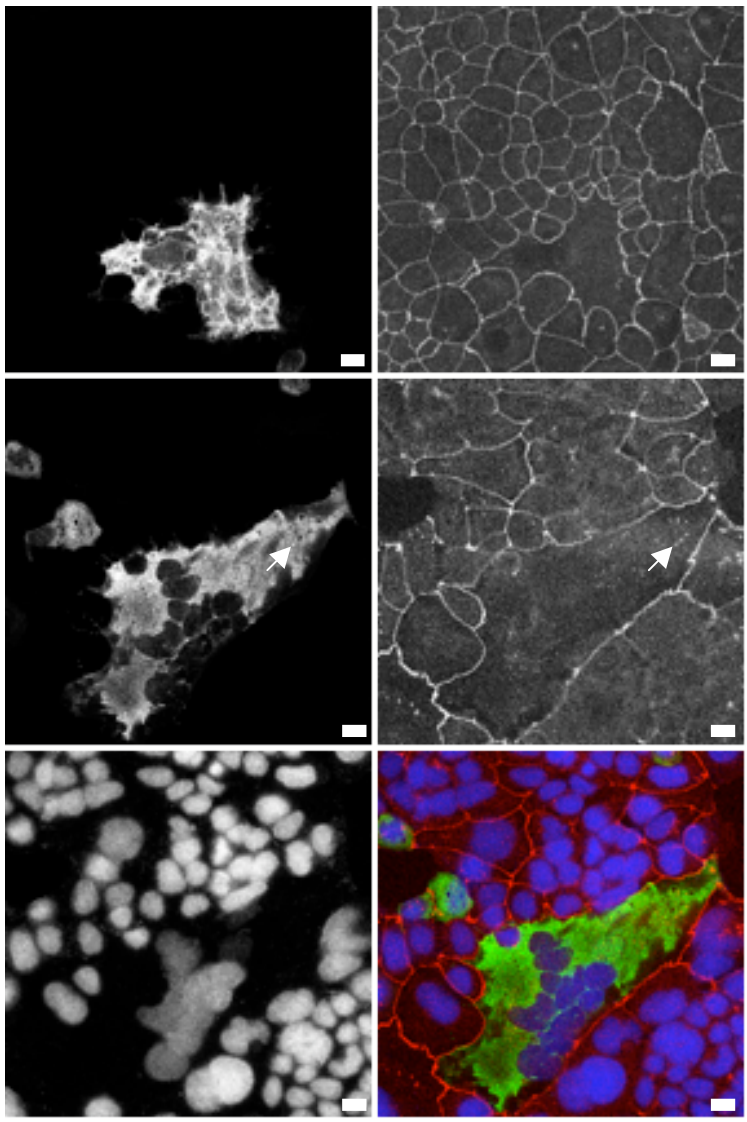

Figure 5.2.2 legend: Cells were transfected with 0.4μg GFP-OCRL1 DNA and left for 24 hours. Cells were then fixed with 4% paraformaldehyde, permeabilised and processed for ZO-1 immunostaining. Images were then taken with a Leica confocal microscope. Top and middle rows: GFP-OCRL1 (left panel), ZO-1 (right panel). Bottom row: Nuclear DAPI stain (left panel), overlay image of pseudocoloured images of GFP-OCRL1 and DAPI (right panel). Arrows indicate punctate ZO-1 inside GFP-OCRL1 positive syncytia. Single confocal sections. Scale bar (10μm).

Figure 5.2.3: Diagram of domain structure of OCRL1 and division for GFP-tagging of N- and C-termini

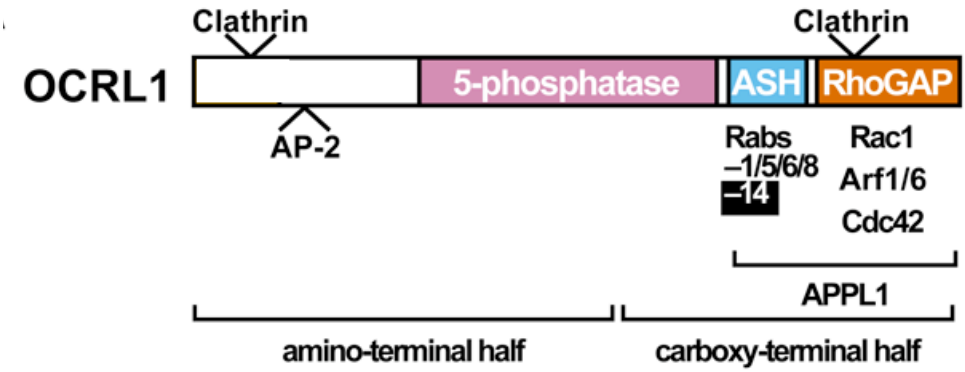

Figure 5.2.3 legend: The diagram above depicts where the division of OCRL1 into two termini was made. The 5-phosphatase domain was split in half at amino-acid number 501. The amino-terminal half consists of OCRL1 residues 1-501 and contains motifs capable of binding AP-2 and clathrin. The carboxyl-terminal half consists of OCRL1 residues 501-901, and contains the ASH and RhoGAP domains, with its linker region, parts of OCRL1 sequence that can bind the proteins listed below the picture.

Figure 5.2.4: Localisation of GFP-tagged N- and C-terminal OCRL1 in HeLa cells

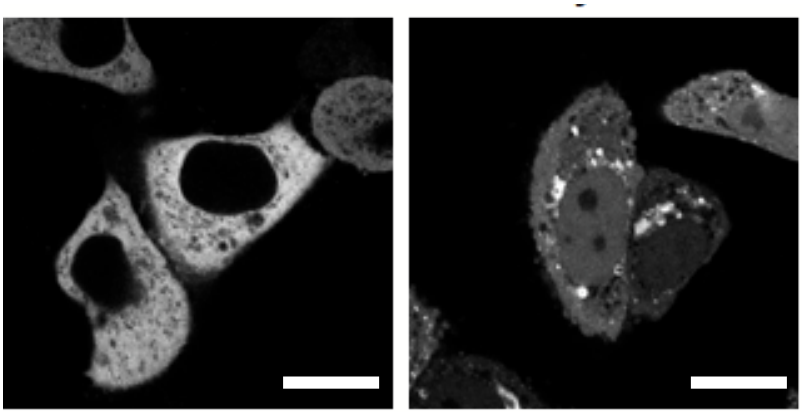

GFP-OCRL1 N-term GFP-OCRL1 C-term

Figure 5.2.4 legend: Cells were plated onto 35mm tissue culture dishes and transfected with 0.4μg either GFP-OCRL1 amino-terminal or carboxy-terminal DNA. After 24 hours of over-expression, live cells were then imaged with a Leica confocal microscope. Single confocal sections. Scale bar (10μm).

Figure 5.2.5: Localisation of GFP N-terminal OCRL1 in Caco-2 cells

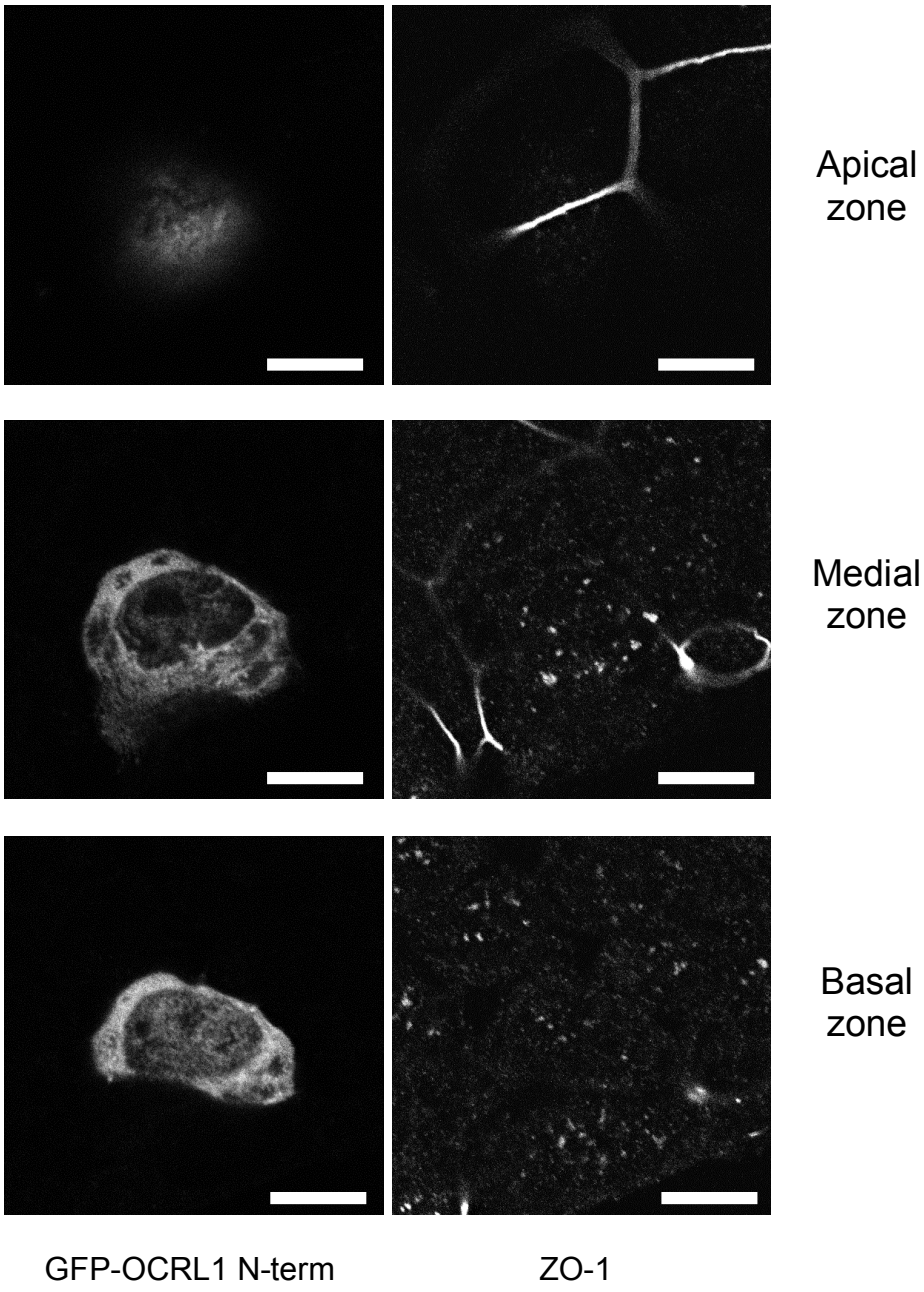

Figure 5.2.5 legend: Cells were transfected with 0.4μg GFP-OCRL1 amino-terminal DNA and left for 24 hours. Cells were then fixed with 4% paraformaldehyde, permeabilised and processed for ZO-1 immunostaining. Single sections were then taken with a Leica confocal microscope. Images are from different confocal sections of the same group of cells. Scale bar (10μm)

Figure 5.2.6: Localisation of GFP-tagged C- terminal OCRL1 in Caco-2 cells

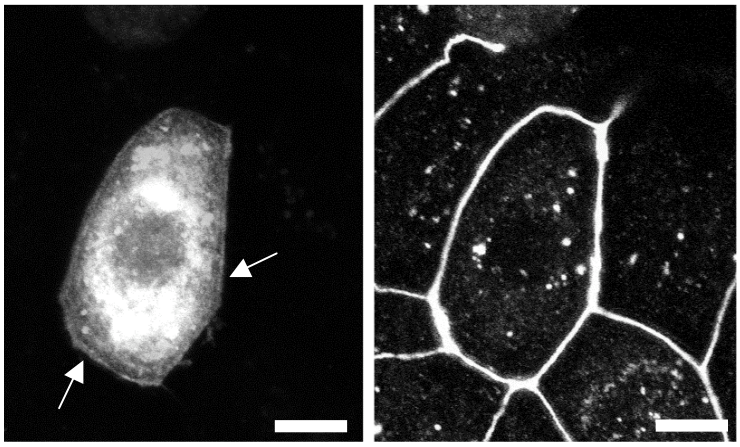

GFP-OCRL1 C-term ZO-1

Figure 5.2.6 legend: Cells were transfected with 0.4μg GFP-OCRL1-carboxy terminus DNA and left for 24 hours. Cells were then fixed with 4% paraformaldehyde, permeabilised and processed for ZO-1 immunostaining. Images were then taken with a Leica confocal microscope. White arrows indicate where ZO-1 positive segments of the periphery co-stained for GFP. Single confocal section. Scale bar (10μm).

Figure 5.2.7: Localisation of GFP-tagged INPP5B in Caco-2 cells

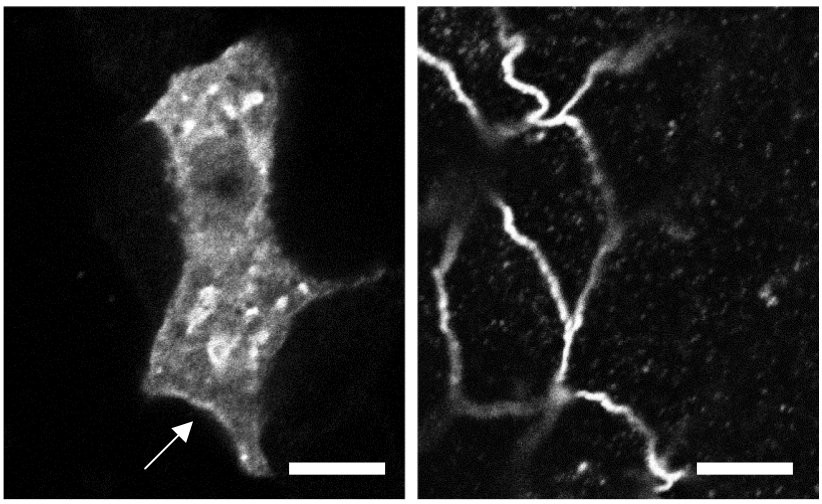

GFP-INPP5B ZO-1

Figure 5.2.7 legend: Cells were transfected with 0.4μg GFP-INPP5B DNA and left for 24 hours. Cells were then fixed with 4% paraformaldehyde, permeabilised and processed for ZO-1 immunostaining. Images were then taken with a Leica confocal microscope. The white arrow indicates where a ZO-1 positive segment of the periphery co-stained for GFP. Single confocal section. Scale bar (10μm).

5.3: OCRL1 and ZO-1 co-immunoprecipitate

Given the partial colocalisation of OCRL1 and ZO-1 (Figure 5.1 and Figure 5.2) we decided to test a potential interaction between the two proteins. We undertook endogenous immunoprecipitations from two different polarised epithelial cell types, MDCK and Caco-2. When Caco-2 cells were grown at high density an interaction between OCRL1 and ZO-1 was not evident (Figure 5.3.1). However, when immunoprecipitating endogenous OCRL1 at lower densities we began to detect an interaction with ZO-1. Interestingly this interaction was best observed when cells were plated so that very few were in contact with one another (Figure 5.3.2). Interestingly the interaction was only observed when cells were plated at low confluency, in agreement with our immunofluorescence results showing colocalisation only when cells were at low confluency (Figures 5.1.1-5.1.3).

Given that GFP-OCRL1 was detected at tight junctions by immunofluorescence, we transfected Caco-2 cells with this construct, and immunoprecipitated it using antibodies to GFP (Figure 5.3.3). In this experiment, we found that a greater amount of ZO-1 than was immunoprecipitated by GFP-OCRL1 than in experiments relying on immunoprecipitation of endogenous OCRL1, suggesting over-expression of OCRL1 may increase the amount of ZO-1 interacting with it. This observation might tie in with the frequently detected syncytial polynuclear cells upon GFP-OCRL1 over-expression (Figure 5.2.2), if the increased formation of

complexes containing both OCRL1 and ZO-1 were to augment tight junction turnover.

In the reverse experiment of immunoprecipitating ZO-1 and Western blotting for OCRL1 in MDCK and Caco-2 cells, a stronger OCRL1 positive band was observed where anti-ZO-1 antibody was used compared to control immunoglobulin (Figure 5.3.4). Consistently however, the control rabbit IgG lanes were not as clean as the sheep IgG control used when immunoprecipitating OCRL1 (Figure 5.3.4). A future experiment to further prove the density-dependent manner of the ZO-1/OCRL1 interaction would be to undergo a series of pull-downs with varying confuencies in parallel with one another. This will be the focus of future studies.

Given that OCRL1 targets to early and recycling endosomes and these organelles are critical for primordial “belt-like” adherens junction formation, these data suggest that OCRL1 may facilitate vesicular traffic of junctional proteins. Recent work published by the Kroschewski lab has revealed key insights into the mechanism of initial cell-cell junction formation with MDCK 2-cell aggregates. In this study, evidence is shown demonstrating that junctional and polarity proteins are delivered to the plasma membrane via apical recycling endosomes [164]. Given that Rab GTPases (specifically OCRL1-binding partners Rab 8 and Rab 1 3) control the trafficking of tight junction proteins, these data suggest OCRL1 may function within this pathway [109-112].

Figure 5.3.1: Immunoprecipitation of OCRL1 at high confluency fails to bring down tight junction protein ZO-1

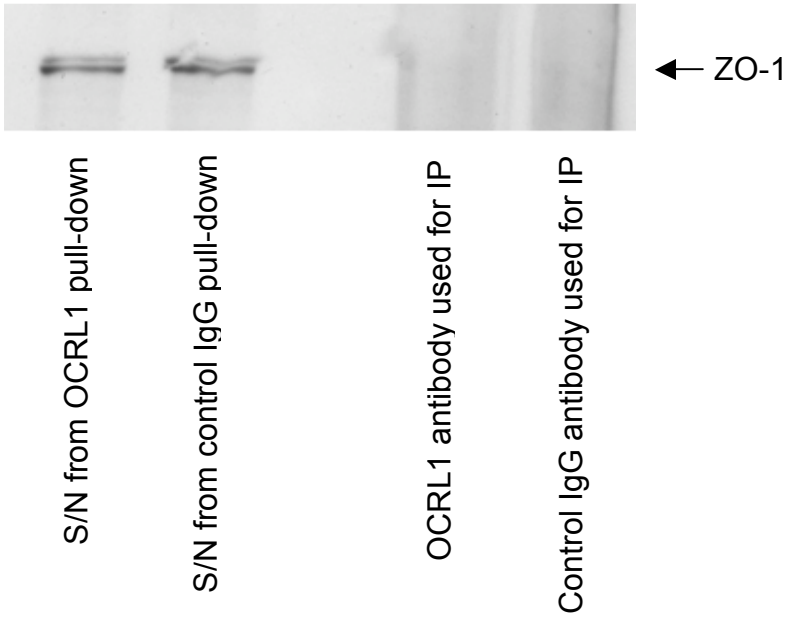

Figure 5.3.1: Western blot for ZO-1. Caco-2 cells lysates were pre-cleared, and then mixed with beads carrying the indicated antibodies. In each case, 30% of precipitated proteins were separated by SDS-PAGE, along with a proportion (equivalent to 1%) of the unbound supernatant. Arrow indicates full-length ZO-1, which runs as a doublet.

Figure 5.3.2: Immunoprecipitation of OCRL1 at low confluency brings down tight junction protein ZO-1

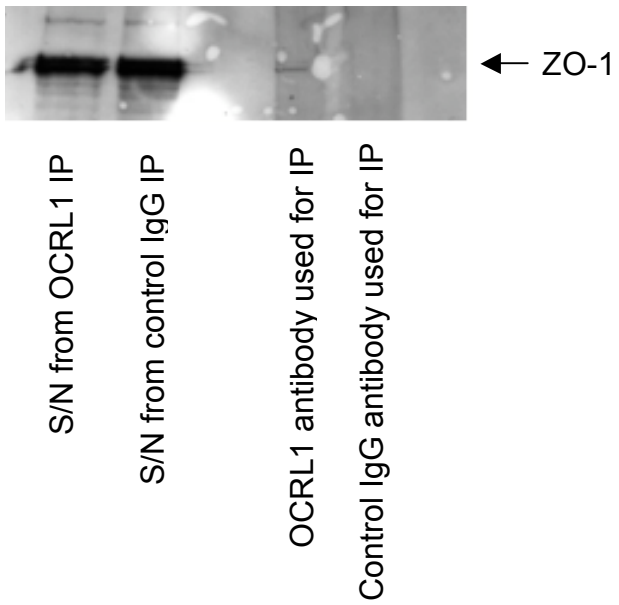

Figure 5.3.2 legend: Western blot for ZO-1. Caco-2 cells lysates were pre-cleared, and then mixed with beads carrying the indicated antibodies. In each case, 30% of precipitated proteins were separated by SDS-PAGE, along with a proportion (equivalent to 1%) of the unbound supernatant. Arrow indicates full-length ZO-1, which runs as a doublet.

Figure 5.3.3: Immunoprecipitation of GFP-OCRL1 brings down tight junction protein ZO-1

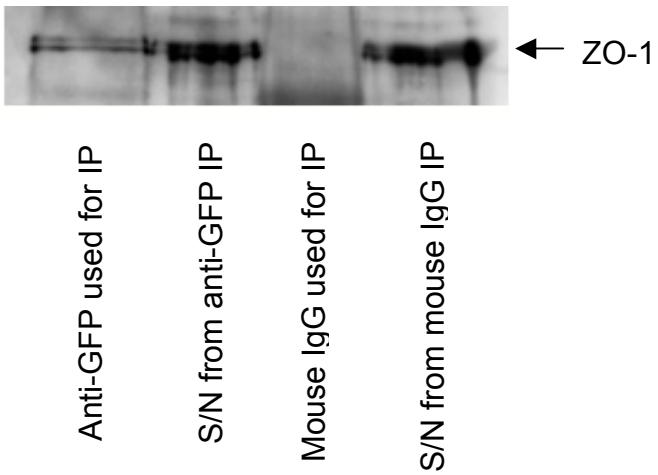

Figure 5.3.3 legend: Western blot for ZO-1. Caco-2 cells were transfected with GFP-OCRL1 and lysates were prepared 24 hours after. Lysates were pre-cleared, and then mixed with beads carrying the indicated antibodies. In each case, 30% of precipitated proteins were separated by SDS-PAGE, along with a proportion (equivalent to 1%) of the unbound supernatant. Arrow indicates full-length ZO-1, which runs as a doublet.

Figure 5.3.4: Immunoprecipitation of ZO-1 brings down OCRL1

Figure 5.3.4 legend: Western blot for OCRL1. Prior to lysis, Caco-2 and MDCK cells were treated with the chemical cross-linker DSP for 30 minutes, followed by three 15 minute washes in blocking solution (see Materials and Methods). Lysates were then made, pre-cleared, and mixed with beads carrying the indicated antibodies. In each case, 30% of precipitated proteins were separated by SDS-PAGE. Arrow indicates full-length OCRL1 determined from the position of OCRL1 in the supernatant (lane not shown).

5.4: Effects of OCRL1 loss in polarised cell types

As Lowe Syndrome arises from the loss of OCRL1, we chose to test for a functional effect by depleting it from Caco-2 cells, using siRNA oligonucleotides. We were able to consistently achieve an 80-90% reduction in OCRL1 levels, with two applications of siRNA over a period of 3 days (Figure 5.4.1). This depletion of OCRL1 was also easily detected at the level of immunofluorescence (Figure 5.4.2). We noticed from our immunofluorescence studies that as cells depleted of OCRL1 contacted one another in culture they covered a much larger area than control siRNA treated cells. To characterise this difference, we chose to immunostain for proteins that target intercellular junctions such as ZO-1 and E-cadherin. By doing so, we could assess any changes in the staining pattern of both proteins but also it served to delineate the cell-cell boundaries, allowing us to measure the area covered by the cells.

Importantly, we noticed that the localisation of ZO-1 to cell edges was unaltered upon OCRL1 depletion (Figure 5.4.3). However, specific localization of ZO-1 to apical membranes, shown by imaging XZ sections, was greatly disturbed (Figure 5.4.4). XZ sections of cells treated with OCRL1 siRNA revealed that not only were the cells smaller, but the localisation of ZO-1 was more basal and less uniform than cells treated with control, non-targetting siRNA. For E-cadherin, its distribution at intercellular junctions seemed to be very similar to that of control siRNA treated cells (Figure 5.4.5). However, we noticed a greater number of internal E-cadherin “flecks” upon OCRL1

depletion. As the recruitment of ZO-1 to cell edges was unaffected by OCRL1 loss, we used the ZO-1 immunostain to measure the area of the cells. Pooling results from two independent knock-down experiments, we found that cells lacking OCRL1 were approximately 2.5 times larger in area, and were 55% the height of control siRNA treated cells (Figure 5.4.6 and 5.4.7). We also tested the effect of OCRL1 depletion on another human polarised cell line, human corneal epithelial (HCE) cells. Again, upon contacting one another, HCE cells depleted of OCRL1 covered a much larger area on coverslips, and were much flatter than control siRNA treated cells (Figure 5.4.8)

A change in the actin cytoskeleton has been seen previously in fibroblasts taken from Lowe Syndrome patients, but could not be observed when depleting OCRL1 in non-polarised cells such as HeLa or COS-7 cells (data not shown) [66, 98]**.** Interestingly, actin binds many components of intercellular junctions and the actin cytoskeleton is integral to cell-cell junction formation and maturation**.** We stained the actin in our Caco-2 cells with fluorescently labeled phalloidin, and upon depletion of OCRL1 we found a very similar phenotype to that seen in Lowe Syndrome fibroblasts. OCRL1 depleted cells displayed far fewer basal actin stress fibres than in cells treated with negative control siRNA (Figure 5.4.9).

To further our understanding of the role of OCRL1 at intercellular junctions, we chose to test the trans-epithelial resistance across HCE cell monolayers during a calcium switch assay. We used HCE cells as they displayed the same cell flattening phenotype as Caco-2 cells, but grew better on the multi-

well plates used for measuring trans-epithelial resistance. Overnight incubation of HCE cells in low calcium medium causes the dissociation of intercellular junctions. Re-addition of medium with regular levels of calcium causes the reformation of intercellular junctions, and by 6 hours most, if not all junctions should be reformed.

We first carried out a calcium switch experiment and observed the localisation of OCRL1 and ZO-1 after overnight incubation and 6 hours post addition of medium containing regular calcium levels. We found that after incubation in low calcium medium, cells lost contact with one another and ZO-1 staining was cytoplasmic. OCRL1 displayed a strong perinuclear localisation, typical in HCE cells. 6 hours after addition of medium containing regular calcium levels, cells formed tight intercellular junctions, as shown by the return of ZO-1 staining to the periphery. At neither time period did OCRL1 show localisation to tight junctions (Figure 5.4.10). This might still allow for OCRL1 recruitment to tight junctions in HCEs, but at an intermediate time during their formation – i.e. before 6 hours.

We decided to repeat the same experiment with cells depleted of OCRL1. We followed the formation of intercellular junctions through immunocytochemistry and also by measuring the trans-epithelial resistance. Trans-epithelial resistance gives a read-out of junctional integrity as it measures across the apical–basolateral axis of the cell monolayer. In control and OCRL1 depleted cells, all junctions between cells were lost after overnight incubation in low calcium medium, as shown by ZO-1 immunostaining. 6 hours post addition of

medium containing regular calcium levels, in both control and OCRL1 siRNA treated cells, ZO-1 recruitment was mostly recovered. However, we more readily found examples of failed ZO-1 recruitment to junctions in OCRL1 depleted monolayers than control siRNA treated monolayers (Figure 5.4.11). The measurement of trans-epithelial resistance revealed only one minor difference over the 6 hour time period after cells were returned to regular calcium levels. In a repeated manner, the first hour of trans-epithelial resistance recovery was slower in OCRL1 depleted HCE cells than control siRNA treated cells. However, the transepithelial resistance was completely recovered in both control and OCRL1 siRNA treated monolayers by 6 hours (Figure 5.4.12). Repeatedly we found that the initial rate of TER recovery was slower in cells treated with OCRL1 siRNA, in comparison to those treated with control siRNA. Although in this experiment, TER is clearly increased at 6 hours in OCRL1 siRNA cells this was not a typical result.

In summary, these data suggest that OCRL1 plays a facilitating but not crucial role in junctional maturation, which may feed into the morphology of the cell. Similar phenotypes are seen when actin cytoskeletal rearrangement is inhibited but also when other junctional components are missing and so this phenotype does not immediately identify the target of OCRL1 [165, 166]. Several lines of evidence point to roles for phosphoinositides in cell polarisation and junction formation[120, 123]. A recent study also revealed that many PDZ domains interact with phosphoinositides [132]. Within the tested proteins ZO-1 was found to bind phosphoinositides. Our preliminary results suggest that OCRL1 is linked to tight junction complexes and epithelial maturation.

Figure 5.4.1: OCRL1 can be efficiently depleted from Caco-2 cells and detected by Western Blotting

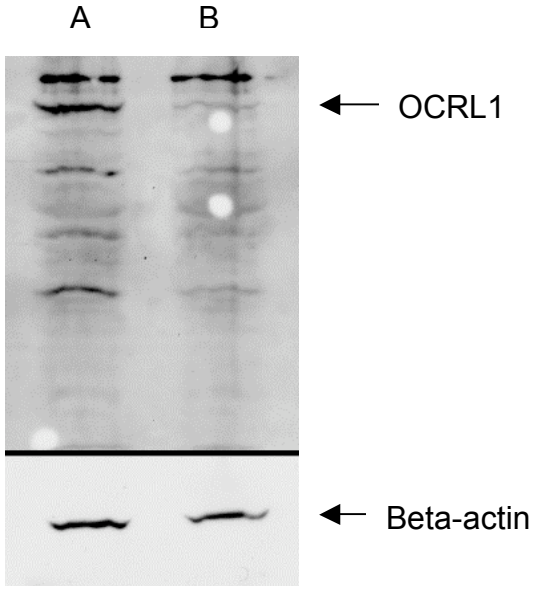

Figure 5.4.1 legend: Caco-2 cells were treated twice with non-targetting, negative control siRNA (lane A) or OCRL1 siRNA (lane B), over a period of 72 hours. OCRL1 and β-actin expression levels were analysed by Western Blot. AIDA densitometry revealed that relative OCRL1 expression is reduced by 90% in comparison to negative siRNA control.

Figure 5.4.2: OCRL1 can be efficiently depleted from Caco-2 cells and detected by immunofluorescence

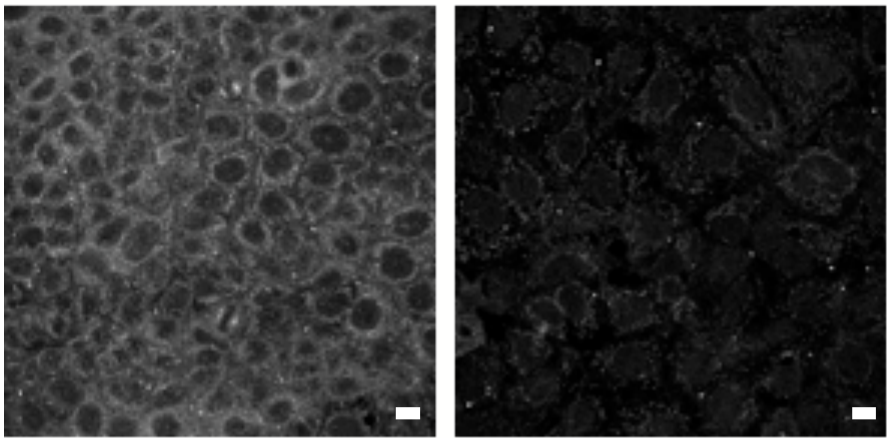

Control siRNA OCRL1 siRNA

Figure 5.4.2 legend: Immunofluorescence for OCRL1. Caco-2 cells were treated twice with OCRL1 siRNA or non-targetting, negative control siRNA, over a period of 72 hours. Cells were then fixed with 4% paraformaldehyde, permeabilised, blocked and processed for OCRL1 immunostaining. Images were then taken with a Leica confocal microscope. Single confocal section. Scale bar (10μm).

Figure 5.4.3: Effect of OCRL1 loss on ZO-1 localisation

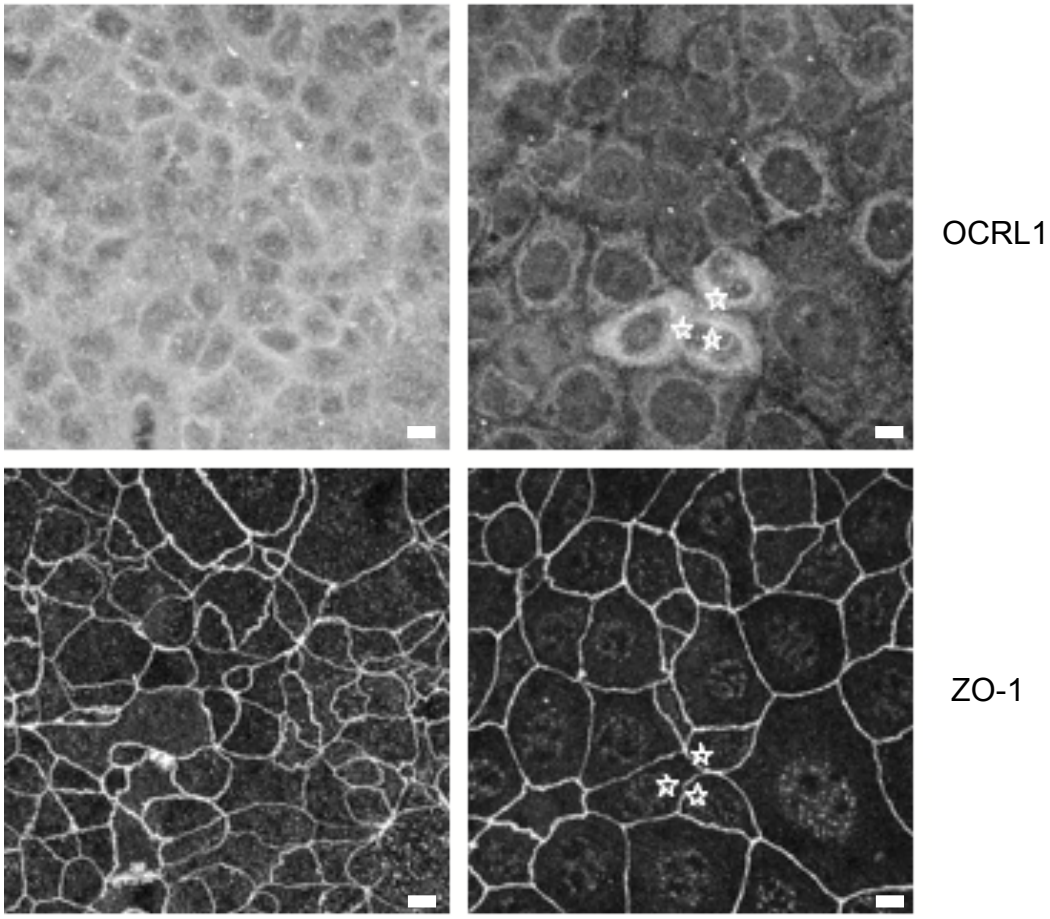

Figure 5.4.3 legend: Caco-2 cells were treated twice with OCRL1 siRNA or non-targetting, negative control siRNA, over a period of 72 hours. Cells were then fixed with 4% paraformaldehyde, permeabilised and processed for OCRL1 and ZO-1 immunostaining. Images were then taken with a Leica confocal microscope. Interestingly, the small number of cells treated with OCRL1 siRNA but still retaining OCRL1 expression (white stars) are smaller than most cells that lack OCRL1 expression. Compressed confocal sections.

Figure 5.4.4: Effect of OCRL1 loss on ZO-1 localisation to apical membrane

Control siRNA

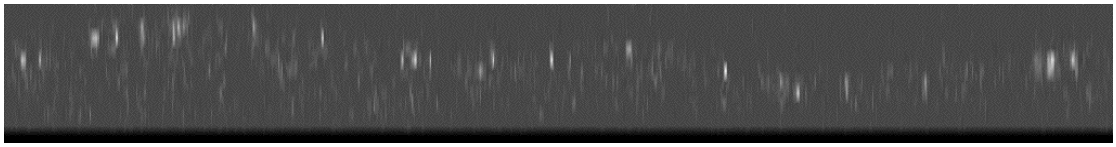

OCRL1 siRNA

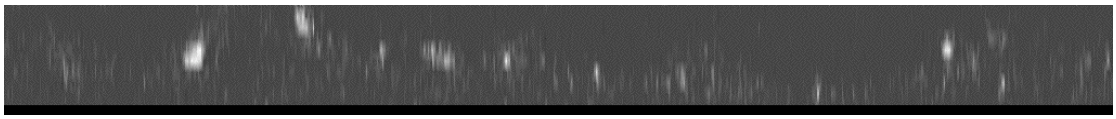

Figure 5.4.4 legend: Immunofluorescent stain of ZO-1. Caco-2 cells were treated twice with OCRL1 siRNA or non-targetting, negative control siRNA, over a period of 72 hours. Cells were then fixed with 4% paraformaldehyde, permeabilised, blocked and processed for ZO-1 immunostaining. XZ sections (1 micron distance per section) were then taken with a Leica confocal microscope. In the case of the OCRL1 siRNA treated sample, all cells in view were depleted of OCRL1.

Figure 5.4.5: Effect of OCRL1 loss on E-cadherin localisation

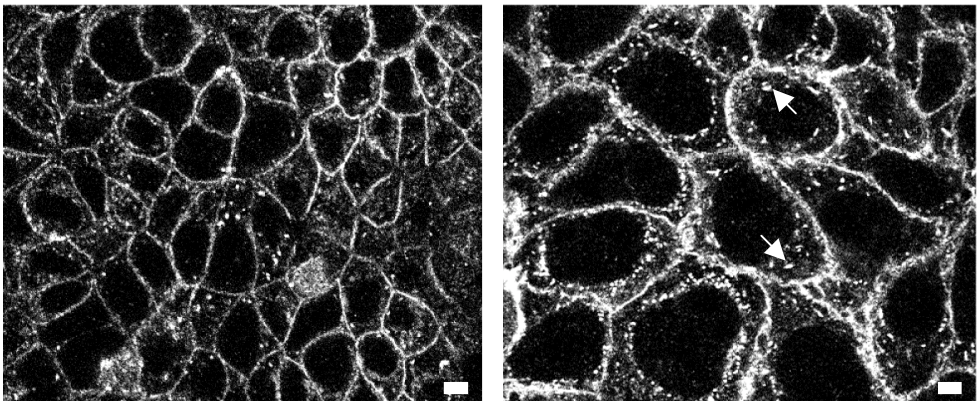

Control siRNA OCRL1 siRNA

Figure 5.4.5 legend: Caco-2 cells were treated twice with OCRL1 siRNA or non-targetting, negative control siRNA, over a period of 72 hours. Cells were then fixed with 4% paraformaldehyde, permeabilised, blocked and processed for E-cadherin immunostaining. Images were then taken with a Leica confocal microscope. White arrows indicate sites of increased punctate staining, much of which is perinuclear. Multiple compressed confocal sections. Scale bar (10μm).

Figure 5.4.6: Quantification of effect of OCRL1 loss on cell area

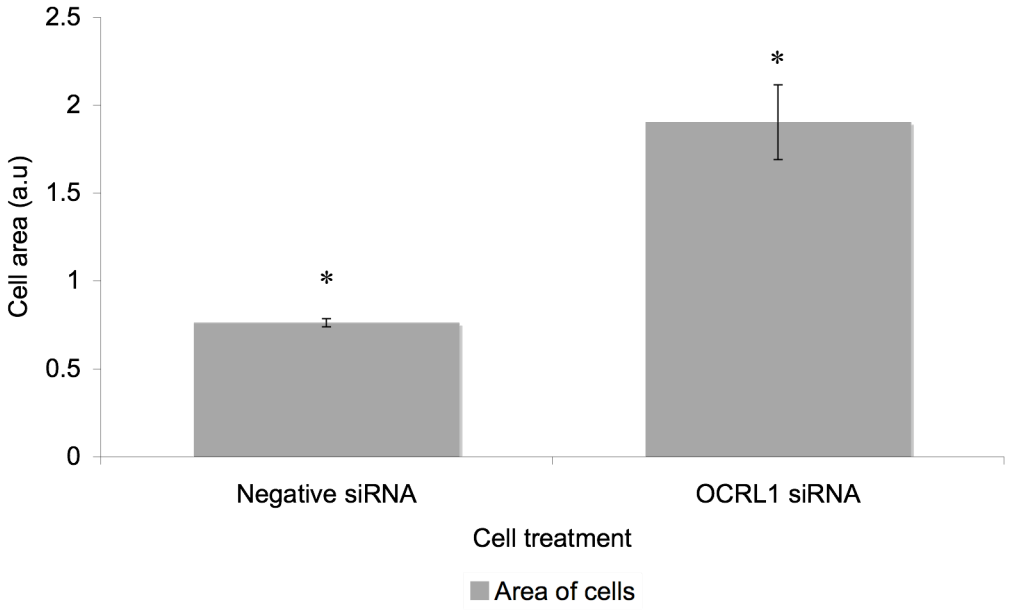

Figure 5.4.6 legend: Using the ZO-1 stain from two different sets of experiments, we measured the area covered of over 200 cells per experiment. Upon loss of OCRL1, cells cover approximately two and a half times the area of cells treated with non-targetting, negative control siRNA. This difference was statistically significant. Error bars represent standard error. * T-tests comparing siRNA treated cells with controls produce p values < 0.05.

Figure 5.4.7: Quantification of effect of OCRL1 loss on cell height

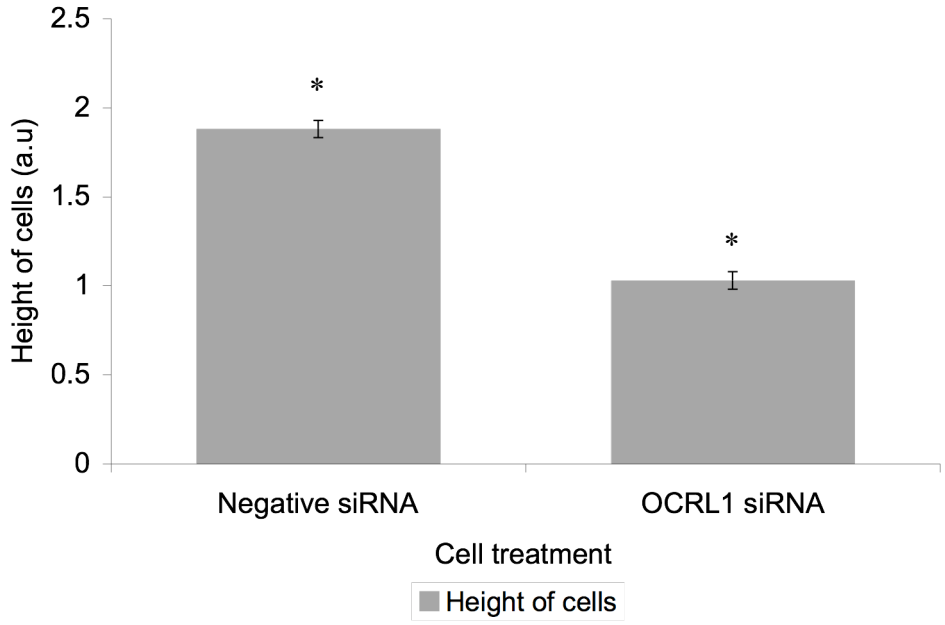

Figure 5.4.7 legend: Using the ZO-1 stain from two different sets of experiments, we measured the height covered in three different regions of the Caco-2 monolayer. Upon loss of OCRL1, cells depleted of OCRL1 are approximately 55% the height of cells treated with non-targetting, negative control siRNA. This difference was statistically significant. Error bars represent standard error. * T-tests comparing siRNA treated cells with controls produce p values < 0.05.

Figure 5.4.8: Effect of OCRL1 loss on ZO-1 localisation in HCE cells

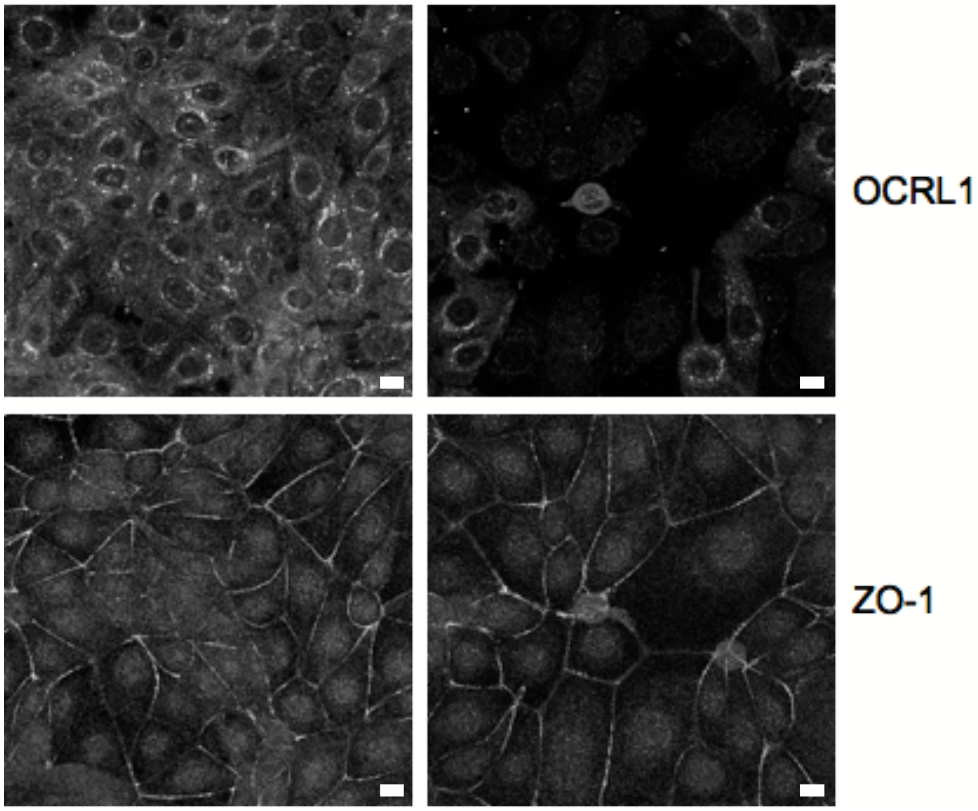

Figure 5.4.8 legend: HCE cells were treated twice with OCRL1 siRNA or non-targetting, negative control siRNA, over a period of 72 hours. Cells were then fixed with 4% paraformaldehyde, permeabilised, blocked and processed for OCRL1 and ZO-1 immunostaining. Images were then taken with a Leica confocal microscope. As with Caco-2 cells (Fig 6.4.3), HCE cells with higher residual OCRL1 tended to have smaller cross-sectional area. 3 compressed confocal sections. Scale bar (10μm).

Figure 5.4.9: Effect of OCRL1 loss on the actin cytoskeleton

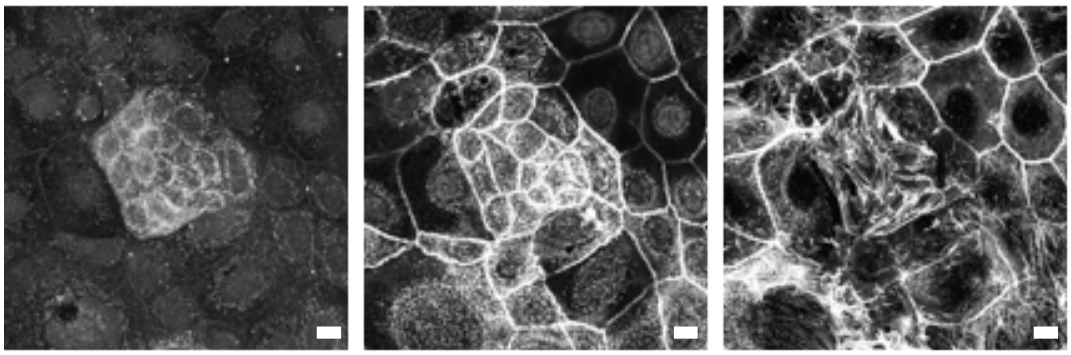

OCRL1 Actin (apical) Actin (basal)

Figure 5.4.9 legend: Caco-2 cells were treated twice with OCRL1 siRNA, over a period of 72 hours. Cells were then fixed with 4% paraformaldehyde, permeabilised, blocked and stained with TRITC-phalloidin. Images were then taken with a Leica confocal microscope. The right hand panel shows that while cells that retained OCRL1 (central cluster) are rich in basal actin stress fibres, most of the remaining cells in the same field that are depleted of OCRL1 have few or no stress fibres. Multiple compressed confocal sections. Scale bar (10μm).

Figure 5.4.10: OCRL1 and ZO-1 localisation over the course of a calcium switch assay

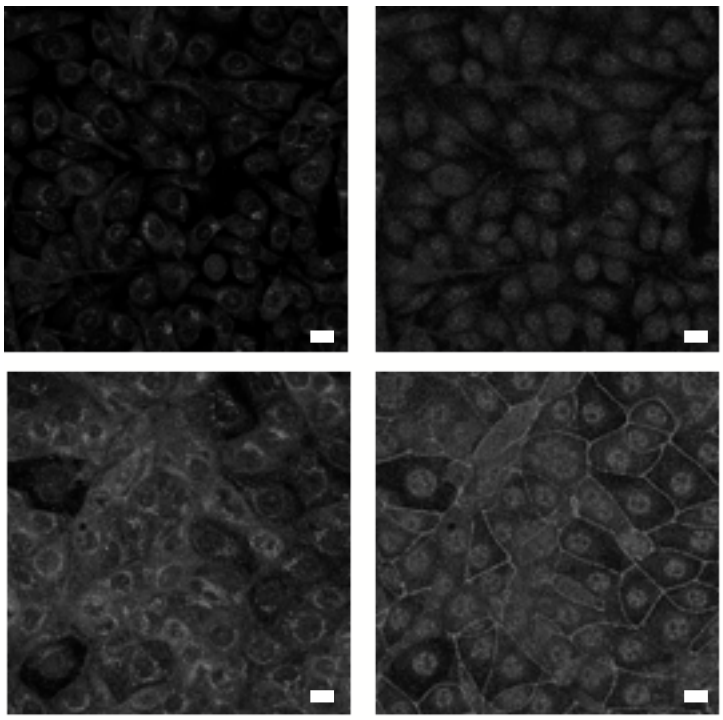

Figure 5.4.10 legend: HCE cells were plated and allowed to grow to 100% confluency. Cells were then washed twice with PBS and placed in low calcium containing media overnight. After overnight incubation, cells were washed twice with PBS and regular calcium containing media was added to cells. After overnight incubation in low calcium containing media, and 6 hours after regular calcium, cells were then fixed with 4% paraformaldehyde. Cells were then permeabilised, blocked and immunostained for OCRL1 and ZO-1. Images were then taken with a Leica confocal microscope. 3 compressed confocal sections. Scale bar (10μm).

Figure 5.4.11: Effect of OCRL1 loss on ZO-1 recruitment after a calcium switch assay

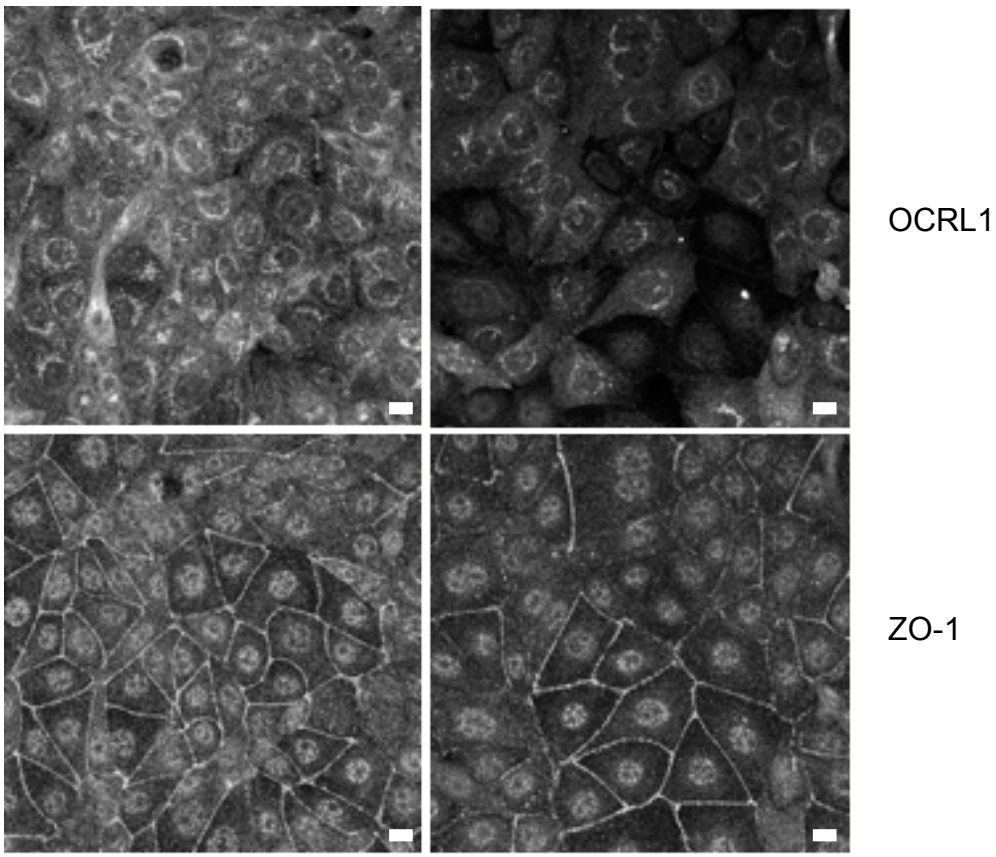

Figure 5.4.11 legend: HCE cells, after being treated with non-targetting, negative control or OCRL1 siRNA, were allowed to grow to 100% confluency. Cells were then washed twice with PBS and placed in low calcium containing media overnight. After overnight incubation, cells were washed twice with PBS and regular calcium containing media was added to cells. 6 hours after regular calcium, cells were then fixed with 4% paraformaldehyde. Cells were then permeabilised, blocked and immunostained for OCRL1 and ZO-1. Images were then taken with a Leica confocal microscope. 3 compressed confocal sections. Scale bar (10μm).

Figure 5.4.12: Trans-epithelial resistance over the course of a calcium switch assay

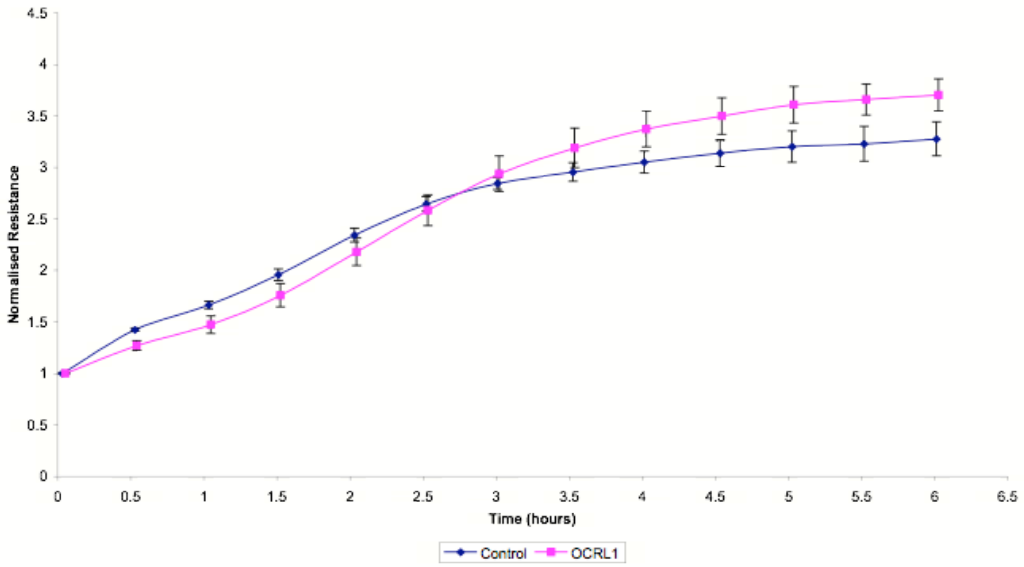

Figure 5.4.12 legend: HCE cells were plated into multi-well slides after being treated with control or OCRL1 siRNA and allowed to grow to 100% confluency. Cells were then washed twice with PBS and placed in low calcium containing media overnight. After overnight incubation, cells were washed twice with PBS and regular calcium containing media was added to cells. During the change of media, cell impedance was measured using an ECIS instrument. This measurement was then converted into trans-epithelial resistance. Measurements from wells in quadruplicate are averaged with error bars indicating standard error. Other repeat experiments showed a similar delay in initial speed of recovery. However, the elevated TER at 6 hours of OCRL1 siRNA treated cells, in comparison to controls, varied between experiments.

Chapter 6: Discussion

6: Discussion

6.1: OCRL1 and localisation of phosphoinositides

The preferred 5-phosphatase activity of OCRL1 upon the membrane lipid PI(4,5)P2 has been the focus of many studies driven at understanding the cellular basis of Lowe Syndrome. Many cellular events are regulated and affected by control of PI(4,5)P2 levels and localisation. Indeed, it has been shown that patients with Lowe Syndrome, lacking the OCRL1 enzyme, have elevated levels of PI(4,5)P2 [36]. However, the site of this aberrant pool of PI(4,5)P2 has not yet been found. We decided to tackle this issue through a number of means: using existing GFP-tagged chimeras of PH domains known to have specific phosphoinositide binding ability, modifying one of these characterised modules to test our hypothesis and also visualising the endogenous localisation of a protein known to bind PI(4,5)P2.

Our first hypothesis was that as OCRL1 resides predominantly at the trans-Golgi network, the increased pool of PI(4,5)P2 upon OCRL1 loss would accumulate in its place. We could demonstrate repeatedly that depletion of OCRL1 using transient RNAi knock-down did not alter the localisation of the PH domain of PLCδ. We next moved on to check whether the localisation of PI(3,4,5)P3 was different upon OCRL1 depletion, as reported by the PH

domains of AKT or Grp1 tagged to GFP. Our hypothesis was that excess PI(4,5)P2 may be converted to PI(3,4,5)P3 by PI3K family members in order to control PI(4,5)P2 levels. It was also possible that OCRL1 targeted a significant pool of PI(3,4,5)P3 [119]. Again, no difference was observed upon transient OCRL1 knock-down.

As no change in localisation upon OCRL1 depletion was observed using GFP-chimeras of AKT, Grp1 and PLCδ PH domains in HeLa cells, we attempted to tailor our GFP-reporter to the site of OCRL1 action. The major pool of PI(4,5)P2 exists at the plasma membrane, which is a relatively strong, anionic environment. Evolutionarily, many proteins that target and bind PI(4,5)P2 also prefer to reside within anionic environments and vice-versa [167]. For this reason, basic amino-acid residues surround the pockets of many PH domains that bind phosphoinositides. Furthermore, proteins with stretches of basic residues are sufficient to target the plasma membrane [167]. This mechanism of coincidence detection of the anionic plasma membrane and PI(4,5)P2 provides these proteins with greater membrane affinity and avidity. Coincidence detection is employed by a great number of proteins in the cell, as a means of targeting their desired organelle. The problem of this system comes when an experiment aims to use plasma membrane targeted domain that binds PI(4,5)P2 (PLCδ -PH), to seek out a (hypothesised) trans-Golgi network pool of PI(4,5)P2. It is this insight that led us to believe that the existing GFP-PH chimeras used to localise phosphoinositides were not suitable or tailored to our studies.

The creation of GFP-POP-PH yielded very consistent, positive and encouraging initial results. This fusion of the mutated OSBP-PH domain and PLCδ-PH domain served to seek out internal, ARF1-positive pools of PI(4,5)P2 upon OCRL1 depletion. However, as we continued to do experiments with this reporter, experiments became less repeatable and were no longer statistically significant. Studies looking at the effect of expression of GFP-POP-PH alone in cells showed that after 24 hours OCRL1 was sequestered within a perinuclear site and the trans-Golgi network compartment as reported by TGN46 staining was disrupted. The reason for this finding may be that the ARF1 binding ability of GFP-POP-PH may have led to ARF1 being sequestered within the TGN, a phenotype that has been previously seen in other studies with overexpression of the OSBP-PH by our laboratory. This finding was disappointing but we believe it may be due to a side-effect of looking at the localisation of lipids using domains from proteins that work within the pathway being tested. For instance, all four PH domains often used to study the localisation of PI(3,4,5)P3 independently affect different downstream functions of the lipid [154]. Furthermore, we believe that the problems encountered with POP-PH are also related to gross over-expression. For this reason we would like to create a POP-PH construct with a weaker promotor than the current CMV promoter used. On the evidence of our current results, we cannot say conclusively that there is an internal accumulation of PI(4,5)P2 reportable by POP-PH. Nevertheless, we would like to revisit our work with GFP-POP, possibly in another cell line where we can establish a role for OCRL1. Our studies using GFP-POP in HeLa cells were conducted very early in this project. Since then, our very recent work

has centered on investigating the role of OCRL1 in Caco-2 cells. As yet, we have not had time to test the effect of OCRL1 loss on GFP-POP localisation in Caco-2 cells.

In summary, we failed to see any changes in phosphoinositide localisation upon OCRL1 knock-down as visualised with GFP-PH domains. Therefore, we still do not know, conclusively, where the elevated level of PI(4,5)P2 is localised. The best and most conclusive evidence we have is the negative data; the PLCδ-PH domain does not move from the plasma membrane upon OCRL1 knock-down. It could therefore be argued that the plasma membrane is the site we sought. This theory is supported by the endogenous localisation of OCRL1 in polarised cell lines and primary cells. In these cells, OCRL1 is readily seen at the plasma membrane, intercellular junctions and sometimes within the nucleus, all sites within the cell that have been shown to contain pools of PI(4,5)P2. Interestingly, many more protein domains are being discovered to interact with PI(4,5)P2. Our general theory of using a protein that binds PI(4,5)P2 and detects the co-incident site at which OCRL1 acts, may still prove to be rewarding in the hunt for the site of elevated PI(4,5)P2 in cells lacking OCRL1 function. Interesting sets of proteins, containing PDZ domains, have recently been shown to bind phosphoinositides [132, 134]. Many of these PDZ domains exist within proteins targeted to intercellular junctions, which makes them very attractive for future OCRL1 related studies. Through tagging GFP to the PDZ domains of proteins such as ZO-1 and syntenin-1, junctional pools of PI(4,5)P2 may be probed. It would be very interesting to characterise the binding site of these domains in order to specifically monitor

levels of phosphoinositides. If we find and characterise PDZ domains of junctional proteins that specifically bind PI(4,5)P2, we could also try tandem dimers of these domains in an effort to more efficiently detect junctional PI(4,5)P2. The specificity of these reporters for PI(4,5)P2 could be tested by depleting PI(4,5)P2 from the plasma membrane of cells using the rapamycin system used by Varnai *et al.* in 2006.

As mentioned above, PI(4,5)P2 has been shown to accumulate within the nucleus. Within the nucleus there is a complement of proteins that function to metabolise phosphoinositides, such as PLC, PI3K and phosphoinositide phosphatase families of proteins [141, 168]. Interestingly, the PDZ domain of Syntenin-2 has been shown to bind the PI(4,5)P2 within the nucleus [21]. Given that OCRL1 is found within the nucleus in some polarised cell types, and also that GFP-tagged C-terminal OCRL1 readily enters the nucleus, it would be interesting to see whether OCRL1 depletion would alter the localisation of this domain.

Furthermore, given the finding that OCRL1 has a different localisation in polarised cells, it would be interesting to re-visit studies with PH domains of PLCδ, Grp1 and AKT in Caco-2 and MDCK cells. In particular, recent studies using 3D cultures of MDCK cells have shown that PI(4,5)P2 and PI(3,4,5)P3 can be specifically detected at apical and basolateral membranes, respectively [123, 142]. It would be interesting to see whether OCRL1 depletion in a fully polarised model, especially the 3D model, would affect the characterised localisation of phosphoinositides. With regard to the 3D model

of MDCK cyst formation, it was shown recently that the recruitment of Annexin A2 to the apical membrane of 3D MDCK cysts through binding to PI(4,5)P2 is integral to full epithelial polarisation, which makes this system well worth looking into further [123]. If a model organism for Lowe Syndrome were to be obtained, it would also be very interesting to undertake these experiments on the affected polarised epithelial tissue.

Through endogenous staining of Annexin A2 in HeLa cells, we found a change in localisation with loss of OCRL1. Annexin A2 moved more towards limiting membranes, with less staining observed in the cytoplasm. This finding fits in nicely with previous published work published linking OCRL1 and actin dynamics [66, 98]. Annexin A2 has been demonstrated to have actin nucleating activity on vesicular actin rockets and on multivesicular bodies (Prof. Jean Gruenberg, Personal Communication). The redistribution of Annexin A2 also links in with a previous finding that Lowe Syndrome patient fibroblasts display a loss of actin stress fibres and an increase in punctate actin staining [66]. It is possible that Annexin A2, which can bind and bundle actin into cables, contributes to this phenotype. In the aforementioned study of Lowe Syndrome patient fibroblasts, other actin-modulating proteins such as gelsolin and α-actinin, both of which have altered activity in the presence of PI(4,5)P2, also change their distribution [169-171]. Further experiments to fully correlate changes in actin dynamics, Annexin A2 localisation and levels and localisation of PI(4,5)P2 would be warranted. Interestingly, data published by our lab shows that in the Lowe Syndrome patient fibroblasts we use in this thesis, vesicular actin rocketing is readily seen in an unstimulated manner [98]. This links in with

data in this thesis, as vesicular actin rocketing is a calcium and PI(4,5)P2-dependent process.

Not only did we observe an intracellular change in distribution of Annexin A2, but we also found Annexin A2 in the medium and on the exofacial leaflet of the plasma membrane. As mentioned above, Annexin A2 has been found to play a key role in the endocytic pathway in epithelial cells. It has been found that it functions to nucleate a small patch of actin on early endosomes, integral to their progression to multivesicular bodies (Personal communication, Prof. Jean Gruenberg). Furthermore, this process is highly dependent upon cholesterol levels. This nucleation may be an analagous process to the previously mentioned vesicular actin rocketing observed in Lowe Syndrome patient fibroblasts. One known mechanism for Annexin A2 presence in the medium is through release of exosomes derived from multivesicular bodies [152]. If PI(4,5)P2 levels on late endosomes/multivesicular bodies increase upon OCRL1 depletion, recruitment of Annexin A2 may occur. This may explain the appearance of Annexin A2 in the medium and on the exofacial face of the plasma membrane.

There are similar changes in Annexin A2 localisation upon loss of OCRL1 and CLCN5 function, which may reflect dysfunction of the same pathway. The activity of many ion channels and pumps has been shown to be affected by PI(4,5)P2. The changes in PI(4,5)P2 upon OCRL1 depletion may lead to dysregulation of the CLCN5 channel activity, an event that has been suggested previously [87]. Therefore changes in Annexin A2 localisation upon

loss of function of CLCN5 or OCRL1 may reflect a difference in the ability to acidify endosomal compartments, which consequently may alter trafficking and possibly the orientation of Annexin A2 within the membrane. We do not know the exact mechanism by which Annexin A2 changes distribution, so this theory may be as likely as a theory in which Annexin A2 responds directly to changes in PI(4,5)P2 upon OCRL1 loss.

Further to this, work from this study has revealed a potential shared mechanism for renal failure in Dent Disease patients and Lowe Syndrome patients. In cells expressing inactive CLCN5 and upon depletion of CLCN5, Annexin A2 changes its distribution in a similar fashion to cells depleted of OCRL1 [78]. It has been proposed before that Annexin A2 at the extracellular face of the plasma membrane may provide a nucleus for calcium oxalate crystal binding, a known cause of renal Fanconi Syndrome. The renal dysfunction observed in Lowe Syndrome patients may however directly correlate with defects in endocytosis, a process highly regulated by PI(4,5)P2 [26, 172, 173]. It is possible that a primarily endosomal defect could be consistent with a junctional defect in polarised cells. Endosomal proteins may be mistargetted through changes in the function and localisation of junctional proteins upon OCRL1 or CLCN5 loss, which often serve as scaffolds for trafficking events [88]. Conversely, if OCRL1 and CLCN5 do work within the same trafficking pathway, then it is possible that CLCN5 depletion may affect endocytosis or delivery of junctional proteins to desired membranes. For these reasons, it would also be interesting to assess the effect of CLCN5

depletion and over-expression on the function and structure of the tight junction.

Although GFP-POP-PH failed in its initial task, it proved to be extremely useful in detecting differences in yeast phosphoinositide levels. The reason for the difference in efficacy of PI(4,5)P2 detection of POP-PH between yeast and mammalian cells may lie in the balance between inositol lipids and inositol phosphates. In yeast, it is permissible for levels of inositol phosphates to be raised, as there is no IP3-dependent release of internal calcium stores. However, if IP3 levels were raised in mammalian cells, this would be catastrophic to the maintenance of cytosolic calcium levels, as the IP3-receptor would be permanently engaged and open.

In yeast, studies frequently use a dimer of the PLCδ-PH domain in order to visualise PI(4,5)P2, in order to maximise its signal at the plasma membrane. However, when used as a monomer, the domain binds to the relatively more abundant IP3 in the cytosol. This is because the PLCδ-PH domain binds both molecules, with a ten-fold greater affinity for IP3 [174]. Therefore, the distinction between plasma membrane and cytosol is harder to visualise. In our experiments, cells were grown at 30 degrees, at which the PLCδ-PH domain was predominantly observed in the cytoplasm, and very infrequently at the plasma membrane. However, the POP-PH fusion was clearly seen at the plasma membrane. We attribute this to co-incident binding of POP-PH to PI(4,5)P2 (via PLCδ-PH) in the plasma membrane and a protein determinant we predict to be ARF-related (via mutated OSBP-PH), from previous studies.

For this reason, POP is able to detect subtle changes in P(4,5)P2 at the plasma membrane upon inactivation of single synaptojanin-like proteins.

We believe that the observed changes in GFP-POP distribution in yeast are representative of these changes in the ratio of PI(4,5)P2 and IP3. For example, it is possible that the removal of GFP-POP from the plasma membrane upon inactivation of synaptojanin-like proteins is due to increased levels of IP3 in the cytoplasm, due to over-activity of PLC1 upon elevated PI(4,5)P2 levels. Furthermore, these differences may be exacerbated if any of the synaptojanin-like proteins act to de-phosphorylate IP3 to IP2. Further studies will focus on elucidating the mechanism of this removal of POP-PH from the plasma membrane, through crossing PLC1 delete strains with the synaptojanin-like inactivated strains. These studies are important, as they reveal that each individual 5-phosphatase controls the specific regulation of PI(4,5)P2 levels. This reveals a difference in PI(4,5)P2 localisation and levels upon inactivation of just one of the synaptojanin-like proteins, previously unseen in the Stefan *et al.* study in 2002.

In summary, current findings and our data suggest that in cells lacking OCRL1 function, PI(4,5)P2 does build up on internal vesicles as shown through increased vesicular rocketing in Lowe Syndrome fibroblasts and relocalisation of Annexin A2 in HeLa cells. However, we have only been able to detect this indirectly through localisation of Annexin A2. It would be interesting to try different GFP-chimeras to PI(4,5)P2 binding modules. One potential avenue to test would be to mutate out the basic residues in the PLCδ-PH domain, in

order to make the probe more PI(4,5)P2-specific and less attracted to anionic environments. Another would be to try other recently discovered PI(4,5)P2 binding modules such as the Tubby domain, or some of the aforementioned PDZ domains, now known to bind PI(4,5)P2 [175]. Furthermore, given that Annexin A2 reports differences in localisation upon OCRL1 loss, it may be profitable to elucidate the part of Annexin A2 sequence that binds PI(4,5)P2 and use it to probe for phosphoinositide changes.

These data also suggest that the changes in PI(4,5)P2 upon OCRL1 loss of function manifest themselves differently depending on the cell type used. Given these insights, we believe that it would be profitable to test the localisation of PI(4,5)P2 in these polarised 3D cell cultures lacking OCRL1, or in fully polarised epithelial tissue of a model organism for Lowe Syndrome.

6.2: OCRL1 and calcium signalling

Loss of OCRL1 function directly increases in the level of PI(4,5)P2 substrate for PLC family members. Our initial hypothesis was that a simple increase in PI(4,5)P2 levels may be sufficient to alter the regulation of cellular calcium handling. However, there are many ways in which an increase in PI(4,5)P2 could affect calcium signalling.

When transiently depleting OCRL1 from HeLa cells, we demonstrated that the elevated level of calcium in the cytoplasm of OCRL1 depleted cells comes from the extracellular medium. The shared sustained calcium response to both thapsigargin and histamine suggests that upon depletion of OCRL1 in

HeLa cells, through an as yet unknown mechanism, there is increased calcium-induced calcium release. These data may be explained by changes in the function and/or activity of store operated calcium channels at the plasma membrane. For instance, OCRL1 may play a role in destabilising the conformational coupling of the IP3 receptor and store operated calcium channels, through ion channel endocytosis. Endocytosis of proteins involved in this pathway may also affect expression levels, if they are targeted for destruction. Furthermore, PI(4,5)P2 may have a positive, direct role in the activation of store-operated calcium channels. Upon OCRL1 depletion, an increase in the association of IP3 receptors and store operated channels, and/or increased activity of store operated calcium channels may be responsible for changes in cellular calcium handling. The identification of Orai1 and STIM-1 as the elusive components of the store operated calcium entry mechanism provides an avenue for further investigation, especially as these can form heterotrimeric complexes containing TRP-C channels that are regulated by PI(4,5)P2 [176-178].

However, when looking at the Lowe Syndrome patient fibroblasts, we observed different phenotypes to those seen with OCRL1 depletion in HeLa cells. These differences may represent the many ways that changes in PI(4,5)P2 levels and localisation could impact calcium signalling. Upon OCRL1 depletion, some increase in basal levels of IP3 in the cytoplasm may occur through a corresponding increase in PLC family member activity upon its preferred substrate, PI(4,5)P2. Conversely, IP3 levels may be increased due to a direct influence of OCRL1 depletion upon IP3 metabolism. As

mentioned earlier, it is possible that OCRL1 functions to dephosphorylate IP3 to IP2. These possibilities can be investigated in a number of ways, such as direct measurement of IP3 levels in resting cells and upon stimulation with a G-protein coupled PLC stimulus such as histamine or ATP. This can be achieved through radioactive labelling of cells with tritiated inositol, which is readily incorporated into the PI(4,5)P2 precursor phosphatidylinositol [179]. Also, monitoring of changes in localisation of the C1 domain of PKC in resting and stimulated cells may reveal significant differences. PI(4,5)P2 is hydrolysed to IP3 and DAG, so changes in the kinetics of C1 domain binding of DAG at membranes upon stimulation may indirectly reflect changes in IP3 levels within the cell. Should a difference be found, this may also represent changes in PKC activity, which is known to be affected by the PLC/IP3 pathway [157, 180].

Another possibility can be proposed with the knowledge that the Golgi apparatus has been shown to be a bona fide IP3 sensitive calcium store. Work in this study and published data suggests that upon OCRL1 depletion in some cell types, especially Lowe Syndrome fibroblasts, PI(4,5)P2 accumulates on internal membranes, as reported by the endogenous staining of Annexin A2. Should these internal membranes be directly verified as positive for PI(4,5)P2 and derived from the Golgi apparatus, an attractive model can be proposed. The hydrolysis of elevated PI(4,5)P2 at the Golgi apparatus by PLC family members may lead to local calcium transients. The increased use of the Golgi apparatus as an IP3-sensitive calcium store may lead to an increase in total Golgi calcium concentration through overcompensation. Excessive re-uptake of calcium ions into stores as a result

of PI(4,5)P2 elevation at Golgi membranes may be responsible for the observed elevation in cytoplasmic calcium in OCRL1 depleted cells. The dynamics of ER and Golgi calcium stores can be efficiently monitored by aequorins targeted specifically to these organelles [83, 84].

Another appealing possibility can be found in work analysing the role of calcium and membrane traffic, which may provide an explanation for the redistribution of Annexin A2. Calcium transients in and around the Golgi apparatus have been shown to affect the secretory competence of cells and alter the function of the Golgi apparatus itself [181]. OCRL1 depletion may cause Golgi apparatus dysfunction leading to errors in organisation of the secretory pathway and membrane traffic as a whole. This potential mechanism may provide another explanation for the redistribution of Annexin A2 to membranes and its increased presence in the medium of OCRL1 depleted cells.

The potential increase of cytosolic calcium levels upon stimulation as a result of OCRL1 depletion may be another contributing factor in the change of Annexin A2 localisation. Cells in the experiments presented in this report are grown in 10% foetal calf serum, which contains many different growth factors capable of eliciting IP3 responses. Annexin A2 binding to PI(4,5)P2 and membranes has been shown to be enhanced by elevated calcium [75, 76]. It is possible that the redistribution of Annexin A2 is due to a change in calcium levels within the cytoplasm, in combination with elevated PI(4,5)P2 at membranes. Experiments with the ratiometric calcium indicator Fura-2 have

suggested that basal cytosolic calcium is unchanged in cells depleted of OCRL1 (data not shown). This does not however rule out the possibility of changes in the flux of calcium ions through the cytoplasm. The possibility exists that OCRL1 depleted cells leak calcium from stores and quickly respond by pumping it out of the cell or back into intracellular stores. Through a mechanism where calcium levels are continually oscillating, in combination with elevation of PI(4,5)P2, the redistribution of Annexin A2 may be explained. Interestingly BAPTA treatment in Lowe Syndrome fibroblasts caused loss of Annexin A2 dependent actin rocketing, known to be a calcium-dependent event. Furthermore, through butan-1-ol treatment, and subsequent reduction of PI(4,5)P2 synthesis, the number of cells displaying spontaneous actin rocketing was dramatically reduced. It could be argued that this experiment also provides support for a role for OCRL1 with phospholipase D. Interestingly, previous data have shown that Synaptojanin inhibits ARF-activated PLD [182]. It is noteworthy that in this publication, they add an unpublished observation that OCRL1 also inhibits ARF-activated PLD. It would be interesting to follow up on this finding, especially considering there is also a characterised PI(4,5)P2 binding site in PLD1 and PLD2 [183]. A feedback mechanism may exist, whereby OCRL1 reduces internal PI(4,5)P2 levels in order to reduce PLD activity. Without OCRL1, this means there may be no negative regulation upon PLD activity.

Annexin A2 has been found to be an inhibitor of G-protein mediated PLC activation [158]. It is possible that a homeostatic mechanism may be in place whereby upon PI(4,5)P2 elevation, Annexin A2 binds and potentially

sequesters PI(4,5)P2 from PLC family members. This possibility can be addressed by a double depletion of Annexin A2 and OCRL1 from cells and analysis of the ability of the cell to respond to histamine or ATP. It would also be interesting to monitor IP3-mediated calcium signalling of cells over-expressing OCRL1. It would be expected that effects on calcium signalling through over-expression of OCRL1 would be similar to that shown for over-expression of synaptojanin-1, another inositol polyphosphate 5-phosphatase [85].

Overall, clear differences in cellular calcium responses to various stimuli have been observed, however inconsistent. All of these differences may well be explained through variation in cell type and the way in which cells adapt to loss of OCRL1 function. Our data demonstrates variability in calcium response in cells lacking OCRL1, which is in line with published work. The recent calcium signalling study by Suchy *et al.* in 2009 also describes a great deal of variation in response to bradykinin between seven different Lowe Syndrome fibroblast lines [184]. Full and thorough characterisation is required for any clear conclusions to be drawn. The studies undertaken in this thesis were performed using the intensiometric calcium dye, Fluo-4. Although this dye is efficient in measuring changes in calcium levels and finding a phenotype in a population of cells, it does not provide any detail on how each single cell responds to a stimulus. These details may prove to be vital in understanding the mechanism of the phenotype we observe. Problems with the Fluo-4 dye and population measurement of calcium signalling lie with the way in which cells couple to one another. What seems to be a uniform

response from a population of cells is actually a mean of many different responses, all inter-dependent upon one another. To continue these studies, we believe experiments using the ratiometric calcium dye, Fura-2 will be helpful in understanding the differences we observe upon OCRL1 loss of function. This dye can be used to measure actual calcium concentrations in single cells and we believe would be helpful in pinning down how and why OCRL1 affects calcium signalling.

As mentioned above, in support of our finding of changes in calcium signalling in Lowe Syndrome fibroblasts and HeLa cells depleted of OCRL1, a paper has been published demonstrating a calcium phenotype, in a different set of Lowe Syndrome fibroblasts, upon stimulation with bradykinin [184]. Although this paper shows the same trend as our data, when comparing the responses provided in this study, there is no statistically significant difference in bradykinin responses between sets of control and Lowe Syndrome fibroblasts ($p= 0.117$). A calcium phenotype in cells lacking OCRL1 function may be very attractive, however, the variation in responses suggest that it is more likely to be wishful thinking rather than a significant and consistent difference.

Given our findings and the phenotype of OCRL1 depletion in polarised cell types, it may be interesting to assess calcium signalling in MDCK and Caco-2 cells upon depletion of OCRL1. Interestingly, phototransduction in the Drosophila eye occurs utilises the PLC signalling pathway. If an OCRL1 knock-out fly model were to be created, changes in PI(4,5)P2/IP3 signalling would be easily probed for. Furthermore, the epithelial tissue and

development of polarity in Drosophila is well characterised and many potential effects of OCRL1 in polarised living tissue could be examined. The draw-back of studies assessing the function of OCRL1 in Drosophila is that flies do not express INPP5B. Therefore a genetic model for Lowe Syndrome in this system may not be tractable to the human condition.

6.3: OCRL1, intercellular junctions and polarised cell types

The most striking of our findings came with the discovery that endogenous OCRL1 localises to very different sites in polarised cells. Given that the phenotype of OCRL1 loss in humans manifests itself in polarised cell types: the epithelial cells of the lens and kidney as well as highly polarised neurons, these findings raise multiple questions. What are the specific mechanisms by which OCRL1 targets the new sites we observe in polarised cells? Is there a specific role that OCRL1 plays in polarised cells, different to non polarised cells? For instance, are there subtle OCRL1-regulated changes in phosphoinositide levels at junctions and the nucleus, and what is the purpose of this regulation? Are there other binding partners for OCRL1 in polarised cell types? Does this new localisation provide us with an insight into cellular processes controlled by OCRL1 that have previously been overlooked?

We have many clues to some of the answers to these questions. We have found, through over-expression of GFP-tagged chimeras of each terminus of OCRL1, that elements within the carboxyl-terminal bring OCRL1 to the tight junction. There are plenty of candidates that may be responsible for the

molecular basis of this localisation. Interestingly, as discussed before, members of the Rab GTPase family, key organisers of membrane traffic, have been shown to localise and control trafficking pathways to and from intercellular junctions [88, 107]. The similarity to OCRL1 change of localisation between polarised and non-polarised cell types exhibited by some Rab GTPases, such as Rab 13, is something that we would like to follow up on. Furthermore, these differences may prove to be clinically important, especially considering that Rab 14 is a binding partner of OCRL1 but not its homologue, INPP5B [44, 55]. As INPP5B is likely to play a compensatory role upon OCRL1 loss, this difference in Rab 14 binding may have some clinical importance and contribute to the phenotypes observed in neurons and epithelia of the lens and kidney.

Another possibility is that OCRL1 targets intercellular junctions via its catalytically inactive Rho-GAP domain. In previous studies, looking at the RhoGAP domain of OCRL1 in isolation, it was found that stimulation of RhoGTPases caused its localisation to the plasma membrane ruffles [47]. The activity of RhoGTPases such as Rho, Rac and Cdc42 is integral to the formation of cortical and perijunctional actin, vital to development of polarised epithelia and intercellular junctions [104, 105, 160-162]. In addition, OCRL1 is a confirmed binding partner of both Rac and Cdc42 [42, 54]. The capacity of the RhoGAP domain to target the plasma membrane suggests that it may contribute to the junctional localisation of OCRL1 in polarised cell types [47]. Recent studies have also shown the importance of PI(4,5)P2 levels at the

apical membrane of polarised cells, a process highly dependent on Cdc42 activity [123].

OCRL1 contains three stretches of proline rich amino-acid sequence, two in the N-terminal and one at the very far region of C-terminal OCRL1. The consensus PxxP motif of proline rich motifs binds to SH3 domains of proteins[185, 186]. Interestingly, in this thesis we identify a new binding partner of OCRL1, in the tight junction protein ZO-1. It is possible that the interaction between the two proteins is direct through this method. Crystallographic studies of the C-terminus of OCRL1 reveal that the RhoGAP domain targets the membrane interface [54]. Through manipulation of this structure in Rasmol, we find that the prolines in the C-terminus are in an accessible region of OCRL1 structure and orientate into the membrane. There are many experiments to do to confirm this. If we were to knock-down OCRL1 and recover junctional localisation with a wobbled construct, then this possibility is easily probed for. If OCRL1 were to target and bind ZO-1 though its polyproline motifs, then this recovery of localisation would fail if the proline residues were mutagenised out to inert residues such as alanines.

Something of which we have little clues to is the observed nuclear localisation of OCRL1 in primary porcine RPE and MDCK cells. The mechanism by which OCRL1 targets the nucleus in polarised cell types is unknown. Intriguingly, the potential of OCRL1 to target the nucleus is realised in all cell types when the C-terminus of OCRL1 or the RhoGAP domain of OCRL1 are over-expressed. In MDCK cells, this nuclear localisation is clearer at lower density, in

monolayers that are yet to fully mature. During this period, there are many changes in transcriptional markers and proliferation. Whether the localisation of OCRL1 at these time points is significant or not, we do not know. There is a great deal of evidence for nuclear PI(4,5)P2, with many phosphoinositide metabolising proteins found to localise to a fairly novel sub-nuclear sites called nuclear speckles [21, 139]. Upon input of the C-terminal sequence into a bioinformatics database (Subnuclear Compartments Prediction System (Version 2.0)) capable of predicting the subnuclear localisation of proteins from primary sequence, we find that C-terminal OCRL1 is predicted to target these confirmed PI(4,5)P2 sites. Admittedly, we have not observed any evidence for OCRL1 in nuclear speckles, but the dynamics of these subnuclear organelles is yet to be established, and it may be that nuclear speckle localisation occurs in a stimulus-dependent manner. The nuclear and junctional localisation of OCRL1 opens up new ideas about OCRL1 biology. One potential mechanism by which the phenotype of OCRL1 loss occurs is through changes in proliferation and differentiation markers. There is a great amount of signalling to and from intercellular junctions and the nucleus [135]. OCRL1 activity may affect transcriptional activity of different proteins integral to the maturation and development of epithelial monolayers. It would be very interesting to study the signalling pathways derived from the junction, and this could be probed through analysis of the promotor activity of transcription factors such as ZONAB, β-catenin, AP-1 and myc.

Given the new localisations of OCRL1 in polarised cell types, it would be very interesting to find how many more interaction partners OCRL1 has, in

comparison to non-polarised cells such as HeLa or COS-7. It would also be interesting to find out whether the interaction between OCRL1 and ZO-1 is direct. It is possible that OCRL1 exists in a complex with other junctional proteins. For instance, the closely related ZO-2 protein shares much of the sequence of ZO-1, and displays similar nuclear and junctional localisation to OCRL1 in polarised epithelia. Further biochemical studies are required for full understanding of OCRL1 localisation and interactions in polarised cells.

It has been found previously that OCRL1 interacts with ARF family GTPases, ARF1 and ARF6 [43]. These proteins, like Rab GTPases, control many vesicular trafficking and signalling pathways. ARF6 has been shown to have roles in organising the actin cytoskeleton in polarised cells [187]. The ARF and Rho GTPase families of proteins may be responsible for the dramatic changes in the actin cytoskeleton upon OCRL1 loss in Caco-2 and HCE monolayers. The links between RhoGTPases and actin are well characterised, and OCRL1 loss may impact the regulation of them in many unpredictable ways. To get a grasp on the potential effect OCRL1 loss has upon RhoGTPase function, a study of their activity via effector domain immunoprecipitations of rhotekin and PAK could be undertaken. PI(4,5)P2 alters the function of a wide number of actin modulating proteins, such as WASP, Annexin A2, gelsolin and profilin [75, 76, 100, 129, 170, 188]. If OCRL1 loss affects the ability of ARF6 to modulate PI(4,5)P2 levels through PI(4)P5K activity, the regulation of their effect on the actin cytoskeleton may be altered. One way of studying the role of OCRL1 in actin dynamics during epithelial

polarisation would be to carry out a full biochemical study of the changes in pools of actin filaments, similar to that carried out by Zhang *et al.* in 2005 [102].

The formation and development of junctions occurs alongside the maturation and development of the epithelial monolayer. Many of the junctional proteins such as ZO-1 and E-cadherin organise the actin cytoskeleton during development. Alongside these events, RhoGTPases also control actin polymerisation via WASP/SCAR signalling, in part through changes in PI(4,5)P2 metabolism [100, 189]. All these events can now be tied in with OCRL1 biology. Due to the high number of proteins that OCRL1 interacts with, it will be hard to elucidate the molecular mechanism by which the actin phenotype in polarised cells occurs. The temporal dynamics of all of these interactions in polarised cells, alongside characterisation of the new interaction partners of OCRL1 will give a better understanding of how the changes in actin cytoskeletal elements and overall cell morphology occur.

6.4:General discussion and overall summary

In this study, we have investigated three distinct pathways related to depletion of OCRL1: localisation of PI(4,5)P2, calcium handling and development of junctions in polarised epithelia.

The key finding from this thesis comes in the finding that OCRL1 exhibits a different cellular localisation and behaviour in a polarised context. Previous work has found that OCRL1 predominantly targets the trans-Golgi network

and endosomes [52]. This localisation has always been perplexing, as the preferred substrate for OCRL1 is highly abundant at the plasma membrane. These studies place OCRL1 and its substrate at the same site, but only at specific time-points. In MDCK cells especially, the shift of endogenous OCRL1 localisation from the junction and nucleus to a more regular perinuclear, vesicular localisation, upon increased cellular density suggests that phosphoinositide levels are altered dynamically at different stages of epithelial maturation. Interestingly, the cellular phenotype we observed in Caco-2 cells upon knock-down of OCRL1 matches the monolayer morphology seen when OCRL1 best targets intercellular junctions i.e. the cells appear to be arrested at the stage where OCRL1 is normally targeted to junctions. To unify the findings from the two polarised cell lines we have used in this thesis, we need to reproduce our Caco-2 monolayer phenotype in MDCK cells, by design of oligonucleotides against canine OCRL1. If we can reproduce our phenotype in MDCKs, this would also answer any questions related to off target effects of our OCRL1 siRNA in Caco-2 cells. Also, we have performed knock-down and over-expression of OCRL1 in non-polarised cells such as HeLa and COS-7, with no evidence for any actin phenotype. However, there are many, as yet uncharacterised changes in the actin cytoskeleton upon these treatments in polarised cell types. We believe that the reason for the difference in effect of OCRL1 loss between polarised and non-polarised cells lies in the dynamics of the cross-talk between the actin cytoskeleton and intercellular junctions.

There is one key experiment that is required to ensure our phenotype occurs purely due to loss of OCRL1. This is a recovery experiment, replacing the loss of OCRL1. We need to design a set of experiments where knock-down of OCRL1 is achieved. Given that epithelial maturation requires the concerted actions of many cells in contact with one another, it would be a good idea to aim for a blanket recovery of the knock-down phenotype using an siRNA resistant OCRL1 stable cell line. If this could be achieved, we will be able to plan for many different experiments testing the mechanism of our observed phenotype, such as mutagenesis of key residues and motifs in OCRL1. Furthermore, it would also be interesting to see whether over-expressed INPP5B compensates for OCRL1 loss.

It is possible that the phenotype observed in Caco-2 cells is due to changes in polarised membrane traffic. In the future, we would like establish whether any changes in polarised traffic occur upon OCRL1 loss in Caco-2 cells. This can be achieved through staining for different markers of polarised traffic such as Na/K ATPase, transferrin receptor, and podocalyxin. Another possible cause for the phenotype we observe upon OCRL1 depletion is a change in cell proliferation. The recent data showing that the ASH domain of OCRL1 binds to APPL1 provides one possible avenue for investigation [54]. It has been shown that the nucleo-cytoplasmic shuttling of APPL1 can regulate the proliferative ability of the cell, via Rab 5 dependent trafficking [124]. If OCRL1 loss affects the way in which APPL1 traffics in and out of the nucleus, the downstream events of its nuclear activity may be affected [190].

The cell biology of OCRL1 depletion presented in this study concurs with clinical data regarding Lowe Syndrome patients. Obvious defects within the polarised epithelia of the lens in Lowe Syndrome patients have previously been demonstrated [191]. The observed increase in stimulation dependent cytosolic calcium upon OCRL1 depletion has very close links with other conditions causing inherited cataract. Calcium handling in the lens is highly regulated and many erroneous cellular processes shown to cause cataract are proposed to be due to dysregulation of calcium handling in the lens [192]. Also, Annexin A2 and actin are very important in the differentiation of lens epithelial cells to lens fibre cells, which is integral in prevention of cataract [148, 193]. Interestingly, it has been reported that Src family members play important roles in cataract formation [194]. Annexin A2 has been shown to be a major phosphorylation target of pp60 v-Src and therefore a link between Annexin A2 and Src in cataract formation may exist [195, 196].

Interestingly, treatment of patients that suffer from manic depression with valproic acid (VPA), a drug that depletes the cell of IP3, leads to chronic renal Fanconi Syndrome [197]. This suggests that a general defect in inositol phosphate metabolism may explain both observations. This link suggests further evidence for PI(4,5)P2-dependent mechanisms playing a role in the pathology of Lowe Syndrome. If a defect in calcium signalling is responsible for the Lowe Syndrome renal disorder then it will be interesting to test if the mechanism of Dent Disease is similar by analysis of the histamine and thapsigargin response in CLCN5 depleted cells. A separate mechanism by which Dent disease might have altered calcium responses is via the

endocytosis of vitamin D, which causes the release of IP3-sensitive calcium stores. Since Dent's disease patients have defects in endocytosis of vitamin D [198, 199], they will have lower release of these stores, which could be tested in the future as a continuation of the current work.

7: References

1. Attree, O. et al. The Lowe's oculocerebrorenal syndrome gene encodes a protein highly homologous to inositol polyphosphate-5-phosphatase. Nature 358, 239-42. (1992).
2. Allen-Baume, V., Segui, B. & Cockcroft, S. Current thoughts on the phosphatidylinositol transfer protein family. FEBS Lett 531, 74-80 (2002).
3. Di Paolo, G. & De Camilli, P. Phosphoinositides in cell regulation and membrane dynamics. Nature 443, 651-7 (2006).
4. Fruman, D. A., Meyers, R. E. & Cantley, L. C. Phosphoinositide kinases. Annu Rev Biochem 67, 481-507 (1998).
5. Hurley, J. H. & Meyer, T. Subcellular targeting by membrane lipids. Curr Opin Cell Biol 13, 146-52 (2001).
6. Czech, M. P. PIP2 and PIP3: complex roles at the cell surface. Cell 100, 603-6 (2000).
7. Cullen, P. J., Cozier, G. E., Banting, G. & Mellor, H. Modular phosphoinositide-binding domains--their role in signalling and membrane trafficking. Curr Biol 11, R882-93 (2001).
8. De Matteis, M. A. & Godi, A. PI-loting membrane traffic. Nat Cell Biol 6, 487-92 (2004).
9. Yin, H. L. & Janmey, P. A. Phosphoinositide regulation of the actin cytoskeleton. Annu Rev Physiol 65, 761-89 (2003).

10. Lemmon, M. A. Phosphoinositide recognition domains. Traffic 4, 201-13 (2003).
11. Balla, T. & Varnai, P. Visualizing cellular phosphoinositide pools with GFP-fused protein-modules. Sci STKE 2002, PL3 (2002).
12. Wang, Y. J. et al. Phosphatidylinositol 4 phosphate regulates targeting of clathrin adaptor AP-1 complexes to the Golgi. Cell 114, 299-310 (2003).
13. Watt, S. A., Kular, G., Fleming, I. N., Downes, C. P. & Lucocq, J. M. Subcellular localization of phosphatidylinositol 4,5-bisphosphate using the pleckstrin homology domain of phospholipase C delta1. Biochem J 363, 657-66 (2002).
14. Osborne, S. L., Thomas, C. L., Gschmeissner, S. & Schiavo, G. Nuclear PtdIns(4,5)P2 assembles in a mitotically regulated particle involved in pre-mRNA splicing. J Cell Sci 114, 2501-11 (2001).
15. Gaullier, J. M. et al. FYVE fingers bind PtdIns(3)P. Nature 394, 432-3 (1998).
16. Gillooly, D. J. et al. Localization of phosphatidylinositol 3-phosphate in yeast and mammalian cells. Embo J 19, 4577-88 (2000).
17. Gaullier, J. M., Ronning, E., Gillooly, D. J. & Stenmark, H. Interaction of the EEA1 FYVE finger with phosphatidylinositol 3-phosphate and early endosomes. Role of conserved residues. J Biol Chem 275, 24595-600 (2000).
18. Shaw, J. D., Hama, H., Sohrabi, F., DeWald, D. B. & Wendland, B. PtdIns(3,5)P2 is required for delivery of endocytic cargo into the multivesicular body. Traffic 4, 479-90 (2003).

19. Roy, A. & Levine, T. P. Multiple pools of PtdIns 4-phosphate detected using the pleckstrin homology domain of Osh2p. J Biol Chem 279, 44683-44689 (2004).

20. De Matteis, M., Godi, A. & Corda, D. Phosphoinositides and the golgi complex. Curr Opin Cell Biol 14, 434-47 (2002).

21. Mortier, E. et al. Nuclear speckles and nucleoli targeting by PIP2-PDZ domain interactions. Embo J 24, 2556-65 (2005).

22. Balla, A., Tuymetova, G., Tsiomenko, A., Varnai, P. & Balla, T. A plasma membrane pool of phosphatidylinositol 4-phosphate is generated by phosphatidylinositol 4-kinase type-III alpha: studies with the PH domains of the oxysterol binding protein and FAPP1. Mol Biol Cell 16, 1282-95 (2005).

23. Godi, A. et al. FAPPs control Golgi-to-cell-surface membrane traffic by binding to ARF and PtdIns(4)P. Nat Cell Biol 6, 393-404 (2004).

24. Varnai, P. et al. Inositol lipid binding and membrane localization of isolated pleckstrin homology (PH) domains. Studies on the PH domains of phospholipase C delta 1 and p130. J Biol Chem 277, 27412-22 (2002).

25. Jost, M., Simpson, F., Kavran, J. M., Lemmon, M. A. & Schmid, S. L. Phosphatidylinositol-4,5-bisphosphate is required for endocytic coated vesicle formation. Curr Biol 8, 1399-402 (1998).

26. Varnai, P., Thyagarajan, B., Rohacs, T. & Balla, T. Rapidly inducible changes in phosphatidylinositol 4,5-bisphosphate levels influence multiple regulatory functions of the lipid in intact living cells. J Cell Biol 175, 377-82 (2006).

27. Gillooly, D. J., Raiborg, C. & Stenmark, H. Phosphatidylinositol 3-phosphate is found in microdomains of early endosomes. Histochem Cell Biol 120, 445-53 (2003).

28. Bache, K. G., Brech, A., Mehlum, A. & Stenmark, H. Hrs regulates multivesicular body formation via ESCRT recruitment to endosomes. J Cell Biol 162, 435-42 (2003).

29. Osborne, S. L. et al. PIKfyve negatively regulates exocytosis in neurosecretory cells. J Biol Chem 283, 2804-13 (2008).

30. Kim, J. et al. The phosphoinositide kinase PIKfyve mediates epidermal growth factor receptor trafficking to the nucleus. Cancer Res 67, 9229-37 (2007).

31. Insall, R. H. & Weiner, O. D. PIP3, PIP2, and cell movement--similar messages, different meanings? Dev Cell 1, 743-7 (2001).

32. Majerus, P. W., Kisseleva, M. V. & Norris, F. A. The role of phosphatases in inositol signaling reactions. J Biol Chem 274, 10669-72 (1999).

33. Astle, M. V. et al. Regulation of phosphoinositide signaling by the inositol polyphosphate 5-phosphatases. IUBMB Life 58, 451-6 (2006).

34. Katan, M. Families of phosphoinositide-specific phospholipase C: structure and function. Biochim Biophys Acta 1436, 5-17 (1998).

35. Lowe, M. Structure and function of the Lowe syndrome protein OCRL1. Traffic 6, 711-9 (2005).

36. Zhang, X., Hartz, P. A., Philip, E., Racusen, L. C. & Majerus, P. W. Cell lines from kidney proximal tubules of a patient with Lowe syndrome lack OCRL inositol polyphosphate 5-phosphatase and accumulate

phosphatidylinositol 4,5-bisphosphate. J Biol Chem 273, 1574-82 (1998).

37. Zhang, X., Jefferson, A. B., Auethavekiat, V. & Majerus, P. W. The protein deficient in Lowe syndrome is a phosphatidylinositol-4,5-bisphosphate 5-phosphatase. Proc Natl Acad Sci U S A 92, 4853-6 (1995).

38. Suchy, S. F., Olivos-Glander, I. M. & Nussabaum, R. L. Lowe syndrome, a deficiency of phosphatidylinositol 4,5-bisphosphate 5-phosphatase in the Golgi apparatus. Hum Mol Genet 4, 2245-50 (1995).

39. Ijuin, T. et al. Identification and characterization of a novel inositol polyphosphate 5-phosphatase. J Biol Chem 275, 10870-5 (2000).

40. Ooms, L. M. et al. The inositol polyphosphate 5-phosphatase, PIPP, Is a novel regulator of phosphoinositide 3-kinase-dependent neurite elongation. Mol Biol Cell 17, 607-22 (2006).

41. Janne, P. A. et al. Functional overlap between murine Inpp5b and Ocrl1 may explain why deficiency of the murine ortholog for OCRL1 does not cause Lowe syndrome in mice. J Clin Invest 101, 2042-53 (1998).

42. Faucherre, A. et al. Lowe syndrome protein OCRL1 interacts with Rac GTPase in the trans-Golgi network. Hum Mol Genet 12, 2449-56 (2003).

43. Lichter-Konecki, U., Farber, L. W., Cronin, J. S., Suchy, S. F. & Nussbaum, R. L. The effect of missense mutations in the RhoGAP-

homology domain on ocrl1 function. Mol Genet Metab 89, 121-8 (2006).

44. Hyvola, N. et al. Membrane targeting and activation of the Lowe syndrome protein OCRL1 by rab GTPases. Embo J 25, 3750-61 (2006).

45. Fukuda, M., Kanno, E., Ishibashi, K. & Itoh, T. Large scale screening for novel rab effectors reveals unexpected broad Rab binding specificity. Mol Cell Proteomics 7, 1031-42 (2008).

46. Shin, H. W. et al. An enzymatic cascade of Rab5 effectors regulates phosphoinositide turnover in the endocytic pathway. J Cell Biol 170, 607-18 (2005).

47. Faucherre, A. et al. Lowe syndrome protein Ocrl1 is translocated to membrane ruffles upon Rac GTPase activation: a new perspective on Lowe syndrome pathophysiology. Hum Mol Genet 14, 1441-8 (2005).

48. Lin, T. et al. Spectrum of mutations in the OCRL1 gene in the Lowe oculocerebrorenal syndrome. Am J Hum Genet 60, 1384-8 (1997).

49. Suchy, S. F., Lin, T., Horwitz, J. A., O'Brien, W. E. & Nussbaum, R. L. First report of prenatal biochemical diagnosis of Lowe syndrome. Prenat Diagn 18, 1117-21. (1998).

50. McCrea, H. J. et al. All known patient mutations in the ASH-RhoGAP domains of OCRL affect targeting and APPL1 binding. Biochem Biophys Res Commun (2008).

51. Ungewickell, A., Ward, M. E., Ungewickell, E. & Majerus, P. W. The inositol polyphosphate 5-phosphatase Ocrl associates with endosomes

that are partially coated with clathrin. Proc Natl Acad Sci U S A 101, 13501-6 (2004).

52. Choudhury, R. et al. Lowe syndrome protein OCRL1 interacts with clathrin and regulates protein trafficking between endosomes and the trans-Golgi network. Mol Biol Cell 16, 3467-79 (2005).

53. Johnson, J. M. et al. Genome-wide survey of human alternative pre-mRNA splicing with exon junction microarrays. Science 302, 2141-4 (2003).

54. Erdmann, K. S. et al. A role of the Lowe syndrome protein OCRL in early steps of the endocytic pathway. Dev Cell 13, 377-90 (2007).

55. Williams, C., Choudhury, R., McKenzie, E. & Lowe, M. Targeting of the type II inositol polyphosphate 5-phosphatase INPP5B to the early secretory pathway. J Cell Sci 120, 3941-51 (2007).

56. Ponting, C. P. A novel domain suggests a ciliary function for ASPM, a brain size determining gene. Bioinformatics 22, 1031-5 (2006).

57. Mao, X. et al. APPL1 binds to adiponectin receptors and mediates adiponectin signalling and function. Nat Cell Biol 8, 516-23 (2006).

58. Nechamen, C. A. et al. Human follicle-stimulating hormone (FSH) receptor interacts with the adaptor protein APPL1 in HEK 293 cells: potential involvement of the PI3K pathway in FSH signaling. Biol Reprod 71, 629-36 (2004).

59. Lin, D. C. et al. APPL1 associates with TrkA and GIPC1 and is required for nerve growth factor-mediated signal transduction. Mol Cell Biol 26, 8928-41 (2006).

60. Liu, J. et al. Mediation of the DCC apoptotic signal by DIP13 alpha. J Biol Chem 277, 26281-5 (2002).

61. Kaplan, D. R. & Miller, F. D. Neurotrophin signal transduction in the nervous system. Curr Opin Neurobiol 10, 381-91 (2000).

62. Caruso-Neves, C., Pinheiro, A. A., Cai, H., Souza-Menezes, J. & Guggino, W. B. PKB and megalin determine the survival or death of renal proximal tubule cells. Proc Natl Acad Sci U S A 103, 18810-5 (2006).

63. Ungewickell, A. J. & Majerus, P. W. Increased levels of plasma lysosomal enzymes in patients with Lowe syndrome. Proc Natl Acad Sci U S A 96, 13342-4. (1999).

64. Del Nery, E. et al. Rab6A and Rab6A' GTPases play non-overlapping roles in membrane trafficking. Traffic 7, 394-407 (2006).

65. Takenawa, T. & Itoh, T. Phosphoinositides, key molecules for regulation of actin cytoskeletal organization and membrane traffic from the plasma membrane. Biochim Biophys Acta 1533, 190-206 (2001).

66. Suchy, S. F. & Nussbaum, R. L. The deficiency of PIP2 5-phosphatase in Lowe syndrome affects actin polymerization. Am J Hum Genet 71, 1420-7 (2002).

67. Jones, D. H. et al. Type I phosphatidylinositol 4-phosphate 5-kinase directly interacts with ADP-ribosylation factor 1 and is responsible for phosphatidylinositol 4,5-bisphosphate synthesis in the golgi compartment. J Biol Chem 275, 13962-6 (2000).

68. Perez-Mansilla, B. et al. The differential regulation of phosphatidylinositol 4-phosphate 5-kinases and phospholipase D1 by

ADP-ribosylation factors 1 and 6. Biochim Biophys Acta 1761, 1429-42 (2006).

69. Balla, T., Bondeva, T. & Varnai, P. How accurately can we image inositol lipids in living cells? Trends Pharmacol Sci 21, 238-41 (2000).

70. Yagisawa, H. et al. Replacements of single basic amino acids in the pleckstrin homology domain of phospholipase C-delta1 alter the ligand binding, phospholipase activity, and interaction with the plasma membrane. J Biol Chem 273, 417-24 (1998).

71. Garcia, P. et al. The pleckstrin homology domain of phospholipase C-delta 1 binds with high affinity to phosphatidylinositol 4,5-bisphosphate in bilayer membranes. Biochemistry 34, 16228-34 (1995).

72. Stefan, C. J., Audhya, A. & Emr, S. D. The yeast synaptojanin-like proteins control the cellular distribution of phosphatidylinositol (4,5)-bisphosphate. Mol Biol Cell 13, 542-57 (2002).

73. Creutz, C. E. & Snyder, S. L. Interactions of annexins with the mu subunits of the clathrin assembly proteins. Biochemistry 44, 13795-806 (2005).

74. Hansen, M. D., Ehrlich, J. S. & Nelson, W. J. Molecular mechanism for orienting membrane and actin dynamics to nascent cell-cell contacts in epithelial cells. J Biol Chem 277, 45371-6 (2002).

75. Hayes, M. J. et al. Annexin 2 binding to phosphatidylinositol 4,5-bisphosphate on endocytic vesicles is regulated by the stress response pathway. J Biol Chem 279, 14157-64 (2004).

76. Rescher, U., Ruhe, D., Ludwig, C., Zobiack, N. & Gerke, V. Annexin 2 is a phosphatidylinositol (4,5)-bisphosphate binding protein recruited to

actin assembly sites at cellular membranes. J Cell Sci 117, 3473-80 (2004).

77. Gokhale, N. A., Abraham, A., Digman, M. A., Gratton, E. & Cho, W. Phosphoinositide specificity of and mechanism of lipid domain formation by annexin A2-p11 heterotetramer. J Biol Chem 280, 42831-40 (2005).

78. Carr, G., Simmons, N. L. & Sayer, J. A. Disruption of clc-5 leads to a redistribution of annexin A2 and promotes calcium crystal agglomeration in collecting duct epithelial cells. Cell Mol Life Sci 63, 367-77 (2006).

79. Gunther, W., Piwon, N. & Jentsch, T. J. The ClC-5 chloride channel knock-out mouse - an animal model for Dent's disease. Pflugers Arch 445, 456-62 (2003).

80. Hoopes, R. R., Jr. et al. Dent Disease with mutations in OCRL1. Am J Hum Genet 76, 260-7 (2005).

81. Cockcroft, S. & Thomas, G. M. Inositol-lipid-specific phospholipase C isoenzymes and their differential regulation by receptors. Biochem J 288 (Pt 1), 1-14 (1992).

82. Rhee, S. G. & Bae, Y. S. Regulation of phosphoinositide-specific phospholipase C isozymes. J Biol Chem 272, 15045-8 (1997).

83. Pinton, P., Pozzan, T. & Rizzuto, R. The Golgi apparatus is an inositol 1,4,5-trisphosphate-sensitive Ca2+ store, with functional properties distinct from those of the endoplasmic reticulum. Embo J 17, 5298-308 (1998).

84. Missiaen, L. et al. Calcium release from the Golgi apparatus and the endoplasmic reticulum in HeLa cells stably expressing targeted aequorin to these compartments. Cell Calcium 36, 479-87 (2004).

85. Johenning, F. W. et al. InsP3-mediated intracellular calcium signalling is altered by expression of synaptojanin-1. Biochem J 382, 687-94 (2004).

86. Lupu, V. D., Kaznacheyeva, E., Krishna, U. M., Falck, J. R. & Bezprozvanny, I. Functional coupling of phosphatidylinositol 4,5-bisphosphate to inositol 1,4,5-trisphosphate receptor. J Biol Chem 273, 14067-70 (1998).

87. Hilgemann, D. W., Feng, S. & Nasuhoglu, C. The complex and intriguing lives of PIP2 with ion channels and transporters. Sci STKE 2001, RE19 (2001).

88. Zahraoui, A., Louvard, D. & Galli, T. Tight junction, a platform for trafficking and signaling protein complexes. J Cell Biol 151, F31-6 (2000).

89. Matter, K. & Balda, M. S. Signalling to and from tight junctions. Nat Rev Mol Cell Biol 4, 225-36 (2003).

90. Gossman, D. G. & Zhao, H. B. Hemichannel-mediated inositol 1,4,5-trisphosphate (IP3) release in the cochlea: a novel mechanism of IP3 intercellular signaling. Cell Commun Adhes 15, 305-15 (2008).

91. Kumar, N. M. & Gilula, N. B. The gap junction communication channel. Cell 84, 381-8 (1996).

92. Baruch, A. et al. Defining a link between gap junction communication, proteolysis, and cataract formation. J Biol Chem 276, 28999-9006 (2001).

93. Hartsock, A. & Nelson, W. J. Adherens and tight junctions: structure, function and connections to the actin cytoskeleton. Biochim Biophys Acta 1778, 660-9 (2008).

94. Irie, K., Shimizu, K., Sakisaka, T., Ikeda, W. & Takai, Y. Roles and modes of action of nectins in cell-cell adhesion. Semin Cell Dev Biol 15, 643-56 (2004).

95. Ikenouchi, J. [Molecular mechanisms in the formation of discrete apical and basolateral membrane domains in polarized epithelial cells]. Tanpakushitsu Kakusan Koso 52, 1863-70 (2007).

96. Ikenouchi, J., Umeda, K., Tsukita, S., Furuse, M. & Tsukita, S. Requirement of ZO-1 for the formation of belt-like adherens junctions during epithelial cell polarization. J Cell Biol 176, 779-86 (2007).

97. Shen, L., Weber, C. R. & Turner, J. R. The tight junction protein complex undergoes rapid and continuous molecular remodeling at steady state. J Cell Biol 181, 683-95 (2008).

98. Hayes, M. J. et al. Annexin A2 at the interface between F-actin and membranes enriched in phosphatidylinositol 4,5,-bisphosphate. Biochim Biophys Acta (2008).

99. Allen, P. G. Actin filament uncapping localizes to ruffling lamellae and rocketing vesicles. Nat Cell Biol 5, 972-9 (2003).

100. Rozelle, A. L. et al. Phosphatidylinositol 4,5-bisphosphate induces actin-based movement of raft-enriched vesicles through WASP-Arp2/3. Curr Biol 10, 311-20 (2000).

101. Yonemura, S., Itoh, M., Nagafuchi, A. & Tsukita, S. Cell-to-cell adherens junction formation and actin filament organization: similarities and differences between non-polarized fibroblasts and polarized epithelial cells. J Cell Sci 108 (Pt 1), 127-42 (1995).

102. Zhang, J. et al. Actin at cell-cell junctions is composed of two dynamic and functional populations. J Cell Sci 118, 5549-62 (2005).

103. Cavey, M., Rauzi, M., Lenne, P. F. & Lecuit, T. A two-tiered mechanism for stabilization and immobilization of E-cadherin. Nature 453, 751-6 (2008).

104. Takaishi, K., Sasaki, T., Kotani, H., Nishioka, H. & Takai, Y. Regulation of cell-cell adhesion by rac and rho small G proteins in MDCK cells. J Cell Biol 139, 1047-59 (1997).

105. Fukuhara, A., Shimizu, K., Kawakatsu, T., Fukuhara, T. & Takai, Y. Involvement of nectin-activated Cdc42 small G protein in organization of adherens and tight junctions in Madin-Darby canine kidney cells. J Biol Chem 278, 51885-93 (2003).

106. Ivanov, A. I., Nusrat, A. & Parkos, C. A. Endocytosis of epithelial apical junctional proteins by a clathrin-mediated pathway into a unique storage compartment. Mol Biol Cell 15, 176-88 (2004).

107. Zerial, M. & McBride, H. Rab proteins as membrane organizers. Nat Rev Mol Cell Biol 2, 107-17 (2001).

108. Pereira-Leal, J. B. & Seabra, M. C. Evolution of the Rab family of small GTP-binding proteins. J Mol Biol 313, 889-901 (2001).

109. Yamamura, R., Nishimura, N., Nakatsuji, H., Arase, S. & Sasaki, T. The interaction of JRAB/MICAL-L2 with Rab8 and Rab13 coordinates the assembly of tight junctions and adherens junctions. Mol Biol Cell 19, 971-83 (2008).

110. Sato, T. et al. The Rab8 GTPase regulates apical protein localization in intestinal cells. Nature 448, 366-9 (2007).

111. Marzesco, A. M. et al. The small GTPase Rab13 regulates assembly of functional tight junctions in epithelial cells. Mol Biol Cell 13, 1819-31 (2002).

112. Zahraoui, A. et al. A small rab GTPase is distributed in cytoplasmic vesicles in non polarized cells but colocalizes with the tight junction marker ZO-1 in polarized epithelial cells. J Cell Biol 124, 101-15 (1994).

113. Nokes, R. L., Fields, I. C., Collins, R. N. & Folsch, H. Rab13 regulates membrane trafficking between TGN and recycling endosomes in polarized epithelial cells. J Cell Biol 182, 845-53 (2008).

114. Morimoto, S. et al. Rab13 mediates the continuous endocytic recycling of occludin to the cell surface. J Biol Chem 280, 2220-8 (2005).

115. Terai, T., Nishimura, N., Kanda, I., Yasui, N. & Sasaki, T. JRAB/MICAL-L2 is a junctional Rab13-binding protein mediating the endocytic recycling of occludin. Mol Biol Cell 17, 2465-75 (2006).

116. Kitt, K. N. et al. Rab14 regulates apical targeting in polarized epithelial cells. Traffic 9, 1218-31 (2008).

117. Kohler, K., Louvard, D. & Zahraoui, A. Rab13 regulates PKA signaling during tight junction assembly. J Cell Biol 165, 175-80 (2004).

118. Guillemot, L., Paschoud, S., Pulimeno, P., Foglia, A. & Citi, S. The cytoplasmic plaque of tight junctions: a scaffolding and signalling center. Biochim Biophys Acta 1778, 601-13 (2008).

119. Schmid, A. C., Wise, H. M., Mitchell, C. A., Nussbaum, R. & Woscholski, R. Type II phosphoinositide 5-phosphatases have unique sensitivities towards fatty acid composition and head group phosphorylation. FEBS Lett 576, 9-13 (2004).

120. van Zeijl, L. et al. Regulation of connexin43 gap junctional communication by phosphatidylinositol 4,5-bisphosphate. J Cell Biol 177, 881-91 (2007).

121. Meyer, T. N., Hunt, J., Schwesinger, C. & Denker, B. M. Galpha12 regulates epithelial cell junctions through Src tyrosine kinases. Am J Physiol Cell Physiol 285, C1281-93 (2003).

122. Hains, M. D., Wing, M. R., Maddileti, S., Siderovski, D. P. & Harden, T. K. Galpha12/13- and rho-dependent activation of phospholipase C-epsilon by lysophosphatidic acid and thrombin receptors. Mol Pharmacol 69, 2068-75 (2006).

123. Martin-Belmonte, F. et al. PTEN-mediated apical segregation of phosphoinositides controls epithelial morphogenesis through Cdc42. Cell 128, 383-97 (2007).

124. Miaczynska, M. et al. APPL proteins link Rab5 to nuclear signal transduction via an endosomal compartment. Cell 116, 445-56 (2004).

125. Akiyama, C. et al. Phosphatidylinositol-4-phosphate 5-kinase gamma is associated with cell-cell junction in A431 epithelial cells. Cell Biol Int 29, 514-20 (2005).

126. Ward, P. D., Ouyang, H. & Thakker, D. R. Role of phospholipase C-beta in the modulation of epithelial tight junction permeability. J Pharmacol Exp Ther 304, 689-98 (2003).

127. Suzuki, T., Seth, A. & Rao, R. Role of phospholipase Cgamma-induced activation of protein kinase Cepsilon (PKCepsilon) and PKCbetaI in epidermal growth factor-mediated protection of tight junctions from acetaldehyde in Caco-2 cell monolayers. J Biol Chem 283, 3574-83 (2008).

128. Santarius, M., Lee, C. H. & Anderson, R. A. Supervised membrane swimming: small G-protein lifeguards regulate PIPK signalling and monitor intracellular PtdIns(4,5)P2 pools. Biochem J 398, 1-13 (2006).

129. Goldschmidt-Clermont, P. J., Machesky, L. M., Baldassare, J. J. & Pollard, T. D. The actin-binding protein profilin binds to PIP2 and inhibits its hydrolysis by phospholipase C. Science 247, 1575-8 (1990).

130. Laux, T. et al. GAP43, MARCKS, and CAP23 modulate PI(4,5)P(2) at plasmalemmal rafts, and regulate cell cortex actin dynamics through a common mechanism. J Cell Biol 149, 1455-72 (2000).

131. Mancini, A., Koch, A., Wilms, R. & Tamura, T. The SH2-containing inositol 5-phosphatase (SHIP)-1 is implicated in the control of cell-cell junction and induces dissociation and dispersion of MDCK cells. Oncogene 21, 1477-84 (2002).

132. Wu, H. et al. PDZ domains of Par-3 as potential phosphoinositide signaling integrators. Mol Cell 28, 886-98 (2007).

133. Zimmermann, P. et al. PIP(2)-PDZ domain binding controls the association of syntenin with the plasma membrane. Mol Cell 9, 1215-25 (2002).

134. Zimmermann, P. The prevalence and significance of PDZ domain-phosphoinositide interactions. Biochim Biophys Acta 1761, 947-56 (2006).

135. Matter, K. & Balda, M. S. Epithelial tight junctions, gene expression and nucleo-junctional interplay. J Cell Sci 120, 1505-11 (2007).

136. Mazzotti, G. et al. Immunocytochemical detection of phosphatidylinositol 4,5-bisphosphate localization sites within the nucleus. J Histochem Cytochem 43, 181-91 (1995).

137. Traweger, A. et al. The tight junction protein ZO-2 localizes to the nucleus and interacts with the heterogeneous nuclear ribonucleoprotein scaffold attachment factor-B. J Biol Chem 278, 2692-700 (2003).

138. Benezra, M., Greenberg, R. S. & Masur, S. K. Localization of ZO-1 in the nucleolus of corneal fibroblasts. Invest Ophthalmol Vis Sci 48, 2043-9 (2007).

139. Boronenkov, I. V., Loijens, J. C., Umeda, M. & Anderson, R. A. Phosphoinositide signaling pathways in nuclei are associated with nuclear speckles containing pre-mRNA processing factors. Mol Biol Cell 9, 3547-60 (1998).

140. Mellman, D. L. et al. A PtdIns4,5P2-regulated nuclear poly(A) polymerase controls expression of select mRNAs. Nature 451, 1013-7 (2008).

141. Deleris, P. et al. SHIP-2 and PTEN are expressed and active in vascular smooth muscle cell nuclei, but only SHIP-2 is associated with nuclear speckles. J Biol Chem 278, 38884-91 (2003).

142. Gassama-Diagne, A. et al. Phosphatidylinositol-3,4,5-trisphosphate regulates the formation of the basolateral plasma membrane in epithelial cells. Nat Cell Biol 8, 963-70 (2006).

143. Pinal, N. et al. Regulated and polarized PtdIns(3,4,5)P3 accumulation is essential for apical membrane morphogenesis in photoreceptor epithelial cells. Curr Biol 16, 140-9 (2006).

144. Levine, T. P. & Munro, S. Targeting of Golgi-specific pleckstrin homology domains involves both PtdIns 4-kinase-dependent and -independent components. Curr Biol 12, 695-704 (2002).

145. Loewen, C. J. & Levine, T. P. A highly conserved binding site in vesicle-associated membrane protein-associated protein (VAP) for the FFAT motif of lipid-binding proteins. J Biol Chem 280, 14097-104 (2005).

146. Dressman, M. A., Olivos-Glander, I. M., Nussbaum, R. L. & Suchy, S. F. Ocrl1, a PtdIns(4,5)P(2) 5-phosphatase, is localized to the trans-Golgi network of fibroblasts and epithelial cells. J Histochem Cytochem 48, 179-90 (2000).

147. Gerke, V., Creutz, C. E. & Moss, S. E. Annexins: linking Ca2+ signalling to membrane dynamics. Nat Rev Mol Cell Biol 6, 449-61 (2005).

148. Talian, J. C. & Zelenka, P. S. Calpactin I in the differentiating embryonic chicken lens: mRNA levels and protein distribution. Dev Biol 143, 68-77 (1991).

149. Zhao, W. Q., Waisman, D. M. & Grimaldi, M. Specific localization of the annexin II heterotetramer in brain lipid raft fractions and its changes in spatial learning. J Neurochem 90, 609-20 (2004).

150. Lowe, C. Oculocerebral syndrome of Lowe. J Glaucoma 14, 179-80 (2005).

151. Karimi-Busheri, F. et al. Expression of a releasable form of annexin II by human keratinocytes. J Cell Biochem 86, 737-47 (2002).

152. Thery, C. et al. Molecular characterization of dendritic cell-derived exosomes. Selective accumulation of the heat shock protein hsc73. J Cell Biol 147, 599-610 (1999).

153. Levine, T. P. & Munro, S. The pleckstrin homology domain of oxysterol-binding protein recognises a determinant specific to Golgi membranes. Curr Biol 8, 729-39 (1998).

154. Varnai, P. et al. Selective cellular effects of overexpressed pleckstrin-homology domains that recognize PtdIns(3,4,5)P3 suggest their interaction with protein binding partners. J Cell Sci 118, 4879-88 (2005).

155. Gray, A., Van Der Kaay, J. & Downes, C. P. The pleckstrin homology domains of protein kinase B and GRP1 (general receptor for

phosphoinositides-1) are sensitive and selective probes for the cellular detection of phosphatidylinositol 3,4-bisphosphate and/or phosphatidylinositol 3,4,5-trisphosphate in vivo. Biochem J 344 Pt 3, 929-36 (1999).

156. Mitchell, C. A. et al. Inositol polyphosphate 5-phosphatases: lipid phosphatases with flair. IUBMB Life 53, 25-36. (2002).

157. Berridge, M. J., Lipp, P. & Bootman, M. D. The versatility and universality of calcium signalling. Nat Rev Mol Cell Biol 1, 11-21 (2000).

158. Schelling, J. R., Gentry, D. J. & Dubyak, G. R. Annexin II inhibition of G protein-regulated inositol trisphosphate formation in rat aortic smooth muscle. Am J Physiol 270, F682-90 (1996).

159. Vasioukhin, V., Bauer, C., Yin, M. & Fuchs, E. Directed actin polymerization is the driving force for epithelial cell-cell adhesion. Cell 100, 209-19 (2000).

160. Bruewer, M., Hopkins, A. M., Hobert, M. E., Nusrat, A. & Madara, J. L. RhoA, Rac1, and Cdc42 exert distinct effects on epithelial barrier via selective structural and biochemical modulation of junctional proteins and F-actin. Am J Physiol Cell Physiol 287, C327-35 (2004).

161. Jou, T. S. & Nelson, W. J. Effects of regulated expression of mutant RhoA and Rac1 small GTPases on the development of epithelial (MDCK) cell polarity. J Cell Biol 142, 85-100 (1998).

162. Jou, T. S., Schneeberger, E. E. & Nelson, W. J. Structural and functional regulation of tight junctions by RhoA and Rac1 small GTPases. J Cell Biol 142, 101-15 (1998).

163. Hellsten, E. et al. Sertoli cell vacuolization and abnormal germ cell adhesion in mice deficient in an inositol polyphosphate 5-phosphatase. Biol Reprod 66, 1522-30. (2002).

164. Ferrari, A., Veligodskiy, A., Berge, U., Lucas, M. S. & Kroschewski, R. ROCK-mediated contractility, tight junctions and channels contribute to the conversion of a preapical patch into apical surface during isochoric lumen initiation. J Cell Sci 121, 3649-63 (2008).

165. Weber, K. L., Fischer, R. S. & Fowler, V. M. Tmod3 regulates polarized epithelial cell morphology. J Cell Sci 120, 3625-32 (2007).

166. Aijaz, S., Sanchez-Heras, E., Balda, M. S. & Matter, K. Regulation of tight junction assembly and epithelial morphogenesis by the heat shock protein Apg-2. BMC Cell Biol 8, 49 (2007).

167. Yeung, T. et al. Membrane phosphatidylserine regulates surface charge and protein localization. Science 319, 210-3 (2008).

168. Irvine, R. Nuclear lipid signaling. Sci STKE 2000, RE1 (2000).

169. Fukami, K. et al. Requirement of phosphatidylinositol 4,5-bisphosphate for alpha-actinin function. Nature 359, 150-2 (1992).

170. Janmey, P. A. & Stossel, T. P. Modulation of gelsolin function by phosphatidylinositol 4,5-bisphosphate. Nature 325, 362-4 (1987).

171. Janmey, P. A., Iida, K., Yin, H. L. & Stossel, T. P. Polyphosphoinositide micelles and polyphosphoinositide-containing vesicles dissociate endogenous gelsolin-actin complexes and promote actin assembly from the fast-growing end of actin filaments blocked by gelsolin. J Biol Chem 262, 12228-36 (1987).

172. Wenk, M. R. & De Camilli, P. Protein-lipid interactions and phosphoinositide metabolism in membrane traffic: insights from vesicle recycling in nerve terminals. Proc Natl Acad Sci U S A 101, 8262-9 (2004).

173. Sun, Y., Carroll, S., Kaksonen, M., Toshima, J. Y. & Drubin, D. G. PtdIns(4,5)P2 turnover is required for multiple stages during clathrin- and actin-dependent endocytic internalization. J Cell Biol 177, 355-67 (2007).

174. Lemmon, M. A., Ferguson, K. M., O'Brien, R., Sigler, P. B. & Schlessinger, J. Specific and high-affinity binding of inositol phosphates to an isolated pleckstrin homology domain. Proc Natl Acad Sci U S A 92, 10472-6 (1995).

175. Quinn, K. V., Behe, P. & Tinker, A. Monitoring changes in membrane phosphatidylinositol 4,5-bisphosphate in living cells using a domain from the transcription factor tubby. J Physiol (2008).

176. Soboloff, J., Spassova, M. A., Dziadek, M. A. & Gill, D. L. Calcium signals mediated by STIM and Orai proteins-A new paradigm in inter-organelle communication. Biochim Biophys Acta (2006).

177. Smyth, J. T. et al. Emerging perspectives in store-operated Ca(2+) entry: Roles of Orai, Stim and TRP. Biochim Biophys Acta (2006).

178. Ambudkar, I. S. & Ong, H. L. Organization and function of TRPC channelosomes. Pflugers Arch (2007).

179. Skippen, A., Swigart, P. & Cockcroft, S. Measurement of phospholipase C by monitoring inositol phosphates using [3H]inositol-

labeling protocols in permeabilized cells. Methods Mol Biol 312, 183-93 (2006).

180. Berridge, M. J. & Irvine, R. F. Inositol phosphates and cell signalling. Nature 341, 197-205 (1989).

181. Dolman, N. J. & Tepikin, A. V. Calcium gradients and the Golgi. Cell Calcium 40, 505-12 (2006).

182. Chung, J. K. et al. Synaptojanin inhibition of phospholipase D activity by hydrolysis of phosphatidylinositol 4,5-bisphosphate. J Biol Chem 272, 15980-5 (1997).

183. Sciorra, V. A. et al. Identification of a phosphoinositide binding motif that mediates activation of mammalian and yeast phospholipase D isoenzymes. Embo J 18, 5911-21 (1999).

184. Suchy, S. F., Cronin, J. C. & Nussbaum, R. L. Abnormal bradykinin signalling in fibroblasts deficient in the PIP(2) 5-phosphatase, ocrl1. J Inherit Metab Dis (2009).

185. Kay, B. K., Williamson, M. P. & Sudol, M. The importance of being proline: the interaction of proline-rich motifs in signaling proteins with their cognate domains. Faseb J 14, 231-41 (2000).

186. Mayer, B. J. SH3 domains: complexity in moderation. J Cell Sci 114, 1253-63 (2001).

187. Boshans, R. L., Szanto, S., van Aelst, L. & D'Souza-Schorey, C. ADP-ribosylation factor 6 regulates actin cytoskeleton remodeling in coordination with Rac1 and RhoA. Mol Cell Biol 20, 3685-94 (2000).

188. Insall, R. H. & Machesky, L. M. Regulation of WASP: PIP2 Pipped by Toca-1? Cell 118, 140-1 (2004).

189. Hilpela, P., Vartiainen, M. K. & Lappalainen, P. Regulation of the actin cytoskeleton by PI(4,5)P2 and PI(3,4,5)P3. Curr Top Microbiol Immunol 282, 117-63 (2004).

190. Pilecka, I., Banach-Orlowska, M. & Miaczynska, M. Nuclear functions of endocytic proteins. Eur J Cell Biol 86, 533-47 (2007).

191. Robb, R. M. & Marchevsky, A. Pathology of the Lens in Down's syndrome. Arch Ophthalmol 96, 1039-42 (1978).

192. Gao, J. et al. Connections between connexins, calcium, and cataracts in the lens. J Gen Physiol 124, 289-300 (2004).

193. Weber, G. F. & Menko, A. S. Actin filament organization regulates the induction of lens cell differentiation and survival. Dev Biol 295, 714-29 (2006).

194. Zhou, J. & Menko, A. S. The role of Src family kinases in cortical cataract formation. Invest Ophthalmol Vis Sci 43, 2293-300 (2002).

195. Burger, A. et al. The crystal structure and ion channel activity of human annexin II, a peripheral membrane protein. J Mol Biol 257, 839-47 (1996).

196. Hayes, M. J. & Moss, S. E. Annexin 2 has a dual role as regulator and effector of V-Src in cell transformation. J Biol Chem (2009).

197. Zaki, E. L. & Springate, J. E. Renal injury from valproic acid: case report and literature review. Pediatr Neurol 27, 318-9 (2002).

198. Morelli, S., Buitrago, C., Vazquez, G., De Boland, A. R. & Boland, R. Involvement of tyrosine kinase activity in 1alpha,25(OH)2-vitamin D3 signal transduction in skeletal muscle cells. J Biol Chem 275, 36021-8 (2000).

199. Piwon, N., Gunther, W., Schwake, M., Bosl, M. R. & Jentsch, T. J. ClC-5 Cl- -channel disruption impairs endocytosis in a mouse model for Dent's disease. Nature 408, 369-73 (2000).